MID-AMERICA TRANSPORTATION CENTER

Report # MATC-KU: 153-3

Final Report
WBS: 25-1121-0005-153-3

Modeling Driver Behavior and Aggressiveness Using Biobehavioral Methods - Phase III

Alexandra Kondyli, PhD
Associate Professor
Department of Civil, Environmental, and Architectural Engineering
The University of Kansas

Vishal C. Kummetha, PhD
Postdoctoral Researcher
Center for Urban Transportation Research
University of South Florida

2022

A Cooperative Research Project sponsored by
U.S. Department of Transportation- Office of the Assistant Secretary for Research and Technology

Modeling Driver Behavior and Aggressiveness Using Biobehavioral Methods – Phase III

Alexandra Kondyli, Ph.D.
Associate Professor
Department of Civil, Environmental, and Architectural Engineering
University of Kansas

Vishal C. Kummetha, Ph.D.
Postdoctoral Researcher
Center for Urban Transportation Research (CUTR)
University of South Florida

A Report on Research Sponsored by

Mid-America Transportation Center

University of Nebraska–Lincoln

February 2022

TECHNICAL REPORT DOCUMENTATION PAGE

1. Report No. 25-1121-0005-153-3	**2. Government Accession No.**	**3. Recipient's Catalog No.**
4. Title and Subtitle Modeling Driver Behavior and Aggressiveness Using Biobehavioral Methods – Phase III		**5. Report Date** February 18, 2022 **6. Performing Organization Code**
7. Author(s) Alexandra Kondyli, Ph.D. https://orcid.org/0000-0002-3462-0000, Vishal Kummetha, Ph.D. https://orcid.org/0000-0001-9464-6838.		**8. Performing Organization Report No.** 25-1121-0005-153-3
9. Performing Organization Name and Address The University of Kansas 1530 W. 15th Street Lawrence, KS, 66045		**10. Work Unit No.** **11. Contract or Grant No.** 69A3551747107
12. Sponsoring Agency Name and Address Mid-America Transportation Center 2200 Vine St PO Box 830851 Lincoln, NE 68583		**13. Type of Report and Period Covered** Draft Final Report (January 2020-December 2021) **14. Sponsoring Agency Code** US DOT TRB RiP # 91994-66

15. Supplementary Notes
Conducted in cooperation with the U.S. Department of Transportation, Federal Highway Administration.

16. Abstract
Mathematical models of car-following, lane changing, and gap acceptance are mostly descriptive in nature and lack decision making or error tolerance. Including additional driver-related information with respect to behavior and cognitive characteristics would account for these lacking parameters and incorporate a human aspect to these models. Car-following, particularly in relation to the intelligent driver model (IDM), is the primary component of this research. The major objectives of this research are to investigate how psychophysiological constructs can be modeled to replicate car-following behavior, and to correlate subjective measures of behavior with actual car-following behavior. To accomplish these objectives the following tasks were performed: thorough literature review, theorized methodological framework for model development, administered behavioral questionnaires, carried out a driving simulator study to collect relevant data, grouped drivers with respect to their static and behavioral traits, established thresholds for introducing biobehavioral parameters to the IDM, and calibrated and validated the IDM based on driver groups as well as based on the introduction of the biobehavioral parameters.
This report builds on the previous project phases and provides a detailed description of the data analysis and model development, in addition to the thorough literature review, methodological framework, and data collection process. Behavioral, driving, physiological, and subjective data were collected from 90 participants, while performing six car-following tasks on the driving simulator. Analysis of trends observed with respect to compensatory and performance changes experienced by drivers is presented. A new model named, b-IDM is proposed. This model includes modifications to the IDM based on driver classification, behavior, and driving performance.

17. Key Words Mental workload, situation awareness, biobehavioral, car-following	**18. Distribution Statement** No restrictions. This document is available through the National Technical Information Service, Springfield, VA 22161. Enter any other agency mandated distribution statements. Remove NTIS statement if it does not apply.

19. Security Classif. (of this report) Unclassified	**20. Security Classif. (of this page)** Unclassified	**21. No. of Pages** 143	**22. Price**

Form DOT F 1700.7 (8-72) Reproduction of completed page authorized

Table of Contents

List of Figures

List of Tables

List of Abbreviations

Cognitive Reflection Task (CRT)
Detection Response Task (DRT)
Driving Activity Load Index (DALI)
Electrocardiography (ECG)
Electroencephalography (EEG)
Heart Rate (HR)
Heart Rate Variability (HRV)
Human Driver Model (HDM)
Human Research Protection Program (HRPP)
Institutional Review Board (IRB)
Intelligent Driver Model (IDM)
Level of Activation (LA)
Mid-America Transportation Center (MATC)
National Aeronautics and Space Administration (NASA)
Nebraska Transportation Center (NTC)
Peripheral Detection Task (PDT)
Situation Awareness (SA)
Situation Awareness Global Assessment Technique (SAGAT)
Situation Awareness Rating Technique (SART)
Situation Present Assessment Method (SPAM)
Standard Deviation (SD)
Standard Deviation of Lateral Position (SDLP)
Standard Deviation of Steering Wheel Movement (SDSTW)
The University of Kansas (KU)
Task Load Index (TLX)
Task-Evoked Pupillary Response (TEPR)
Useful Field of View (UFOV)
Mental Workload (WL)

Disclaimer

The contents of this report reflect the views of the authors, who are responsible for the facts and the accuracy of the information presented herein. This document is disseminated in the interest of information exchange. The report is funded, partially or entirely, by a grant from the U.S. Department of Transportation's University Transportation Centers Program. However, the U.S. Government assumes no liability for the contents or use thereof.

Abstract

Mathematical models of car-following, lane changing, and gap acceptance are mostly descriptive in nature and lack decision making or error tolerance. Including additional driver-related information with respect to behavior and cognitive characteristics would account for these lacking parameters and incorporate a human aspect to these models. Car-following, particularly in relation to the intelligent driver model (IDM), is the primary component of this research. The major objectives of this research are to investigate how psychophysiological constructs can be modeled to replicate car-following behavior, and to correlate subjective measures of behavior with actual car-following behavior.

This report builds on the previous project phases and provides a detailed description of the data analysis and model development, in addition to the thorough literature review, methodological framework, and data collection process. Behavioral, driving, physiological, and subjective data were collected from 90 participants, while performing six car-following tasks on the driving simulator. Analysis of trends observed with respect to compensatory and performance changes experienced by drivers is presented. A new model named b-IDM is proposed. This model includes modifications to the IDM based on driver classification, behavior, and driving performance.

Chapter 1 Introduction

1.1 Problem Statement

Driver behavior is a significant contributor to traffic operational quality and safety, and it is also an important element in traffic simulation tools. These tools introduce driver behavioral variability through various distributions and factors such as speed, spacing, acceleration, deceleration, reaction time, and standstill distance. In addition, the mathematical models of car-following, lane changing, and gap acceptance are mostly descriptive in nature. As a result, these tools do not accurately describe traffic phenomena such as breakdowns or capacity drop and consequently, calibration efforts to field data are needed. Also, the majority of tools are "collision-free" by default, therefore, estimating surrogate safety measures based on these models would be inaccurate. As such, additional information of driver behavior from the cognitive sciences could significantly enhance the ability of existing models to replicate field conditions.

Biobehavioral aspects encompass the variability of cognitive workload and situation awareness with the driving pattern of individuals. In this study, driving variables such as preferred gap, speed, jerk, acceleration, and deceleration, are used together with biobehavioral variables such as level of activation/engagement (LA), mental workload (WL), changes in situation awareness (SA), and static driver properties (age, experience, and driving history), to classify drivers from the study pool into clusters of similar driving traits. This collection of variables and traits are used to identify the best-suited coefficients to improve car-following behavioral predictions, depending on the situation complexity, for a particular driver.

1.2 Objectives

The major goals of this research are to investigate how psychophysiological constructs can be modeled to replicate car-following behavior, and to correlate subjective measures of behavior and aggressiveness with actual car-following behavior. This research is divided in three parts. Part I (Kondyli et al., 2018) summarized the literature review comprising of techniques and past studies aimed at incorporating behavioral aspects into traffic models. It also included the proposed methodological setup of the experiments to be conducted with the use of a driving simulator, as well as finalized survey questionnaires related to driving, cognition, personality, and decision-making processes. Part II of this research project (Kondyli et al., 2020) revisited the literature review, established suitable participants, executed the data collection and sorting, and performed preliminary between-tasks analyses. Part III, which is the focus of this report, provides a thorough analysis of the time-series datasets and numerous physiological measures obtained through the driving simulator experiments and the questionnaires, as well as the model development and validation.

The specific tasks performed during this research project are as follows:

- Conduct a thorough literature review comprising of techniques and past studies aimed at incorporating behavioral aspects into traffic models. Including parameters previously used to categorize drivers;
- Develop the methodological framework to incorporate behavioral aspects into an existing car-following model (i.e., the IDM);
- Classify drivers by self-reported/subjective measures (PANAS, decision making, NASA-TLX (Task load index), attention and executive, and screening questionnaires), biobehavioral measures (level of activation, heart rate, pupil

dilation, and gaze fixation), and performance measures (speed, acceleration, headway, standard deviation (SD) steering wheel angle, and SD of lateral position);

- Collect static and dynamic behavioral parameters using a driving simulator study with 90 drivers;
- Analyze data to establish activation level, workload, situation awareness, compensation, and performance thresholds for the different types of driver categories; and
- Incorporate attained thresholds into the intelligent driver model (IDM) and compare the predictive capability to the unaltered IDM. Validate the feasibility of the modified biobehavioral IDM (b-IDM).

1.3 Outline of the Report

The report starts by presenting the problem statement and objectives in the first chapter. Chapter 2 presents the literature review findings on car-following models, behavioral components (such as situation awareness, mental workload, and level of activation), experimental techniques, and existing biobehavioral methodologies. The methodology is described in Chapter 3, while the data collection procedure is presented in Chapter 4. Chapter 5 presents the process followed during data fusion and analysis. Chapter 6 then presents the results with respect to the various driving tasks. The process of developing and validating the biobehavioral IDM is detailed in Chapter 7. Conclusions and future research are presented in Chapter 8.

Chapter 2 Literature Review

This section provides a detailed review of some of the existing car-following models, especially those that have been used to incorporate some sort of biobehavioral architecture. This chapter also includes literature related to the definitions of several biobehavioral parameters, their measurement methods, and their relationship. Literature was obtained from several journal articles, theses, and publications. Online resources such as Google Scholar, ScienceDirect, University of Kansas (KU) Library resources, WorldCat, and Transportation Research International Documentation (TRID) were used.

2.1 Driver Behavior Models

Driver behavior models have significantly evolved from the first established Greenshields single regime model. The Greenshields model is a starting point for several other more complex traffic flow models such as the Pipes, Lighthill–Whitham–Richards (LWR), Gas kinetic (GK), Edie, Newell, and Drake, listed in a chronological order (Wageningen-Kessels et al. 2015).

Car-following models are an important sub-category of traffic flow. The concept of car-following was first introduced by Pipes in 1953. In 1958, a stimulus-response based approach was developed by Gazis-Herman-Rothery (GHR) in the General Motors laboratories (Saifuzzaman & Zheng 2014). The GHR model relied on a few inaccurate assumptions such as the following driver being able to accurately perceive small changes in speed and react to changes in speed even at very large headways. The need for a more adaptive model that better depicts the car-following behavior led to the establishment of psycho-physical models, that incorporate a certain level of human perspective. This establishes a more realistic approach to model traffic, considering that vehicles are controlled by humans with varying physical and mental restraints.

A discussion consisting of existing psycho-physical models and a few other car-following models such as the intelligent driver model and human driver model are presented in the sections that follow.

2.1.1 Psycho-Physical Car Following Models

Psycho-physical models, as the name suggests, incorporate both psychological and physical dynamics of drivers into the car following algorithms. They are entirely based on how drivers react to the actions of the lead vehicle and assume similar perception thresholds for all drivers (Schulze & Fliess 1997). This major assumption fails to consider the behavior and driving preferences of the individual operating the vehicle. For example, some individuals prefer maintaining shorter headways and accelerate more rapidly, affecting the overall flow and throughput of the roadway. This section presents a detailed review of the existing psycho-physical car following models and their mechanics.

2.1.2 Wiedemann (VISSIM)

This is one of the most well-known psycho-physical model and it acts as the foundation behind the car following algorithm in VISSIM. After first being established in 1974, the model has been constantly modified and calibrated to suit various scenarios.

The Wiedemann model considers six main thresholds as shown in figure 2.1. AX: The desired bumper to bumper spacing between two successive standstill vehicles; BX: The minimum desired headway expressed as a function of AX, speed, and distance; Closing delta velocity (CLDV): Deceleration resulting from the application of brakes because speed of the vehicle is greater than the leader; SDV: The point at which the driver perceives a lead vehicle travelling at a slower velocity; OPDV: The point during a drive when the driver realizes that

he/she is traveling slower than the lead vehicle and starts to accelerate; and SDX: Perception threshold to model maximum preferred following distance (Saifuzzaman & Zheng 2014).

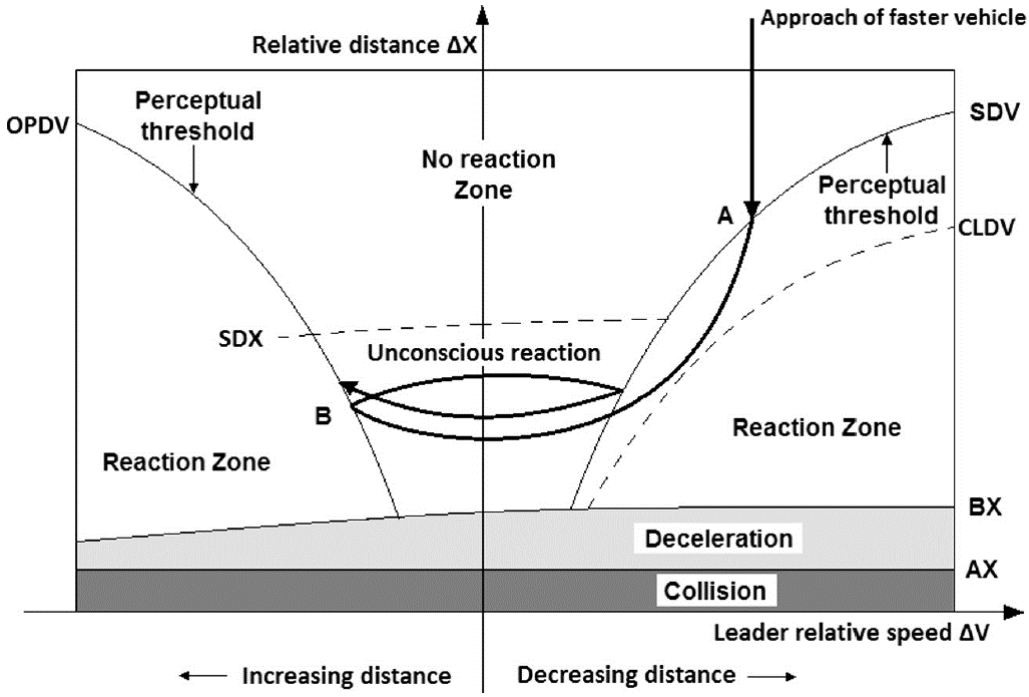

Figure 2.1 Wiedemann car-following model (Wiedemann 1974)

The dark line in Figure 2.1 shows the path followed when a fast-moving vehicle approaches a slow leader. The fast-moving vehicle will approach the slower leader until the perpetual threshold of deceleration is reached (SDV), as shown by point A. At this point, the driver of the fast-moving vehicle applies the brakes and decelerates in order to match the velocity of the leader (Saifuzzaman & Zheng 2014). The zone of unconscious reaction is reached because it is very difficult to accurately predict the speed of the lead vehicle, causing an increase in the headway between the two vehicles. However, when the OPDV threshold is reached (point B), the driver realizes he/she is traveling slower than the leader and starts to accelerate. This process is assumed to continue until the destination is reached unless coupled with a lane-

changing model. Another iteration of the Wiedemann model was also developed specifically to address driving behavior in a freeway facility (Wiedemann 99). Wiedemann 99 also has nine calibration parameters that allow for a more user adjustable model.

In 1998, Fancher and Bareket, proposed a new space known as the “comfort zone” to the Wiedemann model. This zone acts as a threshold for the desired spacing acceptable by the driver as a result of being unable to accurately perceive speed differences (Saifuzzaman & Zheng 2014).

2.1.2.1 Fritzsche (Paramics)

The Fritzsche model is a psycho-physical model first established in 1994. The model has been incorporated in traffic simulation software such as Paramics and is capable of introducing human perception to the car-following (Olstam 2004). There are six main thresholds for this model and they include: perception of negative speed difference (PTN), perception of positive speed difference (PTP), desired speed (AD), risky distance (AR), safe distance (AS), and braking distance (AB). The thresholds together form five regions: free driving, danger, following I, following II, and closing in, as shown in Figure 2.2. Each region captures a specific aspect of car-following as experienced by the driver. The Fritzsche model assumes that a driver will only decelerate when in “danger” or “closing in” to the lead vehicle (Saifuzzaman & Zheng 2014).

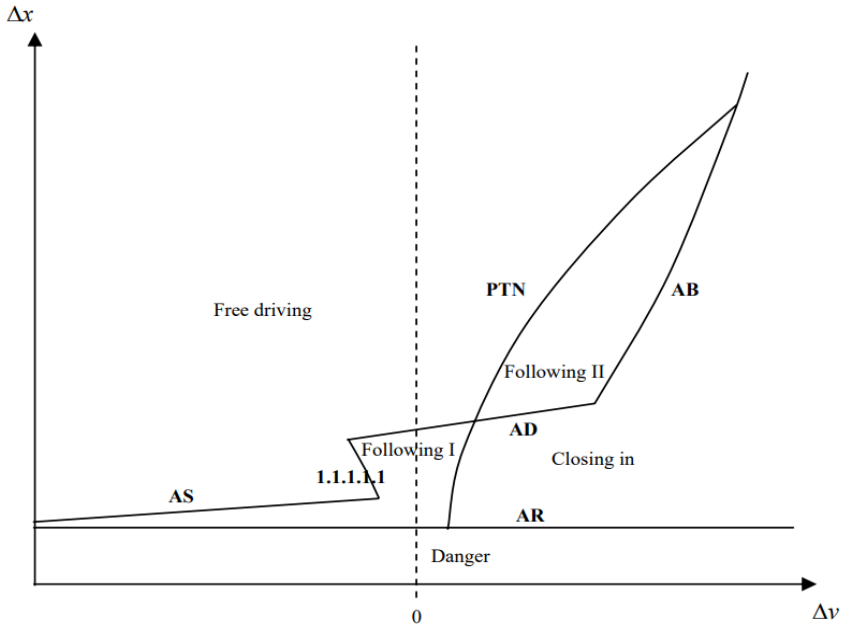

Figure 2.2 Fritzsche car-following model (Olstam 2004)

2.1.2.2 Urban Traffic Psycho-Physical Model

The urban traffic model was established by Schulze and Fliess, in 1997. The phase diagram of the model is shown in Figure 2.3 and can be interpreted as a combination of the Wiedemann and the Fritzsche car-following models. The phase diagram shows seven defined regimes namely: Free driving I, Free driving II, Approximating I, Approximating II, Following I, Following II, and Danger. The green line shows the trajectory of the following vehicle with respect to the changes in the driving regimes.

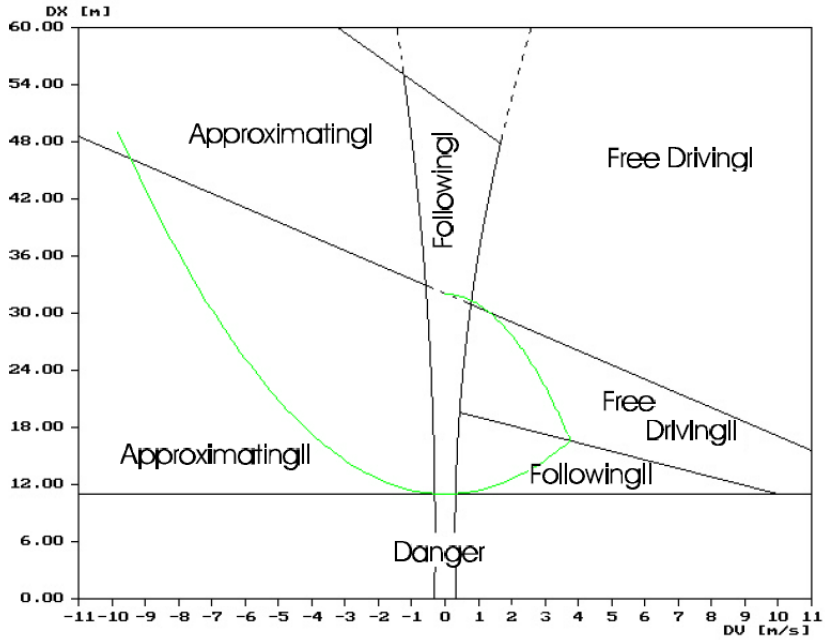

Figure 2.3 Urban traffic psycho-physical model (Schulze & Fliess 1997)

2.1.3 Intelligent Driver Model (IDM)

The IDM model is one of the most commonly used microscopic car-following models. The simplicity of this model with respect to the fewer number of parameters available, makes it easy to apply and calibrate (Hoogendoorn et al. 2012). The IDM captures both the desired speed and desired headway of the driver as shown in equation 2.1 (Saifuzzaman & Zheng 2014).

$$a_n(t) = a_{max}\left[1 - \left(\frac{v_n(t)}{v_0(t)}\right)^{\delta} - \left(\frac{s^*{}_n(t)}{s_n(t)}\right)^2\right] \tag{2.1}$$

$$s^*{}_n(t) = s^*\big(v_n(t), \Delta v_n(t)\big) = s_0 + s_1\sqrt{\frac{v_n(t)}{v_0(t)}} + T_n v_n(t) + \frac{v_n(t)\Delta v_n(t)}{2\sqrt{a_{max} b_{des}}}$$

Where,

$a_n(t)$ is the acceleration of the vehicle at time t

a_{max} is the maximum acceleration of the vehicle

$v_0(t)$ is the desired speed

$v_n(t)$ is the actual speed at time t

$\Delta v_n(t)$ is the approaching rate at time t

$s^*_n(t)$ is the desired minimum gap between two vehicles

s_0 is the minimum spacing at standstill

$s_n(t)$ is the spacing between two vehicles

b_{comf} is the comfortable deceleration

T_n is the desired time headway

δ characterizes how acceleration decreases with speed

Researchers studying the IDM have established typical values for city and highway settings (Kesting & Treiber 2013). However, these values can usually be tweaked within the constraints to provide a better calibrated model. A summary of typical values along with model constraints are shown in Table 2.1.

Table 2.1 Typical IDM Constraints (Kesting & Treiber 2013)

Parameter	**Typical City Values**	**Typical highway values**	**Constraints**
Desired speed, v_0	15.0 m/s	33.3 m/s	1 to 70 m/s
Time headway, T_n	1.0 s	1.0 s	0.1 to 5 s
Minimum spacing, s_0	2 m	2 m	0.1 to 8 m
Acceleration component, δ	4	4	1 to ∞
Maximum acceleration, a_n	1.0 m/s^2	1.0 m/s^2	0.1 to 6 m/s^2
Comfortable deceleration, b_{comf}	1.5 m/s^2	1.5 m/s^2	0.1 to 6 m/s^2

The developers of the IDM, Kesting and Treiber, suggested modification to the model that would improve its predictive capabilities by using external visual indicators such as brake lights, turn signals, tailgating, and head light flashes. An example of a binary input to replicate car-following behavior when the brake lights of the lead vehicle are activated and the acceleration ($\dot{v}_l$) is less than the acceleration of the follower (a_c) is shown in equation 2.2

$$Z_b = \begin{cases} 1 & \dot{v}_l < a_c, \\ 0 & Otherwise. \end{cases} \tag{2.2}$$

A typical value of a_c is -0.2 m/s^2 and it corresponds to the rate of change of velocity when neither the brakes or throttle is applied (vehicle decelerates uniformly) (Kesting & Treiber 2013). Other visual indicators can also be individually represented in similar equations.

A limited number of papers also discuss incorporating behavioral parameters into the IDM. In 2005, Fuller introduced the task capability interface (TCI) model to study the effects of task demand on risk-taking. Hoogendoorn et al. in 2012 combined the task-capability interface model with the IDM to predict changes to driving parameters. Figure 2.4 shows the TCI model that weighs the balance between the capability of the driver (C) and the demand of the task (D).

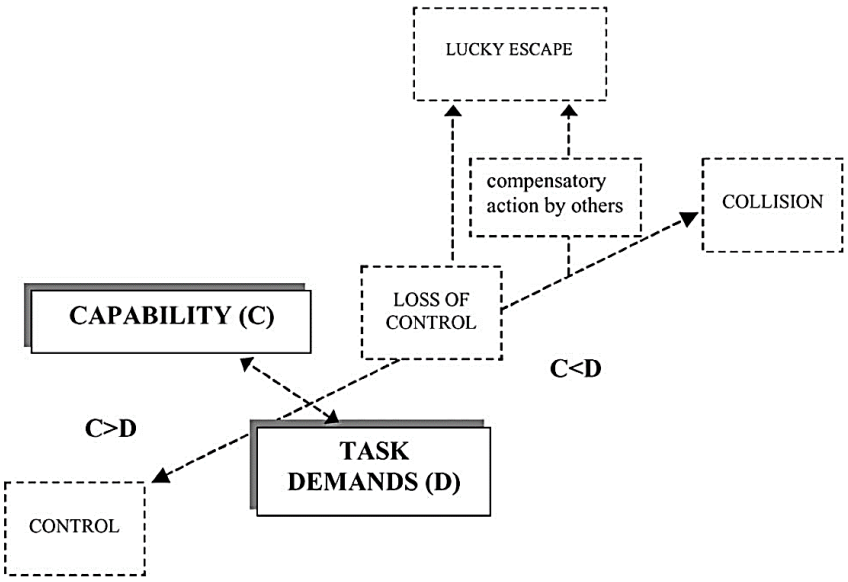

Figure 2.4 Task demand and capability interface (Fuller 2005)

The IDM was modified by incorporating the difference between task demand and the capability of the driver. The task demand and driver capability are applied as a factor scaled between 0 and 1. This implies that the difference between the task demand and capability will range from -1 to 1 as follows:

$$m_d(t) = m_t(t) - m_c(t)\,; \quad 0 < m_t(t) < 1, 0 < m_c(t) < 1, \text{and} -1 < m_d(t) < 1 \tag{2.3}$$

Where,

$m_t(t)$ is the task demand

$m_c(t)$ is the capability of the driver

$m_d(t)$ is the difference between task demand and driver capability

When the driver's capability is much greater than the demand of the task, the driver will perform better (task is easy), resulting in a negative value for the difference. A theoretical

framework of the methodology is shown in Figure 2.5. The driver tries to minimize the difference between varying task demand and capability by attempting compensatory actions like reducing speed. However, when compensatory actions alone are not sufficient to neutralize the difference, performance effects can be noticed (changes in mental workload and situation awareness) (Dee Waard & Brookhuis, 1991).

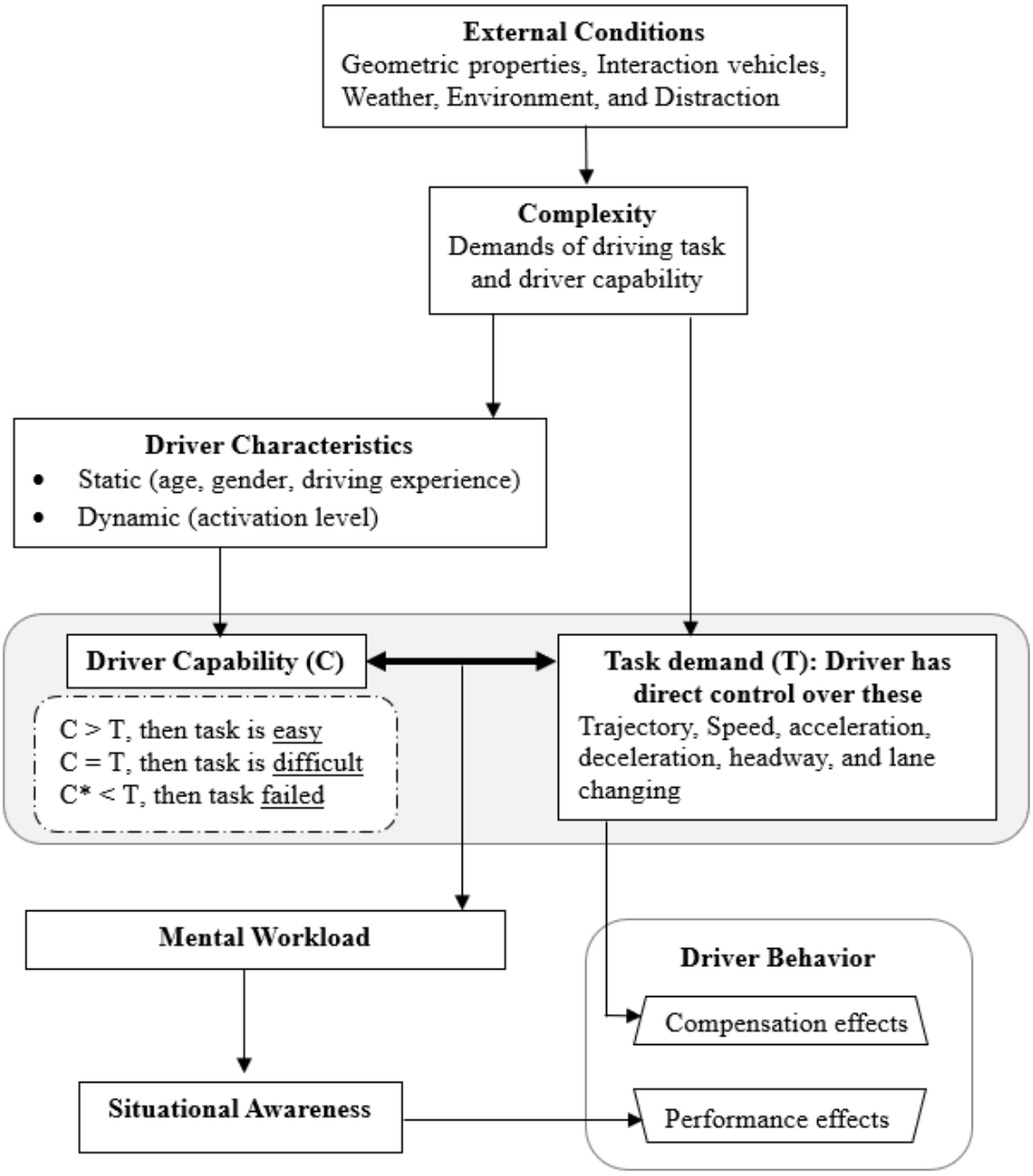

Figure 2.5 Framework developed by Hoogendoorn et al. (2012) to modify the IDM

The a_{max}, b_{comf}, $T_{n,}$ and v_0 parameters were modified to incorporate the difference between task demand and driver capability. When the difference between task demand and driver capability results in a negative value, the a_{max}, b_{comf}, and v_0 parameters increase because of the driver having a greater capability than the required task demand. However, T_n decreases because the driver is

assumed to be capable of accepting a smaller time gap as his/her capability is greater than the demand of the task. The difference between task demand and capability was incorporated as a cubic function as shown below in Equations 2.4-2.7.

$$a_{max}(t) = (-m_d(t)^3 a_{max}) + a_{max} \tag{2.4}$$

$$b_{des}(t) = (-m_d(t)^3 b_{max}) + b_{max} \tag{2.5}$$

$$v_0(t) = (-m_d(t)^3 v_0) + v_0 \tag{2.6}$$

$$T_n(t) = (m_d(t)^3 T_n) + T_n \tag{2.7}$$

Substituting equations 2.4, 2.5, 2.6, and 2.7 into equation 2.2 results in:

$$a_n(t) = ((-m_d(t)^3 a_{max}) + a_{max}) \left[1 - \left(\frac{v_n(t)}{(-m_d(t)^3 v_0(t)) + v_0(t)}\right)^{\delta} - \left(\frac{{s^*}_n(t)}{s_n(t)}\right)^2\right] \tag{2.8}$$

$${s^*}_n(t) = s_0 + ((m_d(t)^3 T_n) + T_n) v_n(t) + \frac{v_n(t)\Delta v_n(t)}{2\sqrt{((-m_d(t)^3 a_{max}) + a_{max})((-m_d(t)^3 b_{max}) + b_{\max})}}$$

After incorporating possible compensatory actions, the next step involves incorporating performance effects into the model. De Waard and Brookhuis established that performance effects and demand are related with an inverted parabola function. This relationship was used to establish the following equation, with α, β, and γ being parameters:

$$m_p(t) = -(\alpha m_d(t)^2 + \beta m_d(t) + \gamma) \tag{2.9}$$

Equation 2.9 shows that performance effects will have a greater magnitude if the capability of the driver is less than the demand of the task (if $m_d(t)$ is positive). The following equation

(2.10) shows the result of incorporating both performance effects and task-capability interface into the IDM:

$$a_n(t) = (1 - m_p(t))((-m_d(t)^3 a_{max}) + a_{max})\left[1 - \left(\frac{v_n(t)}{(-m_d(t)^3 v_0(t)) + v_0(t)}\right)^{\delta} - \left(\frac{{s^*}_n(t)}{s_n(t)}\right)^2\right] \quad (2.10)$$

Saifuzzaman et al. in 2015 performed extensive literature reviews to incorporate task difficulty using the TCI, developed by Fuller (2005), into car following models such as Gipps' and the IDM, where task difficulty is the product of the interaction between driver capability and task demand (Saifuzzaman et al. 2015). In the research performed by Saifuzzaman et al. (2015), an assumption that desired time headway selection is inversely proportional to the driver capability is made. When a driver selects to follow a smaller time headway than is usually desired, the ability to perform an evasive maneuver in case of an emergency is reduced, thus making the task difficult and uncomfortable. In general, if a driver elects a smaller desired time headway (assuming drivers are a good judge of their risk and discomfort), he/she can be categorized as more capable than someone with a larger time headway (Saifuzzaman et al. 2015).

$$TD_n(t) = \left(\frac{V_n(t-\tau'_n)\tilde{T}_n}{(1-\delta_n)s_n(t-\tau'_n)}\right)^{\gamma} \quad (2.11)$$

$$\tau'_n = \tau_n + \varphi_n$$

Where,

$TD_n(t)$ represents the task difficulty perceived by the driver *n* at time *t*;

s_n is the spacing between two vehicles (front of follower to rear of leader);

$\tilde{T}_n$ is the desired time headway;

V_n is the speed of the subject vehicle;

δ_n is a risk parameter;

γ is the driver sensitivity parameter towards task difficulty level;

τ_n is the reaction time of the driver;

φ_n is the increase in reaction time as a result of increased difficulty; and

$\tau'_n$is the modified reaction time.

The parameter δ_n captures the risk perceived by drivers (usually less than 1). A positive number indicates that the driver perceives the risk associated with reduced capability. However, a negative parameter indicates that the driver underestimated the risk. Also, the modified reaction time (τ'_n) captures the change in reaction time associated with varying task difficulty.

The result of incorporating equation 2.11 into the IDM is shown in equation 2.12.

$$a_n(t+\tau'_n) = a_{max}\left[1 - \left(\frac{v_n(t)}{v_0(t)}\right)^{\delta} - \left(\frac{s^*_n(t) * TD_n(t+\tau'_n)}{s_n(t)}\right)^2\right] \quad (2.12)$$

The implementation of models that depend on desired measures such as speed, spacing, and headway, has a limitation that these measures cannot be readily observed in nature (Saifuzzaman & Zheng 2014). A correlation has to be made in order to depict how the desired measures are affected by changes in human factors such as mental workload, situation awareness, and level of activation. In this study, the focus was to modify Hoogendoorn's framework and establish a methodology to capture/incorporate the compensatory and performance effects resulting from an imbalance in task demand and driver capability.

2.1.4 Human Driver Model (HDM)

The HDM was first proposed by Treiber et al. in 2006. It incorporated four extensions in terms of finite reaction times, imperfect estimation capabilities, spatial anticipation, and temporal anticipation to the IDM (Trieber et al. 2006). The model is based on the reaction time and the number of vehicles ahead for which the drivers can anticipate spatial information. Figure 2.6 shows the relationship between the reaction time and anticipated vehicles on traffic regimes, where abbreviations are oscillating congested traffic (OCT), homogeneous congested traffic (HCT), moving and pinned localized clusters (MLC/PLC), and triggered stop-and-go (TSG). It can be seen that the greater the number of vehicles anticipated, the more the reaction time available to mitigate a crash. Anticipation is especially useful in the TSG regime, where predicting behavior of more lead vehicles can be useful to avoid crashes.

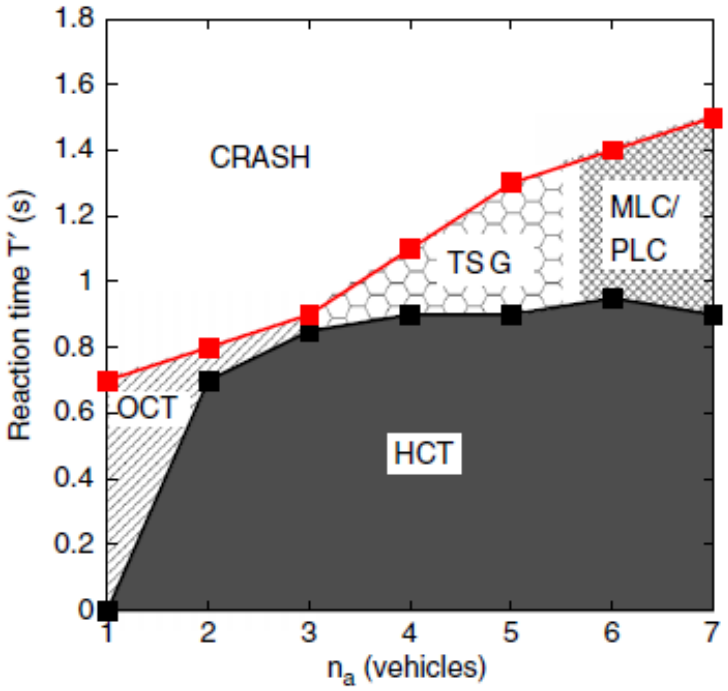

Figure 2.6 Regimes of the HDM

2.2 Driver Classification

Classification of drivers is a strategy used to easily group individuals based on common traits, style, and characteristics (Murphey et al. 2009, Feng et al. 2017). This makes establishing constraints to strategically categorize a sample/population easier and more efficient, especially when developing a model, than individual traits that have numerous unique variables. The number of classes can be pre-determined by the researcher or post-determined based on sample/population characteristics.

Several studies have been able to categorize participants/drivers based on their behavior and driving style. Kondyli, in 2009, classified drivers using three behavioral types: aggressive, average, and conservative, where the aggressive driver tends to drive at high speeds (15 mph over speed limit), perform six discretionary lane changes, short merging, and shows no remorse when cutting individuals off. The average driver was categorized as one that drives at speeds not

exceeding 10 mph over the speed limit and performs five discretionary lane changes. A conservative driver, on the other hand, would demonstrate more cautious maneuvers when lane changing, maintain longer headways, and not drive in excess of 5 mph over the speed limit (Kondyli & Elefteriadou 2011). Participants were categorized using field observations and background surveys.

Lin et al. (2006) also carried out a study, using a virtual reality driving simulator, to classify ten drivers by analyzing physiological measures in response to an unexpected obstacle. Drivers were classified into two categories, aggressive and gentle, based on driving trajectory and steering deviation. Event-related potentials (ERP) were then extracted and compared to the driving measures (Lin et al. 2006). A noticeable power difference at 10Hz and 20Hz was observed between aggressive and gentle drivers.

A study by Murphey et al. (2009) used jerk (defined as the rate of change of acceleration and deceleration) analysis to predict driver's style classification using the Powertrain System Analysis Toolkit simulation program. Four categories of driving style were established: 1) calm: anticipates other road user's movements and avoids hard acceleration/deceleration, 2) normal: drives with moderate acceleration/deceleration, 3) aggressive: drives with abrupt changes in acceleration and braking, and 4) no speed: vehicle not moving (Murphey et al. 2009). The calm driver is classified to be the most fuel-efficient. An algorithm capable of predicting driver class based on fuel efficiency and jerk parameter was developed. A similar study was conducted by Feng et al. (2017) using longitudinal jerk to identify aggressive drivers. Driving data from a previously conducted study was randomly sampled to obtain profiles of 88 drivers. Drivers were classified using acceleration, jerk, and gas pedal travel parameters. Two classifications were used: aggressive and normal (Feng et al. 2017). The two groups were then further examined

using driving behaviors such as speeding, tailgating, and risk of crash. The studied concluded that the aggressive group consisted mostly of young male drivers and had a higher jerk (20-30 years old).

Manjunatha and Elefteriadou (2019) performed a study that involved classifying participants through a cluster analysis based on individual mental workload and situation awareness. The result was two distinct clusters A and B. The properties of the participants from the two clusters were then compared to the responses from the pre-screening questionnaire. Individual properties were age, gender, driving frequency, take joy in driving, aggressiveness, accident history, and traffic violation tickets issued. The comparison showed that individuals in group B, with lower mean age, enjoyed driving but received more traffic violations (Manjunatha & Elefteriadou 2019).

In this study, the number of categories will be dependent on what is observed from the drive (speed, headway, jerk) and survey questionnaires (age, experience, accident history, traffic violations), along with the mutual behavioral traits (mental workload, situation awareness, level of activation) of the selected participants.

2.3 Situation Awareness, Mental Workload, and Level of Activation

This section summarizes key definitions of the level of activation, situation awareness, and mental workload. It also discusses the experimental techniques that can be used to collect the respective data.

2.3.1 Situation Awareness (SA)

Situation awareness (SA) has been defined as the ability to perceive (Level 1 SA), comprehend (Level 2 SA), and project future status (Level 3 SA) of elements in an environment (Endsley 1995). A common misconception is that SA is only affected by perception (ability to

locate an element). However, comprehension of the situation and the driver's ability to project future scenarios are more significant factors where as being able to identify an element without placing where it fits and how it affects an environment is not valuable. The SA of a driver is known to affect his/her capability during a task in that high SA generally implies a more alert driver unless affected by cognitive overload (Endsley, 1995). Figure 2.7 shows the Endsley, 1995 model developed to process how SA is related to decision making and performance.

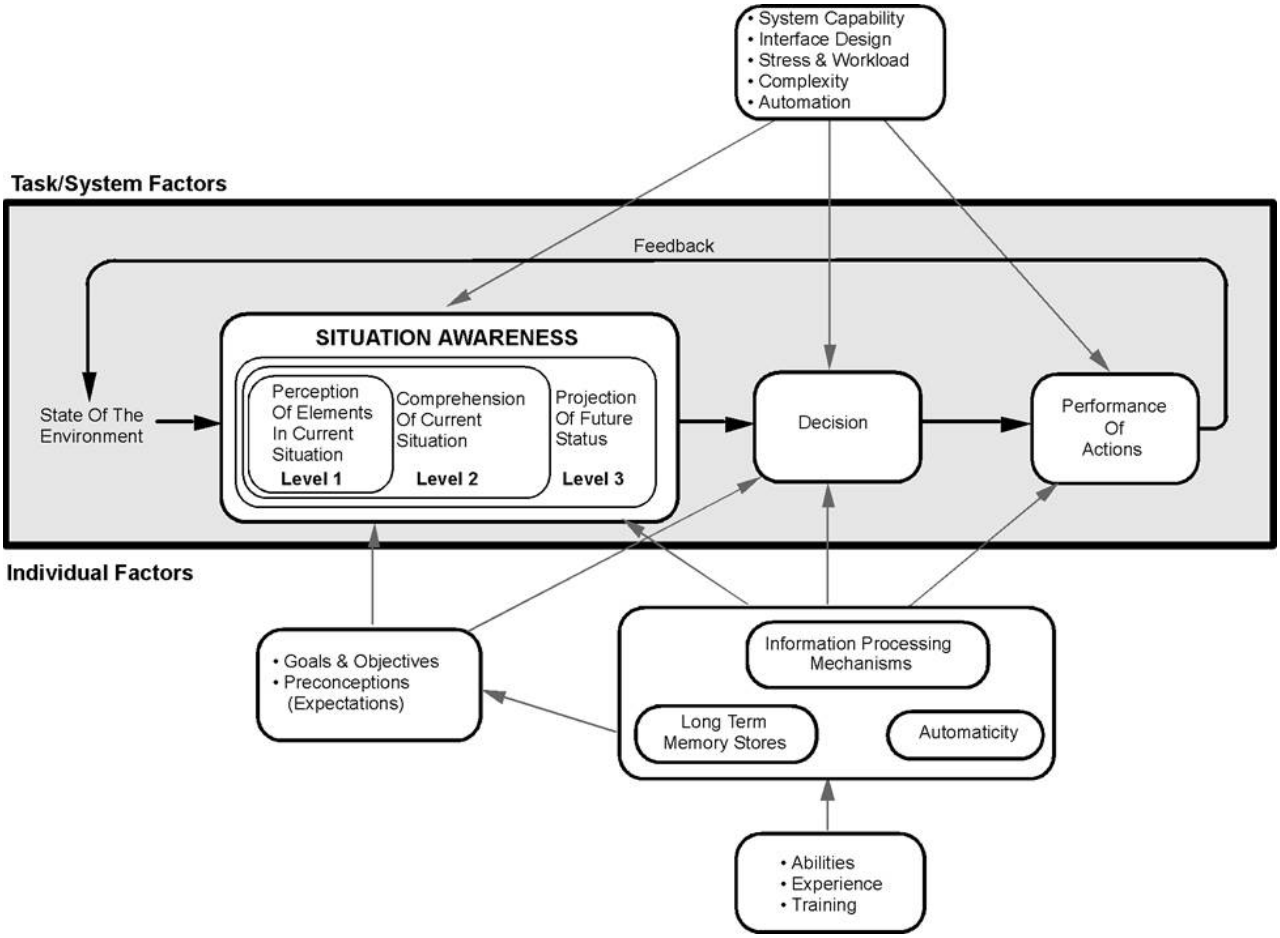

Figure 2.7 Levels of SA in relation to decision-making and performance (Endsley 1995)

SA can be measured using several techniques. They can be divided into freeze probe, real-time probe, self-rating, observer-rating, and physiological techniques. A short description about each technique is provided in the sections that follow.

2.3.1.1 Freeze-Probe Technique

These are typically used in a simulation environment, where a scenario is paused and queries about the situation are asked. Usually, all operator displays are blank and questions related to participant alertness are administered (Salmon et al. 2006). A commonly used freeze probe technique is the situation awareness global assessment (SAGAT) developed by Endsley in 2000. The SAGAT consists of queries designed to assess all three levels of SA. Freeze probe techniques are generally considered as highly intrusive as they interfere with the primary task. However, there has been no conclusive evidence regarding their level of intrusiveness (Salmon et al. 2006).

2.3.1.2 Real-Time Probe Technique

This involves administering the questions targeted at establishing SA without pausing/freezing the simulation. During the task, participants are presented with queries pertinent to the environment and their answers along with response times are noted. A commonly used real-time probe technique is the situation present assessment method (SPAM). Although generally regarded as less intrusive than the free-probe technique, no conclusive evidence exists to support this claim (Salmon et al. 2006).

2.3.1.3 Self-Rating Technique

This technique involves administering questionnaires about SA after the completion of a task. They are relatively easy and cheap to administer. A commonly used self-rating technique is the situation awareness rating technique (SART). SART is a multidimensional scaling technique

that consists of ten subscales each rated from one (low) to seven (high). The subscales include: Instability of situation, variability of situation, complexity of situation, arousal, spare mental capacity, concentration, division of attention, information quantity, information quality, and familiarity. These ten subscales are categorized in three domains: attentional demand (D), attentional supply (S), and understanding (U). Situation awareness is then calculated by U – (D – S) (Selcon & Taylor 1989).

Although SART is a widely used measure of SA, comparisons of the efficiency of SAGAT (best known measure of SA) and SART exist. A study by Endsley, in 2000, reported significant correlation between overall SART scores and level 1 SAGAT. However, a study carried out by Salmon et al. (2009) showed no correlation between SART and SAGAT or performance measures. This raises concerns about self-rating techniques being susceptible/biased to the last performed task.

2.3.1.4 Observer-Rating Technique

This technique requires the presence of an expert to judge the level of SA of the participant. The observer provides a score based on the tasks performed in the field. The main advantage of this technique is that it is not intrusive. However, multiple observers (experts in SA) are required to ensure accurate results without being subject to individual observer bias. Also, the technique is relatively expensive due to the time required from several observers (Salmon et al. 2006).

2.3.1.5 Physiological Technique

A typical physiological technique used to measure SA is eye-tracking. SA can be measured using gaze overlays, fixation patterns, and saccades. Studies have shown that analyzing fixation patterns and saccades can provide information on the relation between

duration of fixation and the perception of objects/words (Just & Carpenter 1980). Eye-trackers are ideal for a simulation environment and provide real-time continuous data. Also, they are non-intrusive and do not affect the performance of the primary task (Salmon et al. 2006). However, devices and relevant software can be very expensive.

A study by Coyne and Sibley, in 2015, used eye-tracking to establish SA in an unmanned aerial vehicle study. Twenty participants were recruited to carry out military training missions at the Naval Research Laboratory involving identifying vehicles and carrying out target assignments through a map. The SmartEye Pro 6.1 was used to track eye movements and gaze at 60Hz along with the SA probe technique (Coyne & Sibley 2015). The study concluded that as task demand increased, participants spent less time looking at their map targets, thus negatively impacting their target assignment. The study showed, in both instances (eye tracker and probe), that SA decreased with an increase in task demand (Coyne & Sibley 2015).

2.3.2 Mental Workload (WL)

Mental workload, also known as cognitive workload, can be defined as the allocation of attention based on the mental resources available for information processing (Patten et al. 2006). The primary role of any driver is to safely navigate from point A to B. However, depending on environmental conditions, emergency situations that require sudden maneuverability, and driver characteristics like age, experience, and behavior, mental resources required by the driver to safely carry out the primary task of driving vary. These changes in WL can be used to represent how the driving performance is affected. Workload has been measured using subjective, performance, and physiological methods. A brief description of each of these measures is discussed below along with their respective sensitivities to task demand.

2.3.2.1 Subjective Measures

Subjective measures are a data collection technique that uses questionnaires and surveys to pose questions to participants. Participants reply based on their individual experience on the topic in question. Questionnaires and surveys can be administered before, during, or after the study. The three most commonly used techniques to measure subjective WL are the NASA- task load index (TLX), driver activity load index (DALI), and the rating scale mental effort (RSME). Each technique is briefly discussed in the sections that follow.

2.3.2.1.1 NASA- Task Load Index (TLX)

The NASA-TLX is one of the simplest and the most widely used subjective measures. The NASA-TLX questionnaire calculates WL experienced by participants as a weighted average of six subscales: mental demand, physical demand, temporal demand, performance, effort, and frustration experienced during the task, each on a 20-point scale ranging from "very low" to "very high" (Stojmenova & Sodnik 2015). Participants are then required to assign a weight, from 0 to 5, to a pair of subscales shown on flash cards (6 subscales resulting in 15 possible pairwise combinations). It is usually administered after the completion of a task or event and has been used in several WL studies. However, it has been shown that the answers to the questionnaire are strongly influenced by the last task performed (Stojmenova & Sodnik 2015). Also, the NASA-TLX does not provide time-varying data but instead relies on participant's memory and ability to recall events that have already occurred.

2.3.2.1.2 Driver Activity Load Index (DALI)

The NASA-TLX was specifically designed to capture the WL of pilots. However, a modified version known as DALI was developed by Pauzie around 1994 to assess WL related to driving with and without secondary tasks. The DALI replaces some subscales from the NASA-

TLX not applicable to driving. The six subscales for the DALI are: effort of attention, visual demand, auditory demand, temporal demand, interference, and situational stress (Pauzie et al. 2008). Although the DALI was developed for driving, NASA-TLX is still more commonly cited and used to measure WL in simulation studies (Stojmenova & Sodnik 2015).

2.3.2.1.3 Rating Scale Mental Effort (RSME)

The RSME is conceptually similar to the NASA-TLX and DALI, however, it consists of a nine-point scale ranging from "absolutely no effort" to "extreme effort" (Sartang 2017). Participants mark their level of effort after completion of each task. It is relatively easier and cheap to use. However, not a lot of studies utilize RSME to compute WL with respect to driving thus not favored over the NASA-TLX.

2.3.2.2 Performance Measures

Performance measures are based on changes to variables collected from the drive. Examples of performance measures during the drive include: lane keeping ability, speed control, and car-following ability (De Waard 1996). De Waard in 1996 concluded that varying WL results in changes to speed, car-following parameters such as mean headway and standard deviation of the headway, and lane keeping parameters such as standard deviation of lateral position (SDLP) and steering wheel movement (SDSWM). A couple of studies also found that an increase in WL significantly increased the time to traverse the same route (De Waard 1996). The main issue with performance measures is that they vary by task and the same measure sometimes cannot be used as a basis for comparison of WL (Sirevaag et al. 1993). For example, a driver might choose to slow down when observing a crash near the roadway, however, when driving through a work zone he/she might choose to focus more on keeping in their lane (SDLP). Studies summarized by De Waard (1996), have shown varying results with respect to SDLP and

SDSWM. In some studies, as WL increased, the SDLP increased (more lateral variability) while in others it decreased. However, this could be because of the layout of the driving scenarios used. (Some regions were on a horizontal curve and required lane changing, thus introducing ambiguities in the data). Hence, extra caution must be observed during the planning and design of the experiment (scenarios). Ideally, performance measures should be coupled with other WL measures to provide a more holistic picture.

2.3.2.3 Physiological Measures

Physiological measures are used to assess mental workload from reactions within the human body. This type of measure provides exact results without interaction from other variables other than those being examined (De Waard 1996). Participants also do not need to reflect and fill questionnaires, as data is continuous and readily available for the entire task. Most physiological measures focus on these four areas: heart, brain, eyes, and muscles. A brief description of measures in these areas is presented.

2.3.2.3.1 Heart

Electrocardiography (ECG) is primarily used in health care centers to monitor electrical activity in the heart and diagnose critical heart conditions such as attacks and arrhythmias. The ECG can be used to provide a continuous stream of data showing the impact of various driving tasks on the electrical activity of the heart expressed over a defined time period. ECG captures several variables than can be analyzed to assess mental workload and they include: heart rate (HR), heart rate variability (HRV), and Inter-Beat-Interval (IBI). Other devices such as heart rate monitors and chest straps can also be used to track changes to HR. However, they may be less accurate due to a lower sampling frequency. Both the ECG equipment and heart rate

monitors/chest straps are considered as intrusive techniques because electrodes or contact points must be placed on the participant.

Numerous researchers have utilized the ECG and HR monitors to study changes in WL. Kahneman et al. (1969) used ten volunteers to perform arithmetic tasks with three levels of difficulty. The study not only measured HR but also pupil diameter and skin resistance. The HR was recorded using a cardiotachometer with electrodes placed on the upper arms of participants (Kahneman et al. 1969). From the study, it was evident that there was an increase in the HR with an increase in question difficulty (with the most difficult question causing a change by up to 5 beats/min). However, the HR (beats/min) values were seen to peak much earlier than the pupil diameter (mm) and skin resistance (ohms).

Dahl and Spence in 1971 performed a similar study using thirteen categories of tasks (Initial resting, digit symbol, word list, recall, discrimination, color reading, color naming, strop color-word, white noise on, color word IR-RI, color work RI-IR with noise, Noise off, and final resting). The study consisted of 61 participants (three sample groups) and participants' task demand was measured using the Bergum's taxonomic analysis (9-point rating scale system to determine task demand) for each category. Not all groups performed all categories of tasks and HR was measured using a photocell transducer in two of the groups while the third used an ECG. The study showed that there was a significant correlation between the subjective score and mean HR of the participants. It was also seen that the HR increased almost linearly, with an increase in task demand (Dahl & Spence 1971). A summary of other studies listed by De Waard (1996) showed similar trends in mean HR. An increase in task demand is seen to cause an increase in HR.

2.3.2.3.2 Brain

Electroencephalography (EEG) is a clinical technique used to measure changes in electrical activity in the brain. The brain is a complex organ that controls most of the functions in the human body. The EEG device uses electrodes attached to the scalp of an individual to detect changes in electrical charges arising from the activity in the brain cells. The following paragraphs discuss the various regions of the brain and their functions. The EEG electrode positions corresponding to the regions of the brain are discussed.

The brain can be divided into six regions: frontal lobe, parietal lobe, occipital lobe, cerebellum, temporal lobe, and the brain stem, each responsible for different functions. The frontal lobe is the anterior-most region of the brain, located in the forehead. It is responsible for problem solving, emotions, response, reasoning, and consciousness. The parietal lobe is located at the same level behind the frontal lobe. The parietal lobe is responsible for controlling sensory functions such as voluntary movements, touch, and visual attention. The occipital lobe is the most posterior region of the brain and is responsible for anything related to vision. The cerebellum is located at the base, in line with the ears and is responsible for coordination and balance. The brain stem is located deep in the center of the brain and links directly to the spinal cord. Figure 2.8a and 2.8b show the different regions of the brain.

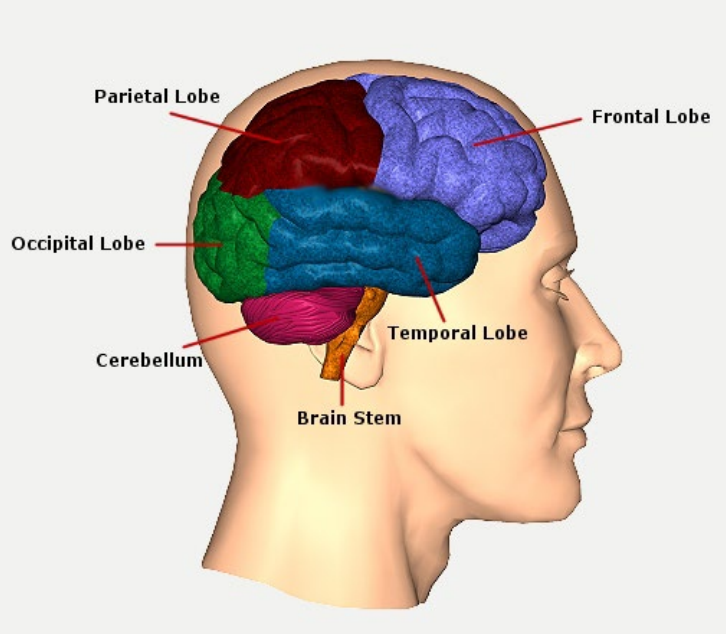

(a)

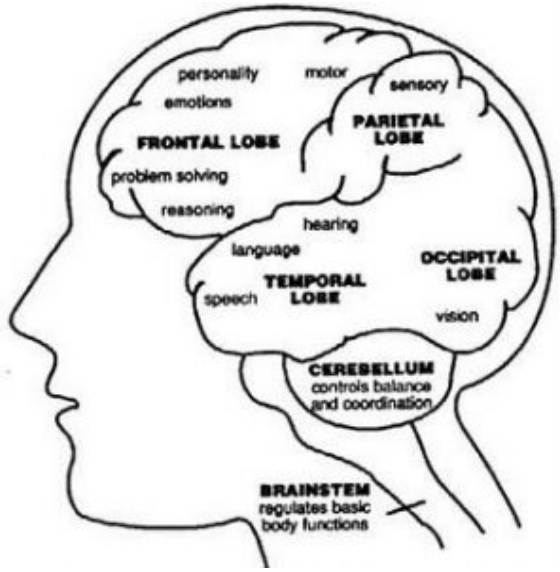

(b)

Figure 2.8 Regions of the brain (Lehr 2015)

The EEG electrodes are placed in positions shown in Figure 2.9. The first alphabet in each position refers to a region of the brain. For example: the frontal lobe is represented by the letter “F”, parietal lobe by the letter “P”, temporal lobe by the letter “T”, and occipital lobe by the letter “O”. Other letters such as “FP” represent the frontopolar and “A” represents the auricular (ear electrode). The number represents the hemisphere location of the brain, with even numbers located in the right and odd numbers in the left. The 10% and 20% refer to the distance between adjacent electrodes with respect to the front-back or right-left dimension of the skull.

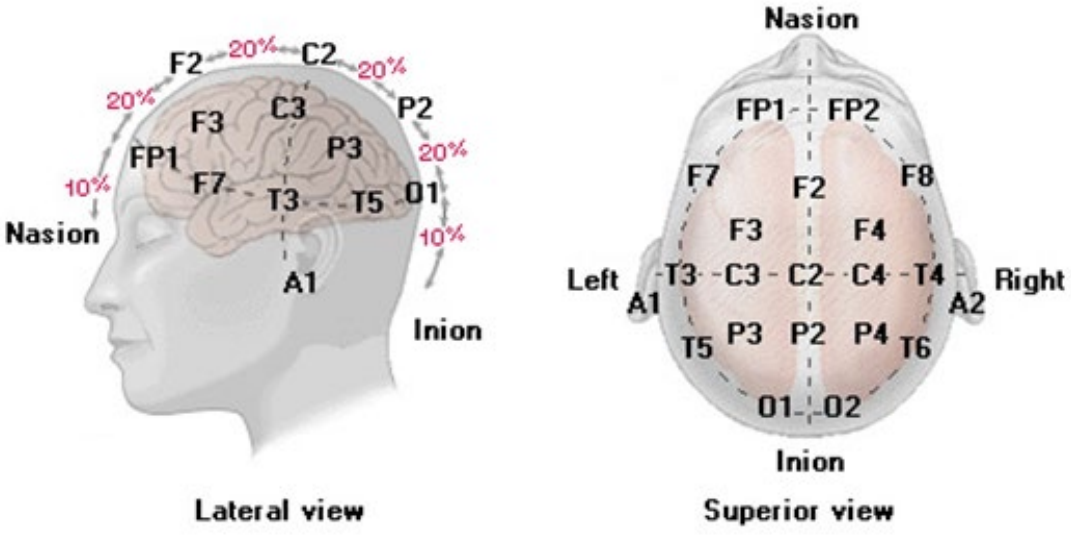

Figure 2.9 EEG electrode positions

The EEG provides two main ways of determining mental workload: extracting raw EEG data by synchronizing the timeline of the drive and using ERPs (Kincses et al. 2008). Analyzing the raw EEG signal can be complex and requires filtering noise from AC power lines (60Hz filter in the United States), blinking, and other muscle movements. The raw EEG signal can be typically separated into the following frequency bands using fast Fourier transformation: delta

(0.5-4Hz), theta (4-8Hz), alpha (8-13Hz), beta (13-40Hz), and gamma (>40Hz). Power spectrum analysis is the most common method to detect changes in mental workload through raw EEG signal (Walter 2015). Data is usually divided into epochs consisting of critical task moments. The power spectrum analysis provides insight into the signal power of the different frequencies with respect to the various regions of the brain (electrode positions). Studies have shown that the power of alpha band increases in the drowsy or more relaxed driver state while an increase in the power of beta band is associated with tension and cognition (Kim et al. 2014). A decrease in alpha band activity and an increase in theta band activity is usually associated with increased mental workload (De Waard 1996, Kramer 1991).

ERPs related to cognitive load are mainly associated with the P300 amplitude (usually peaks around 300ms or more), as several studies have used this as a reference to identifying changes in WL (Prinzel III et al. 2001). The P300 amplitude is sensitive to the participants expectancy disrupted by mental workload (Prinzel III et al. 2001). A summary of studies carried out by De Waard (1996) shows a decrease in P300 amplitude and an increase in latency, with increased task load.

The P300 amplitude can be further split into P3a (latency 250-280ms) and P3b (latency 280-500ms). Where, the P3a (novelty P300) is associated with re-orienting and attention shifting and the P3b is associated with cognitive processing (Light et al. 2010). A study by Causse et al. (2015) showed a decrease in P3b amplitude with an increase in WL as the high WL task requires more processing power/working memory than the low WL task. The drop in P3b amplitude at the PZ electrode of a participant is shown in Figure 2.10.

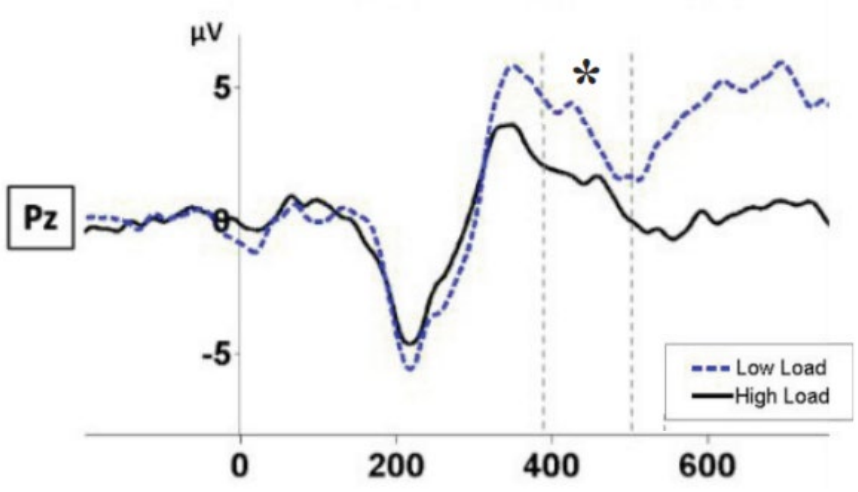

Figure 2.10 Effect of WL on ERP (Causse et al. 2015)

2.3.2.3.3 Eyes

Eye-tracking devices that track eye movement of the driver without disrupting the primary task of driving are very useful in determining the areas of focus of the driver. Some advanced devices are also capable of tracking pupil dilation—the phenomenon causing changes to the pupil diameter due to varying levels of cognitive workload, also known as task-evoked pupillary response (TEPR) (Strayer et al. 2013, Gangeddula et al. 2017). Several studies have shown that as cognitive workload increases, the diameter of the pupil increases (Hess & Polt 1964, Kahneman et al. 1969, Klingner 2010, Szulewski et al. 2014). Hess and Polt, using five test subjects ranging in age and educational qualification, carried out one of the first studies in 1964. Since advanced eye tracking devices did not exist at the time of the study, the researchers used an animation motion camera (essentially an older version of a video camera) to take multiple pictures of the test subject's face at equal time intervals, concentrating on the eyes (Hess & Polt 1964). Four mathematical questions ranging in difficulty were asked (vocally) and the pupil diameter recorded. The pupils were observed to reach a larger peak diameter, with increase

in difficulty of the mathematical problem. It was also seen that the pupil diameter increase ranged from 4% to 29.5% when compared to the non-stimulated pupil diameter, depending on the participant and question difficulty (Hess & Polt 1964).

Klingner, in 2010, carried out extensive studies on changes to pupil diameter using the Tobii 1750 eye tracker and the Neuroptics VIP-200 ophthalmology pupillometer as a reference instrument. The study first concluded that the Tobii eye tracker was not as precise as the Neuroptics ophthalmology pupillometer. However, the results from the Tobii eye tracker were still adequate to show variations in pupil diameter. The study also presented a visual take on the auditory stimuli presented by Hess and Polt. Mathematical problems varying in difficulty (easy, medium, and hard) were presented on a screen for a duration of eight seconds, before prompting a response (Klingner 2010). The participants were asked to attempt the questions to the best of their ability, without requiring the final answer to be correct. The results obtained are shown in Figure 2.11 (b), where pupils were seen to get to a larger peak diameter with increased question difficulty. Also, the pupil diameter increased more steeply with an increase in question difficulty (a reflection of cognitive workload). In this experiment, Klingner ensured to control the brightness and contrast of the visual cues as changes to these could cause pupil dilation and contraction. This aspect was carefully enforced in the scenario design of this research.

Figure 2.11 (a) shows the visual response of the human eye to an increase in cognitive workload.

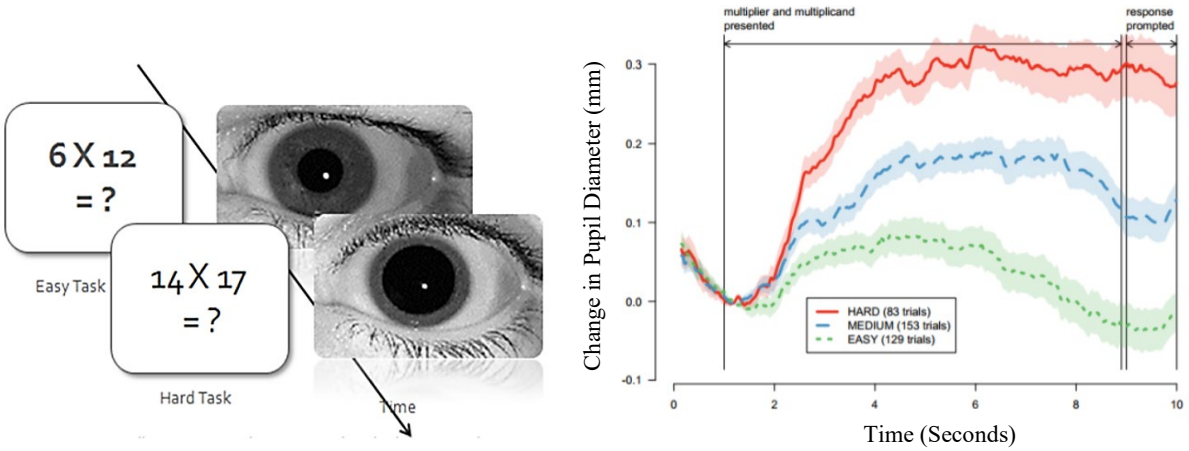

(a) (b)

Figure 2.11 WL on pupil diameter ((a)-Hossain & Yeasin 2014, (b)-Klingner 2010)

A study performed by Szulewski et al. in 2014, validated the results obtained by Klingner. Similar experimental setup and arithmetic problems were used. However, only two levels of difficulty (easy and hard) were tested. The results showed an added dimension to those obtained by Klingner, with easy questions causing a peak pupil dilation three seconds quicker than hard questions. However, maximum pupil diameter attained was still larger for hard questions than for easy questions (Szulewski et al. 2014). A study by Marquart and De Winter in 2015, consisting of thirty participants, validated the measurement of workload using pupillometry by comparing the data to that obtained using the well-established NASA-TLX questionnaire. However, the authors suggested using caution when tackling tasks that cause pupil reflexes due to light sensitivity. They also recommend using multiple measures (HR, EEG) to eliminate instances of extreme variability (Marquart & De Winter 2015).

This property of the pupils can be used to assess cognitive workload continuously throughout a drive. Advanced software tools have been developed by device manufacturers to analyze the observed changes and patterns in pupil dilation/contraction and compare it to

baseline conditions, identifying any changes resulting from the task. This can be used in simulation environment, to track changes in cognitive load experienced by the driver.

2.3.2.3.4 Coordination between Vision and Muscles

These measures typically require participants to react to a visual or sensory stimulus. Common measures include the peripheral detection task, the detection response task, and the ISO 17488.

The peripheral detection task (PDT) presents visual stimuli throughout various locations in a driving scenario. Stimuli are presented as small colored squares or circles. Participants' reaction time to detect and respond to the task by pressing a button usually located on the steering wheel (coordination between vision and muscle), is measured (Patten et al. 2004).

The detection response task (DRT) is a more refined version of the PDT and was primarily devised to determine the effect of a secondary task on WL. The DRT equipment presents frequent artificial stimuli during a task and records participant performance in the form of response time, hit rate, and miss rate (ISO 17488 2016). There are three types of DRT stimuli commonly used in studies. The head-mounted light-emitting diode (LED), fixed LED location mounted inside a vehicle, and a tactile electrical vibrator attached to the driver's shoulder (ISO 17488 2016). As the stimuli are presented, participants are required to acknowledge them using a micro-switch, typically attached to the thumb. Changes to the response time, hit rate, and miss rate of stimuli are analyzed to determine the intensity of WL being experienced. However, because both the PDT and DRT present simultaneous alternative tasks for the driver to complete, they compete with the primary task of driving and are thus not very effective in establishing actual WL.

The ISO 17488 (2016) presents several coordinated studies on mental workload and resource allocation. The studies show that an increase in hit rate and reduction in stimuli response time can be associated with lower mental demand, as performance with respect to the task is improved. Strayer et al. (2013 & 2014) compared the results of the DRT to other subjective (NASA-TLX) and physiological measures such as the EEG and HR, using both driving simulators and instrumented vehicles. The results showed that the DRT data is equally capable in tracking WL when compared to the other measures.

2.3.2.4 Sensitivity of the Various Measures

De Waard observed that some WL measures were more sensitive at a particular intensity of the task demand than others. This can be clearly observed in Figure 2.12. However, it can also be noted that most measures were only sensitive at high WL and not during low WL. De Waard concluded that one measure of WL might not be a sufficient representation for the entire task and multiple measures would provide a better basis for comparison.

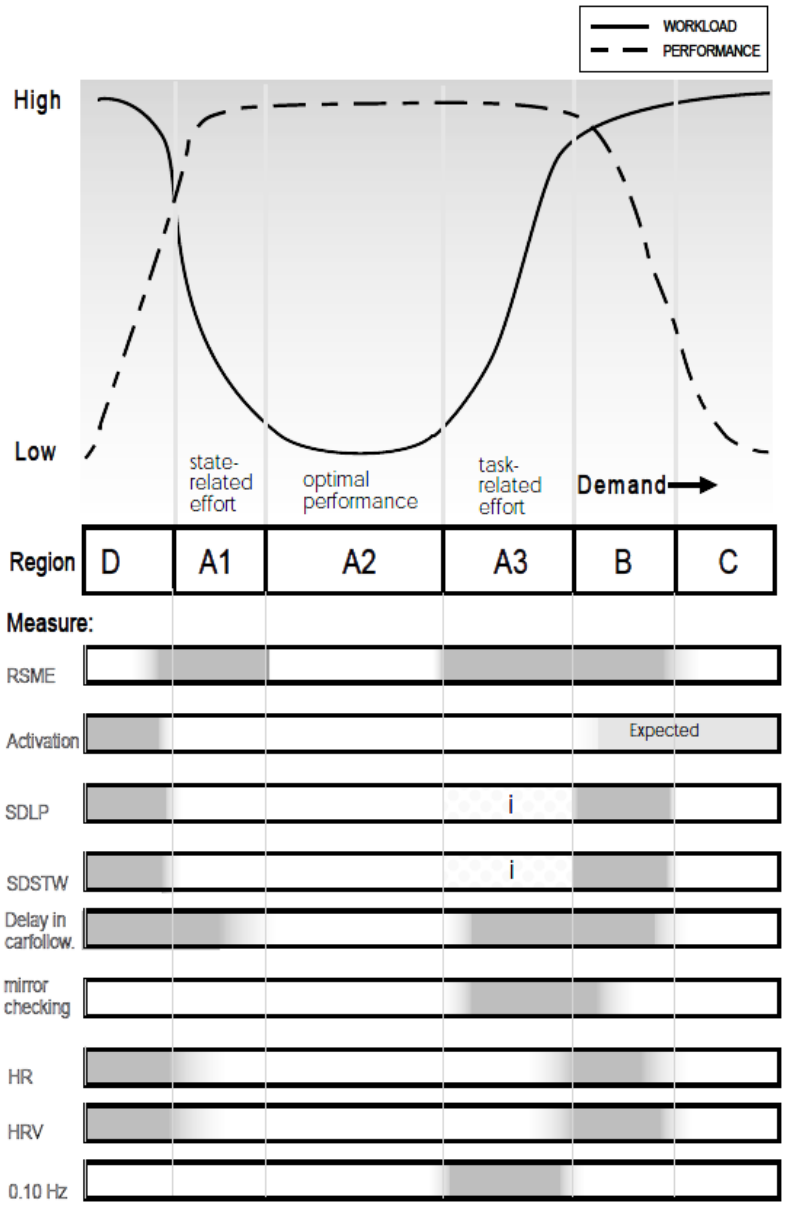

Figure 2.12 Sensitivity of workload measures (De Waard 1996)

Where, SDLP is the standard deviation of lateral position and SDSTW is the standard deviation of steering wheel movements.

2.3.3 Level of Activation (LA)

The level of activation or arousal has been identified by several researchers as a key measure of engagement, motivation, and enthusiasm involved in responding to a task. The LA was directly related to the ability of an individual to perform the task of driving (Tampere et al. 2009). However, the LA was not only affected by the primary task of driving, but also by secondary tasks such as cell phone use and operating the media controller or navigation system (Tampere et al. 2009).

De Waard and Brookhuis (1991), suggested measuring LA using the three classic EEG bands: theta, alpha, and beta, representing the frequency ranges 4-7 HZ, 8-13 HZ, and 14-30 HZ, respectively. To prevent susceptibility to isolated changes, De Waard and Brookhuis proposed combining the spectral power of all three bands (filtered and divided into epochs) using the formula $(\alpha+\theta)/\beta$ (De Waard & Brookhuis 1991). In 1995, Pope et al. identified the electrode positions P3, PZ (P2), P4, and CZ(C2), to capture the "engagement index" of a driver, also known as the LA. The results of this study were validated by Prinzel III et al. (2001). However, both Pope et al. (1995) and Prinzel III et al. (2001) used the inverse of the formula suggested by De Waard & Brookhuis (1991).

A study by Tejero and Choliz in 2002 used the EEG Fourier spectral power analysis suggested by De Waard and Brookhuis in a real-world driving study. Participants were required to drive 90 km on a highway while being monitored by researchers. The study showed that LA increased when speed varied, as opposed to keeping a constant speed. They concluded that the act of modifying speed creates a source of engagement, thus increasing the LA of the driver.

2.4 Relationship Between WL, SA, LA and Performance

In 1995, Endsley theorized four constructs that link SA and WL. They include:

- **Low SA with low WL**: Operator had little idea of what was happening due to inattentiveness or lack of motivation;
- **Low SA with high WL**: Tasks that require more processing capabilities from the operator might have to missing/overlooking of some elements in a given task (only a subset of information is processed along with incomplete perception);
- **High SA with low WL**: This state is what was ideally preferred by an operator, with information that could be easily comprehended without requiring high mental processing; and
- **High SA with high WL**: In this state, the operator was using more mental resources but was also successful at comprehending/adjusting to the situation.

Following these constructs, it is clear that SA and WL depend on the task, experiment design, and individual traits/behavior. A determent in SA was only expected when the operator was trying to attain SA and the demand of the task exceeds capability (Endsley 1995).

The relationship between WL and task demand was well established by several studies. De Waard suggested a U-function as shown in Figure 2.12, where WL initially started off at high and decreased as a task got familiar. As the task difficulty gradually increased, there might not have been any significant changes to WL until a threshold was reached (region A3). After, WL increased steeply with an increase in task demand (regions with high sensitivity and easy measurability of WL) and performance slump was recorded (De Waard 1996).

From Figure 2.13, it can be seen that as WL increased, the LA also increased . However, the relationship was not entirely linear.

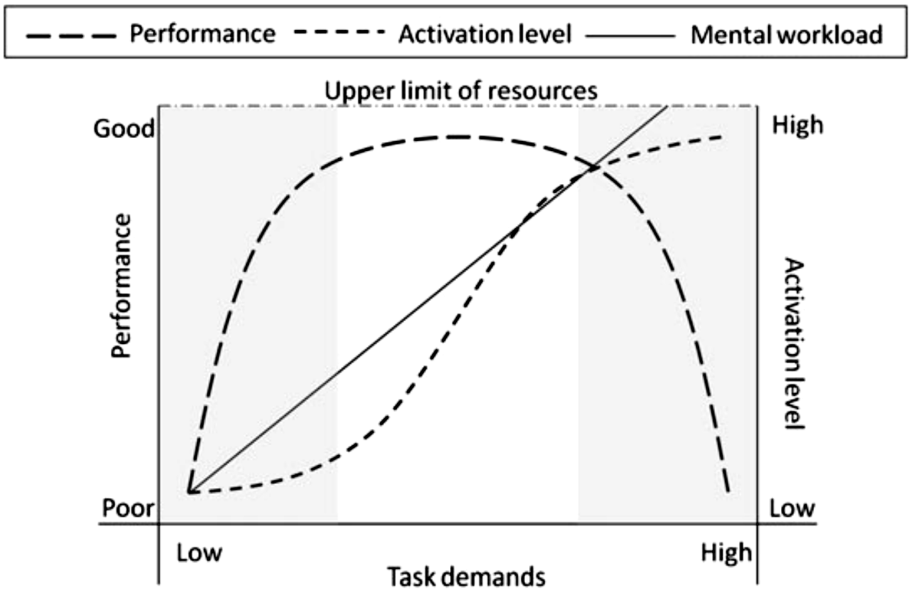

Figure 2.13 Relationship of WL, LA, and performance (Young et al. 2015)

In 2017, Zhang and Kumada studied the relationship between WL and mind wandering. The experiment was performed in a low-fidelity driving simulator. Forty participants drove a 25-minute scenario with car-following tasks. A real-time probe was applied randomly and participants rating of mind wandering was recorded. After the completion of the scenario, NASA-TLX was completed to establish the WL. The study also correlated the measured WL to performance measures such as the standard deviation of lateral position (SDLP) and standard deviation of steering wheel movement (SDSTW). No significant relationship was seen between the performance measures and WL.

From Figure 2.14, it can be clearly established that as WL increased, mind wandering decreased. Mind wandering could be directly attributed to SA. However, from this experiment, the levels of WL were not clear. It would seem that it only captured the region between low and high WL.

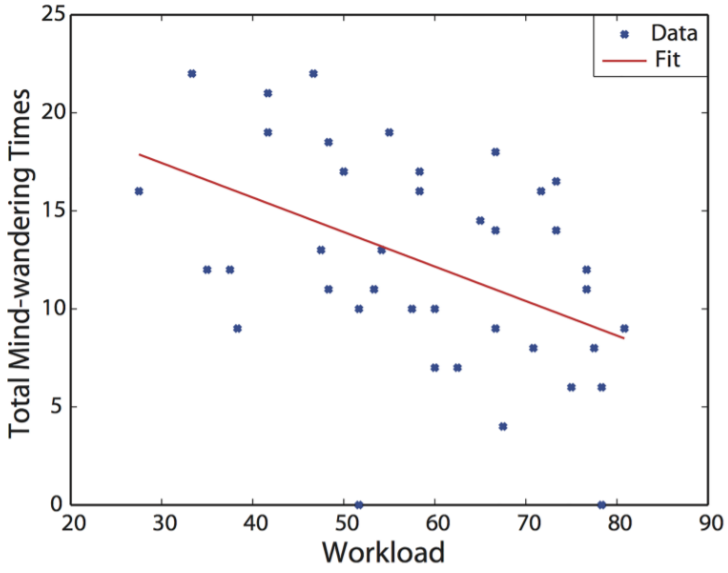

Figure 2.14 Mind wandering and WL (Zhang & Kumada 2017**)**

In general, it can be theorized that high levels of WL indicated low SA, but low levels of WL did not necessarily indicate a high level of SA. In situations with low to medium WL, SA increased gradually before reaching an optimum and decreasing sharply. Also, both WL and SA were dependent on LA.

Chapter 3 Methodology

The methodology was divided into two main phases. The first phase involves a simulator study to establish different levels of driver classification through performance parameters and biobehavioral trends and the second phase incorporates the classifications with their subsequent biobehavioral parameters into the IDM along with validation of the developed model. A framework for the proposed methodology is provided in Figure 3.1.

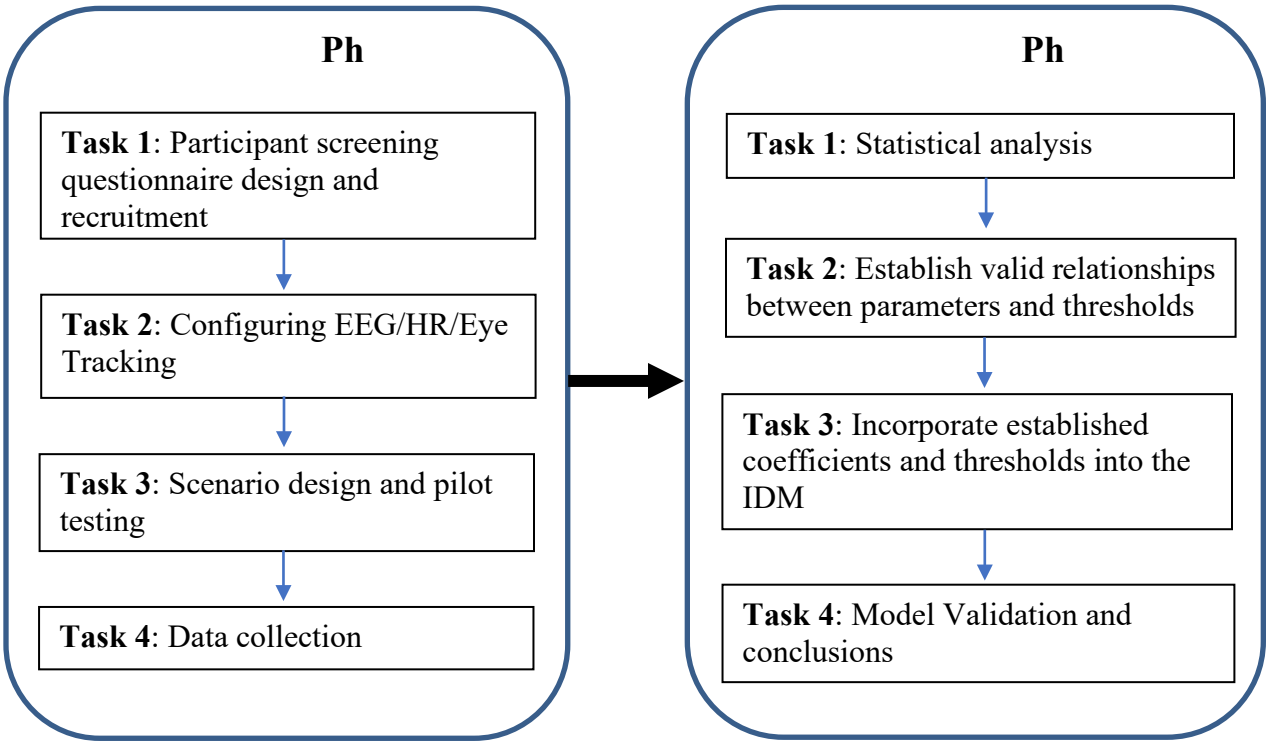

Figure 3.1 Methodological framework

The theory behind developing a framework that can be used to incorporate biobehavioral parameters such as LA, WL, and SA, with respect to changes in driving performance is explained in the paragraphs that follow.

When describing the theory behind the proposed framework, terms such as task demand, driver capability, task difficulty, mental workload, and situation awareness, are used. The definitions of these terms with respect to this project are shown in Table 3.1.

Table 3.1 Important definitions

Term	Definition
Task demand	The amount of effort required to successfully meet the set requirements of a task, independent of the individual (Kahneman 1973).
Driver capability	The individual traits/biological characteristics of a driver that affect his/her ability to complete a task. Some traits include: speed, reaction time, information processing ability, experience, knowledge of driving, and motor coordination (Fuller 2005).
Task difficulty	The strategies or behavior followed to cope with changes to task demand during a task (Mosaly et al. 2017). Fuller (2005) quotes task difficulty to be inversely proportional to the difference between task demand and driver capability.
WL	The proportion of mental capacity required by an individual to perform a task (Brookhuis and De Waard 1991).
SA	The ability to perceive, comprehend, and project future status of elements in an environment (Endsley 1995).

The external conditions in a specific scene contribute towards the complexity of the driving task at hand. Differences in conditions, such as the geometric properties, weather, number of interaction vehicles, and sources of distraction, add a certain level of complexity to the driving environment. The capability of the driver to handle tasks of varying complexity mostly depends on his/her physical and mental characteristics. For example: it can be expected that older drivers have slower reaction times than younger drivers due to their diminishing physical capabilities. Also, some individuals may prefer to drive faster and follow smaller headways (aggressive), while others tend to be more conservative. Static and dynamic

characteristics are identified as distinguishable variables between drivers. Where the age and experience of the driver coupled with the activation level can affect driving performance. Activation level describes the driver arousal state before and during the drive e.g., a drowsy or less motivated driver will have a lower activation level than a mentally aroused driver.

Also, the capabilities of the driver and the demands of the task are closely related. If the capabilities of the driver are greater than those required by the task, then the task will be easily completed (Hoogendoorn et al. 2012). It also means drivers can complete this task at a lower activation level and by utilizing fewer mental resources (WL). If the capability of the driver is equal to the task demand, the task becomes difficult as the driver is using all the available capabilities to successfully complete the task (Hoogendoorn et al. 2012). The driver will require a higher LA and alertness to complete this task. However, if the capability of the driver is less than that required by the task, the driver will fail to complete the task. The capability of the driver is also constrained by the physical capability/condition of the vehicle.

The interaction between driver capability and demand can be quantified with respect to the changes in WL and SA. Slight imbalance between the WL and SA can result in the driver compensating by adjusting longitudinal control variables such as speed, acceleration, and headway. For example: if a task is challenging (increased WL), the driver might choose to reduce his/her overall speed or increase his/her headway in order to be safe and maintain a comfortable level of SA. In essence, he/she is compensating for the lack of capabilities at that instance by making these changes to driving.

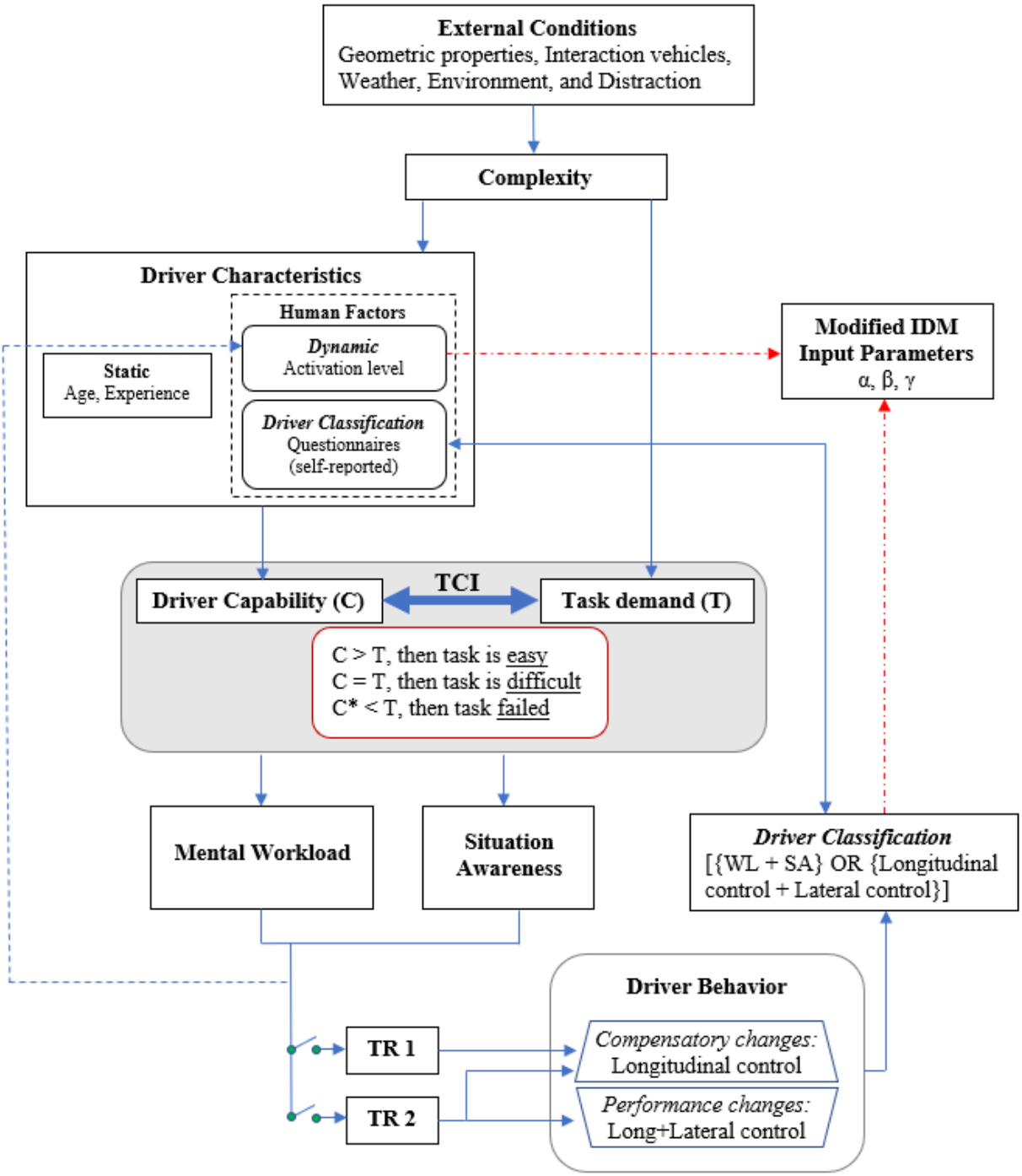

$C^* = \min \{VC_{max} \text{ or } C\}$. Where VC is the capability of the vehicle.

Figure 3.2 Theoretical framework for incorporating biobehavioral parameters

This leads to a trigger that is activated through small imbalances between WL and SA (TR 1) as seen in Figure 3.2. However, if the imbalance between driver capability and task demand is high e.g. task is difficult for the driver to successfully complete due to their current capability, the driver tries to restore this imbalance resulting in both compensatory and performance effects (setting off TR 2). Where compensation effects are theorized to only affect longitudinal driving variables, performance effects are theorized to affect longitudinal and lateral (SDLP) driving variables. Essentially, this implies that task difficulty is split into TR1 and TR2, depending on the extent of the imbalance between task demand and driver capability.

Speed and headway (longitudinal parameters) have been previously established to represent compensation behavior of drivers (Alm & Nilsson 1995 and Hoogendoorn et al. 2012). Measures such as SDLP, SDSTW, and route time, have been established to represent driver performance (Brookhuis et al. 1985, Brookhuis et al. 1991, Brookhuis & De Waard 1994, and De Waard 1996). Route time indicates the time taken by the driver to complete a set route, depending on the speed and the preferred headway (longitudinal control).

Drivers were also categorized by behavioral (LA, WL, SA) and static characteristics (age, experience, number of speeding tickets, number of accidents), into two or three groups (depending on the sample population). The resulting effect of the driver from a particular group trying to match his/her capability to the task demand was used to establish how drivers in different classes react to the same task. Would the driver experience lower mental workload, implying lower compensation and performance effects, while completing a difficult task? Or would the driver increase the speed and follow shorter headways during an easy task, to increase the level of difficulty to match his/her optimal capability? The established classifications were

also compared to the driving variables such as average speed, average headway, and maximum acceleration, to measure the accuracy of self-perception in driver classification.

3.1 Proposed Modification to the IDM

In order to incorporate the theoretical framework shown in Figure 3.2, modifications to the IDM are required. The IDM parameters that can be affected by an imbalance in the task-capability interface are assumed to be the desired speed and desired time gap. This assumption was made because the desired variables capture what the driver wants to do at that moment but is unable due to a higher than usual task demand. Equations 3.1 and 3.2 show how the overall acceleration of the IDM was modified when triggers (TR) 1 or 2 are activated.

Compensation only (TR 1):

$$a_n(t) = a_{max}\left[1 - \left(\frac{v_n(t)}{(\alpha+\beta)v_0(t)}\right)^{\delta} - \left(\frac{s^*{}_n(t)}{s_n(t)}\right)^2\right]; \quad 0 < (\alpha+\beta) \leq 1 \tag{3.1}$$

$$s^*{}_n(t) = s_0 + \left(\frac{1}{\alpha+\beta}\right)T_n v_n(t) + \frac{v_n(t)\Delta v_n(t)}{2\sqrt{a_{max}b_{comf}}}$$

Where,

α = Compensation coefficient

β = Activation level coefficient

Compensation and Performance (TR 2):

$$a_n(t) = a_{max}\left[1 - \left(\frac{v_n(t)}{(\{\alpha+\gamma\}+\beta)v_0(t)}\right)^{\delta} - \left(\frac{s^*{}_n(t)}{s_n(t)}\right)^2\right]; \quad 0 < \{\alpha+\gamma\}+\beta) \leq 1 \tag{3.2}$$

$$s^*{}_n(t) = s_0 + \left(\frac{1}{\{\alpha+\gamma\}+\beta}\right)T_n v_n(t) + \frac{v_n(t)\Delta v_n(t)}{2\sqrt{a_{max}b_{comf}}}$$

Where,

γ = Performance coefficient

Together with incorporating compensation, LA, and performance coefficients, a visual cue parameter that incorporates the effect of active brake lights (*bl*) on the lead vehicle was implemented to the model, essentially depicting a reaction time threshold. Upon activation of brake lights on the leader and the time-gap (*T(t)*) between the leader and follower at time (*t*) was determined to be lower than the desired time-gap (T_n), the modified IDM model was triggered to recalculate the car-following trajectory using the acceleration/deceleration (*a(t)*) at that instance. However, if *T(t)* was greater than T_n, it was assumed that the driver does not apply brakes or accelerate, resulting in a uniform deceleration of -0.2m/s^2 (Kesting & Treiber 2013). *T(t)* and T_n were used to establish constraints because it was theorized that drivers more readily perceive time-gap than the acceleration of the leader. Equation 3.3 shows the implementation of brake light parameter along with the resulting acceleration/deceleration.

$$bl = \begin{cases} 1 & On, \\ 0 & Off. \end{cases}$$

$$\text{If } bl = 1 \text{ then, } a_n(t)^* = \begin{cases} a(t) & 0 \le T(t) \le T_n \\ -0.2\, m/s^2 & T_n \le T(t) \le 5 \end{cases} \quad (3.3)$$

Where, $a_n(t)^*$ describes the starting acceleration/deceleration during car-following computations.

Any brake light observed from a time-gap of greater than five seconds will not be considered as this will be the threshold to represent active car-following. Four brake lights events were added to every driving task to collect data on respective car-following behavior.

3.2 Data Collection Techniques

A list of the techniques used during data collection to establish the coefficients α, β, and γ are listed in Table 3.2.

Table 3.2 Measuring techniques aggregated with respect to the coefficient

Coefficient	**Methodological Definition**	**Measuring Event/Technique**
α	Compensation coefficient	*Measuring WL:* • HR • Pupil dilation and TEPR • NASA-TLX *Measuring SA:* • Gaze overlay • SART *Measuring longitudinal control:* • Speed • Headway • Acceleration
β	LA coefficient	EEG
$\alpha + \gamma$	Compensation + Performance coefficient	*Measuring WL:* • HR • Pupil dilation and TEPR • NASA-TLX *Measuring SA:* • Gaze overlay • SART *Measuring longitudinal control:* • Speed • Headway • Acceleration *Measuring lateral control:* • SD of steering wheel position • SD of lateral position

Chapter 4 Data Collection

This section discusses the design of the scenarios and the strategies that will be followed during data collection. The simulation study was carried out from May 08, 2019 to June 17, 2019. Data were obtained in three formats: subjective, driving variables, and physiological. The subjective data were collected using electronically administered questionnaires such as the screening questionnaire, NASA-TLX, and SART. Driving variables are derived from the simulation tasks and they include: average speed, maximum speed, average headway, minimum headway, maximum acceleration, maximum deceleration, jerk, standard deviation of lateral position, number of collisions, maximum brake force, and average brake force. Physiological variables were collected using the EEG, HR monitor, and eye tracker.

4.1 Participant Recruitment

The study was first submitted to the Human Research Protection Program (HRPP) at the University of Kansas (KU), for approval. The study was advertised in several public places (libraries, universities/colleges, grocery stores, and community centers) around towns in Kansas and Missouri including: Lawrence, Overland Park, Shawnee, and Kansas City, using flyers, emails, and targeted advertising within Facebook. 90 participants were recruited to participate in this research, equally split between males and females. The descriptive statistics of the participants are shown in Table 4.1. The participants' recruitment was carried out in three age groups 18-24, 25-49, and 50-65 years, depending on availability and willingness to participate. Participants were screened using a questionnaire and selected if they were between the age of 18 and 65 years, with at least one year of driving experience, in possession of a valid U.S. driver's license, annual mileage no less than 1000 miles, satisfactory completion of pre-screening and

behavioral questionnaires, and good health (free from seizures, eye conditions, ear problems, heart conditions, arthritis, excessive motion sickness, and possibility of pregnancy).

Table 4.1 Descriptive statistics of participants

Age Group	Group ID	Males	Females	Mean and SD by age group
18-24 years	1	25	20	20.3 ± 1.4 years
25-49 years	2	14	15	35.0 ± 8.0 years
50-65 years	3	6	10	56.3 ± 3.7 years
	Sum	45	45	31.4 ± 14.2 years

A $50 gift card was issued to the participants after the completion of the study as compensation for their time. Participants were required to complete a 45-minute screening questionnaire prior to their driving appointment, covering the demographic information, medical conditions, driving preferences and history, mood and personality measure, empathy and moral decision-making measures, and attention and executive function measures. A summary of the participants' demographic data is shown in Appendix A.

The next subsections comprise of behavioral/personality information gathered during the screening process. This research included a series of behavioral self-report measures aimed to capture cognitive effort, personality, and social decision-making variables that could account for aspects of driving performance that have not been considered before in car-following behavior. The objective with the inclusion of these measures was to investigate whether current mood and generally stable descriptors of individual differences among drivers can improve the intelligent driver model by incorporating predictors of driver behavior based on cognitive and socio-affective variables. Our selection of behavioral measures was guided by this objective. Our measures incorporated well-established tests of (a) mood and personality; (b) cognitive

engagement; and (c) empathy and social decision-making. The specific self-report measures employed are briefly summarized below:

4.1.1 Mood and Personality Measure

There are several measures available through the literature that provide mood and personality assessments such as:

- Positive and Negative Affect Schedule (PANAS): The PANAS is a self-report measure designed to assess both positive and negative affect (Watson et al. 1988). The PANAS consists of 20 adjectives pertaining to negative affect (i.e., distressed or nervous) and positive affect (i.e., excited or proud), with ten items for each subscale. Items are rated on a five-point Likert scale: 1 = "Very slightly or not at all" to 5 = "Extremely." The subscales are obtained by taking the average of each item within that subscale.
- Need for Cognition: This test is designed to assess the tendency to engage in and enjoy effortful cognitive endeavors (Cacioppo et al. 1984).

4.1.2 Cognitive Engagement Measures

- Cognitive Reflection Task (CRT): This questionnaire assesses individuals' ability to suppress an intuitive and spontaneous wrong answer in favor of a reflective and deliberative right answer (Frederick 2005). Three common CRT questions include:

  Qn 1: "A bat and a ball cost $1.10 in total. The bat costs $1.00 more than the ball. How much does the ball cost? _____ cents." (Correct answer: 5 cents)

  Qn 2: "If it takes five machines 5 minutes to make five widgets, how long would it take 100 machines to make 100 widgets? _____ minutes." (Correct answer: 5 minutes)

  Qn 3: "In a lake, there is a patch of lily pads. Every day, the patch doubles in size. If it takes 48 days for the patch to cover the entire lake, how long would it take for the patch to cover half of the lake? _____ days." (Correct answer: 47 days)

- Neuroticism-Extroversion-Openness Five Factor Inventory: this is a 60-item survey to measure the five primary personality characteristics of openness, conscientiousness, extraversion, agreeableness, and neuroticism (Costa & McRae 1989).

4.1.3 Empathy and Moral Decision-Making Measures

- Interpersonal Reactivity Index (Davis 1983). This questionnaire measures individual differences in empathy.
- The Empathy Quotient (Baron-Cohen & Wheelwright 2004): This questionnaire also measures individual differences in empathy.
- Psychological Entitlement Scale (Campbell et al. 2004): This scale measures psychological entitlement, which refers to the stable and pervasive sense that one deserves more and is entitled to more than others. This sense of entitlement will also be reflected in desired or actual behaviors. The concept of psychological entitlement is intrapsychically pervasive or global; it does not necessarily refer to entitlement that results from a specific situation (e.g., "I am entitled to social security because I paid into the system," or "I deserve an 'A' because I performed well in class"). Rather, psychological entitlement is a sense of entitlement that is experienced across situations.
- Ethical dilemmas such as the Trolley/Footbridge Dilemmas: These are short vignettes describing different scenarios and the participant has to decide or evaluate the 'right' course of action. The tasks are meant to measure moral decision making in context.

4.2 Equipment

The data were collected using the KU driving simulator, a fixed-based simulator in an Acura MDX chassis (half cab). The simulator provides a 170º horizontal field of view as shown in Figures 4.1 and 4.2, with three forward screens and one rear screen. The rear screen renders the view of both side-view mirrors and the rear-view mirror, providing an immersed driving experience.

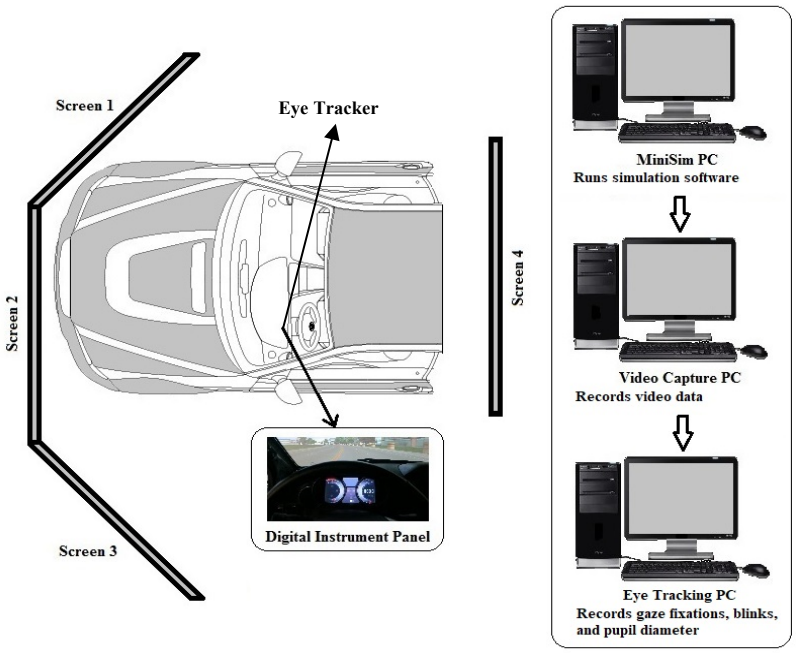

Figure 4.1 Layout of the KU driving simulator

The simulation run and respective data are recorded on the MiniSim (MiniSim User's Guide 2015) computer while the video of the participant's drive is captured on the video capture computer. Separate systems were used for the eye-tracking and EEG recordings. All the data were later synchronized using the available system times.

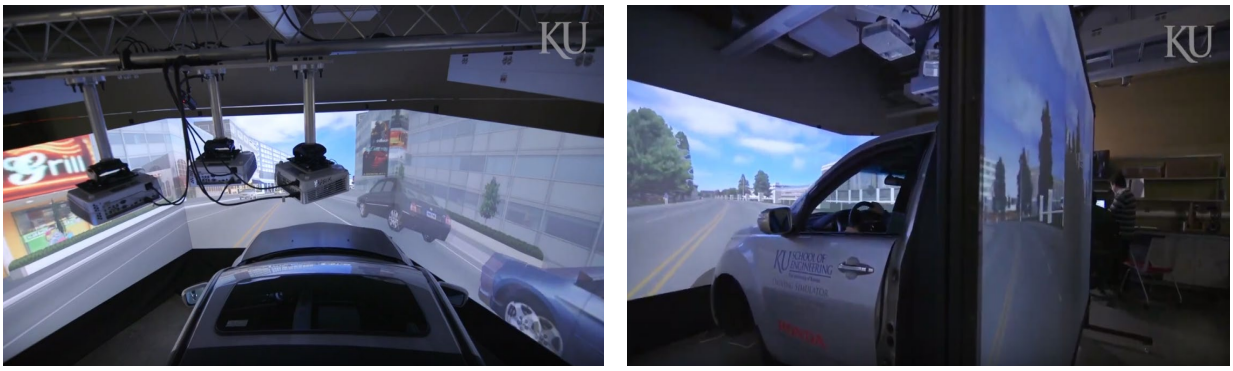

Figure 4.2 KU driving simulator in action

4.3 Configuring the EEG, HR Monitor, and Eye Tracker

The LA (arousal) was a key variable in this research. Changes to the level of activation have been directly associated with the changes in neural activity occurring in the driver's brain (Brookhuis et al. 1991). The EEG was used to monitor any changes in activation level associated with the various tasks presented during the drive. It was also used to capture an initial state of mind of the driver at the beginning of the drive.

During the drive, participants' overall attentional trajectory was captured using the EEG at a sampling frequency of 500Hz (Neuroelectrics User Manual: Enobio 8 2019). A portable, lightweight, wireless, and rechargeable system for EEG recording is available for this project. The system (Enobio 8) allowed for the reliable reproduction of EEG and EMG signal with a rapid setup that took less than 20 minutes and was optimal for multi-component, multi-method studies. The accompanying software allowed for visualization of time-frequency 2D/3D features (3D EEG scalp map) in real time, including the power spectrum and spectrograms, as well as easy channel labeling. The software further provided continuous online EEG signal quality with an option to filter out noise due to AC power lines (60Hz frequency in the United States). Eight EEG electrode positions were used, and they include: P3, PZ, P4, CZ, T7, T8, O1, and FZ (Pope

et al. 1995 and Prinzel III et al. 2001). These electrode positions allowed for the capturing of the functions shown in Table 4.2.

Table 4.2 Selected electrode positions

Electrode Position	**Brain Region**	**Captured Function**
P3, PZ, P4	Parietal	Sensory and Object recognition
CZ	Central	Motor
T7, T8	Temporal	Memory
O1	Occipital	Vision
FZ	Frontal	Concentration, Planning, Judgement

The Polar H10 chest strap was used to monitor the heart rate at 1Hz. The obtained data needed to be manually synchronized with the frames of miniSim. Participants were shown how to correctly place the device against their chest to ensure accurate data collection.

A Fovio-FX3 eye tracker was installed directly over the instrument cluster of the simulator chassis (EyeWorks 3 User Manual 2019). The eye tracker collects mental workload through TEPR at 1Hz and gaze points at approximately 60Hz. Other eye-related measures such as pupil diameter, blink rate, gaze point vector coordinates, and gaze fixations, are also available.

Due to the restriction of not being able to pause a scenario (in miniSim) to perform the SAGAT by Endsley (1995), another measure is devised. SAGAT was mostly verified by studies on airplane pilots and military professionals (combat SA). However, driving might not require the same level of skills to project the status of future events, especially if the task is routine/instinctive (following, braking, lane changing). Also, studies suggested that SAGAT might interfere and make the primary driving task feel discontinuous, therefore not accurately representing the car-following behavior.

The devised method made use of probe questions (similar to Endsley 1995), visual cues, and time spent gazing, to estimate the SA of the driver, without pausing the scenario. Five SA probe locations were present in every task and require participants to answer questions related to the last five seconds of activity. The questions were tailored to cover all three components of SA (perception, comprehension, and projection). Table 4.3 summarizes the number of points and criteria to obtain them.

Table 4.3 SA scores and criteria

Type	**SA Points**	**Criteria**
Full	1	Correct response and gaze match
Partial	0.5	Wrong response and gaze match
None	0	(Wrong response and no gaze match) OR (*Correct response and no gaze match)

*Correct response without a gaze match was considered a guess

Studies summarized by Karwowska & Siminski in 2015 showed that the lower limit for perception time (time to locate an object) was around 0.32 seconds and the higher limit was 0.82 seconds. Using this as a constraint, a gaze match was considered successful if the participant spent at least 0.3 seconds gazing at the visual cue. Any gaze fixations less than 0.3 seconds were considered as a no match (miss), due to insufficient perception time.

An example of how a SA probe was administered is as follows: a deer crossing sign was shown five seconds before the probe question was asked. The probe question asked was “Do you expect a crossing deer?”. Participants were required to say their answer out loud, either “yes/no” or “I do not know”. In post-processing, participants gaze was monitored to see if they spent more than 0.3 seconds looking at the sign and if this is positive, a gaze match is granted. If the

participants said “yes”, then a perfect SA score was recorded for that question. However, if a “no” was selected but they still spent time looking, partial credit was given. These questions were designed to consider all three components of SA i.e., ability to perceive the sign, comprehend to what the sign was saying, and project any upcoming events (status of the crossing deer). A list of the probe questions is shown in Table 4.4.

Table 4.4 Probe questions for SA

Qn	Probe Question	Possible Answers
1	Do you expect crossing deer?	Yes: Deer crossing sign shown No: Deer crossing sign not present
2	Is an off ramp approaching soon?	Yes: Exit sign shown No: No sign shown
3	Did the sign say ‘speeding kills’?	Yes: Sign said speeding kills No: Sign says something else or no sign present
4	Did you avoid a road kill?	Yes: Road kill present No: Road kill not present
5	A green color car on the shoulder	Yes: Car present was green No: Car present was black
6	A red car merged two spots ahead	Yes: Car that merged was red No: Car that merged was green
7	Does the left shoulder close ahead	Yes: Left shoulder closed sign shown No: No sign shown
8	Did you see or avoid a worn out tire?	Yes: Tire present No: Tire not present
9	The current speed limit is 70 mph	Yes: Speed limit is 70 mph No: Speed limit is not 70 mph

Three questions with outcome ‘yes’ and two with outcome ‘no’ are randomly placed in each task to counterbalance the full and partial credit system. A SART questionnaire was also

administered at the end of the task to observe how the devised method compared to existing subjective measures.

4.4 Scenario Design

After recording baseline thresholds for the EEG and heart rate, participants received an extensive tutorial of the driving simulator. Before the tutorial, the eye-tracker was calibrated to the driver's view point. The tutorial comprised of driving at low and high speeds, lane changing activity, familiarizing participants with distances and headways in a simulator setting, gas and brake pedal responsiveness, and steering wheel sensitivity. During the tutorial, participants were also screened for simulator sickness. Any participants who showed severe signs of simulator sickness were advised to forfeit the study and received a compensation of $10.

A preliminary driving scenario, shown in Figure 4.3, was designed with two phases: free driving and car-following. The free driving phase was used to capture the participant's desired speed and maximum acceleration components on an empty four-lane divided rural highway, while the car-following phase captured the participant's desired time-gap and preferred standstill distance. Participants were instructed to only focus on maintaining a comfortable gap to the lead vehicle during the car-following phase. Each phase was configured to be driven at both 55 mph and 70 mph speed limits, to capture the variability in performance. Eight probe questions were also presented to obtain an estimate of baseline SA. A breakdown of the full appointment schedule for each participant is shown in Table 4.5.

Figure 4.3 Preliminary scenario

Table 4.5 Time breakdown by activity

<table>
<tr><th>Description</th><th>Approximate Time</th></tr>
<tr><td>Consent form explanation.</td><td>5 minutes</td></tr>
<tr><td>Equipping participants with EEG & HR monitor.</td><td>10 minutes</td></tr>
<tr><td>Baseline EEG and HR data: Watching short video.</td><td>5 minutes</td></tr>
<tr><td>Introduction to simulator driving, calibrating the eye tracker, and tutorial.</td><td>10-15 minutes</td></tr>
<tr><td colspan="2">Preliminary scenario:
<table><tr><td>Free driving (no other roadway traffic) with 55 mph and 70 mph speed limits.</td><td>3 minutes</td></tr><tr><td>Following (one lead vehicle): lead speed changes first from 70 mph to 55 mph, then speeds up to 65 mph.</td><td>4 minutes</td></tr><tr><td>Total time</td><td>7 minutes</td></tr></table></td></tr>
<tr><td colspan="2">Actual scenario:
<table><tr><th rowspan="2">Traffic density</th><th colspan="4">Task</th></tr><tr><th>1</th><th>2</th><th>3</th><th>4</th></tr><tr><td>Medium</td><td>8 minutes</td><td>5 minutes</td><td colspan="2">–</td></tr><tr><td>High</td><td>5 minutes</td><td>5 minutes</td><td>5 minutes</td><td>5 minutes</td></tr><tr><td>Total time</td><td colspan="4">35 minutes</td></tr></table></td></tr>
<tr><td>NASA-TLX + SART Questionnaires</td><td>20 minutes</td></tr>
<tr><td colspan="2">Average duration per participant = 95 minutes</td></tr>
</table>

Before finalizing the configuration of the tasks, pilot testing was carried out on three participants to establish any design flaws in the scenario and assess the quality of data output.

The identified flaws were corrected to ensure that the all required data variables were being properly captured.

The actual scenario incorporates six tasks with varying levels of difficulty arising from varying traffic density, lane changing/deviation activity, heavy vehicle density, number of open lanes, and secondary tasks replicating visual distraction. Task 6 was designed to be the most complex while task 1 was the least. Each task was five miles long on a straight roadway with no horizontal curves and had a posted speed limit of 70 mph. Simulation traffic was configured to be free flowing, without any form of congestion or speed drop. Participants were asked to drive as they would normally, with similar car-following and lane changing behavior. The tasks were assigned and performed in a random sequence to eliminate any order-related bias. At the end of each task (including preliminary), drivers were required to fill out the NASA-TLX and SART questionnaires. A comprehensive description of all tasks is presented in the following sections.

4.4.1 Task 1

The first task, also considered as the baseline, was designed to capture car-following behavior during regular non-intensive highway driving. Participants were required to exhibit naturalistic behavior. The vehicles on the right lane were programmed to travel at 70 ± 2 mph, while vehicles on the left lane were programmed to travel a bit faster at 74 ± 2 mph. This provides an opportunity for the driver to exhibit a more naturalistic speed profile. The left and right lane speed configuration was consistent in all the driving tasks. The task contained no heavy vehicles and had a medium traffic density (25-28 pc/mi/ln), shown in Figure 4.4.

Figure 4.4 Task 1 design layout and driver view

4.4.2 Task 2

The second task was very similar to the first task. However, the roadway had a higher density of vehicles (35-38 pc/mi/ln). Also, lane changing and lane deviations were introduced to the behavior of leading traffic (one passenger car per mile) to further increase complexity. Figure 4.5 shows a snapshot from the task.

Figure 4.5 Task 2 design layout and driver view

4.4.3 Task 3

This task incorporated an inactive work zone that consisted of a closed left shoulder as shown in Figure 4.6. The speed limit was maintained at 70 mph to facilitate speed correlations with other tasks. The presence of barriers and channelizers were theorized to increase the situation complexity. Also, the traffic composition for this task consisted of 10% heavy vehicles along with two to three lane deviations/changes per mile.

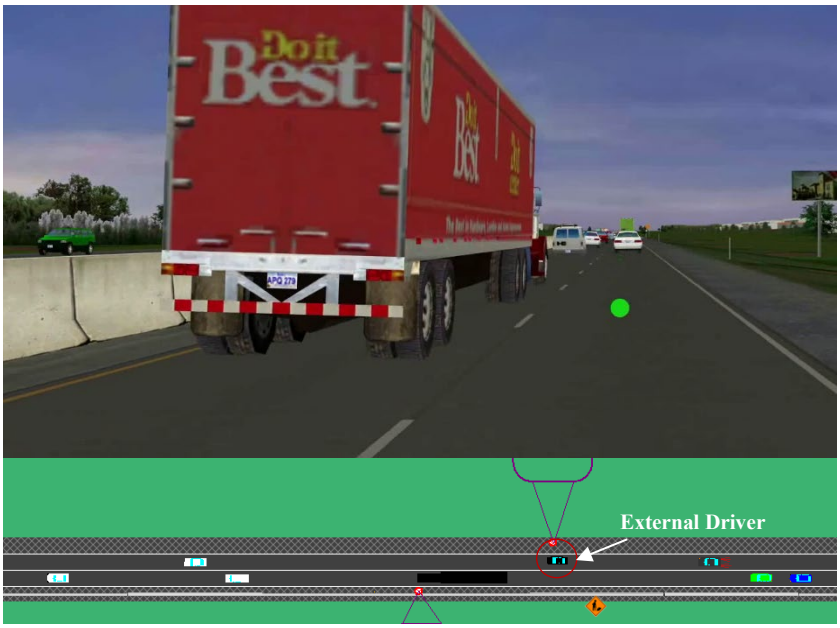

Figure 4.6 Task 3 design layout and driver view

4.4.4 Task 4

Task 4 consisted of a five-lane highway with three lanes closed in one direction. The two open lane edges were delineated using concrete barriers and traffic channelizers. The speed limit was still set at 70 mph for easy comparisons and in order to prevent loss of speed perception in a fixed-base driving simulator (Hurwitz et al. 2005). An active work zone with moving construction workers and equipment was present along both sides of the roadway. The task also consisted of 20% heavy vehicles, medium traffic density, and 3-5 lane changes/deviations per mile. This setup was designed to further increase the complexity of the drive. Changes to the driver's mental workload and situation awareness were expected as a result of the increased complexity. Figure 4.7 shows the configuration of task 4.

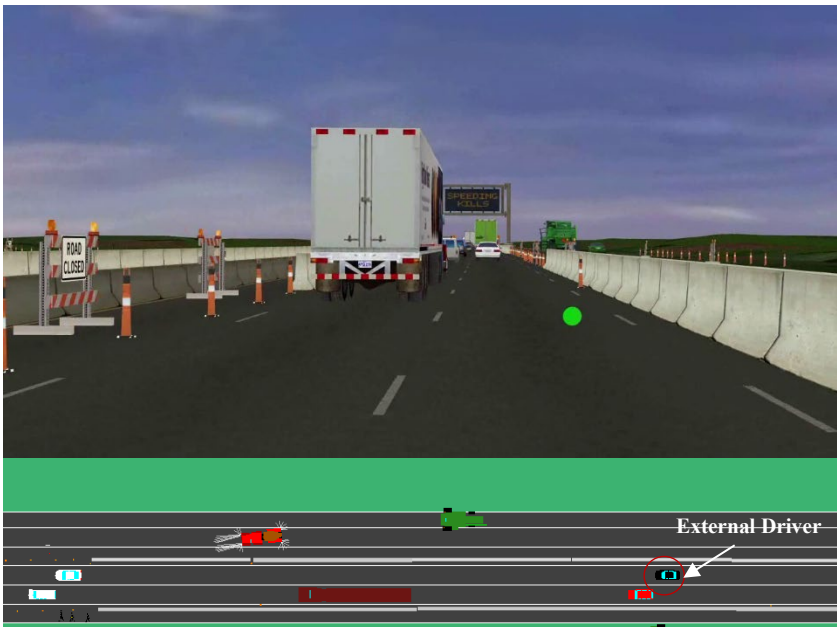

Figure 4.7 Task 4 design layout and driver view

4.4.5 Task 5

Task 5 was created very similar to task 4. However, a higher percentage of heavy vehicles was used (20%).

Figure 4.8 Task 5 design layout and driver view

4.4.6 Task 6

Task 6 and task 5 were essentially the same apart from the presence of a secondary task. The secondary task used an application developed using Visual Basic Studio (VBA.NET), shown in Figure 4.9. The application required participants to match the shown number correctly from the presented tiles during the drive. A computer-generated voice was used to alert the participants on when to start and stop attempting the secondary task. Four short distraction events lasting a distance of 2000 feet (approximately 15 seconds depending on speed) each were configured into the task. Participants were advised to attempt tasks only when they felt comfortable during the events as their primary task was still driving.

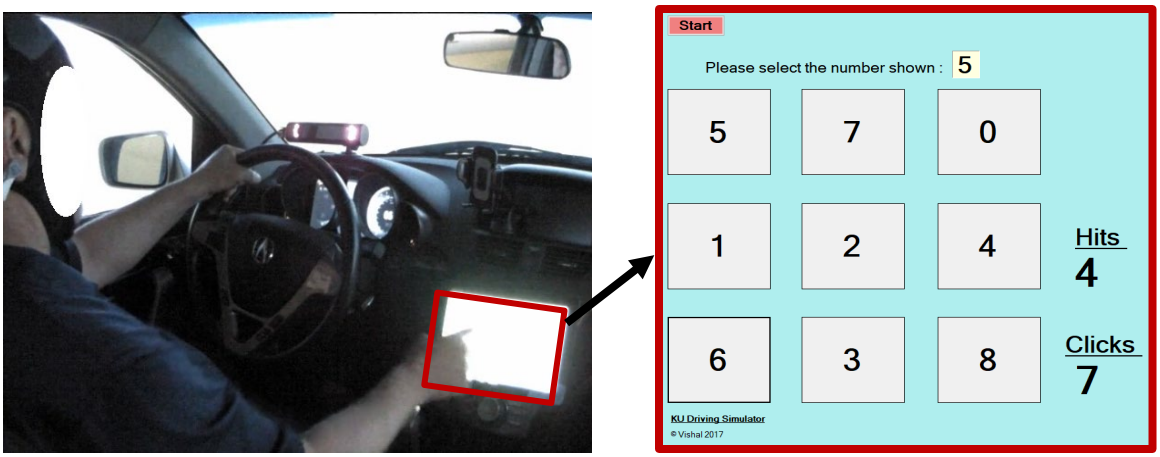

Figure 4.9 Secondary task used to simulate visual distraction

Participants' reaction to having additional tasks competing with the primary task of driving was critically assessed. The distraction provides data with respect to mental workload, situation awareness, level of activation, and driving performance on car-following behavior when engaged in an activity other than driving. A summary of all tasks and their composition is provided in Table 4.6.

Table 4.6 Task configuration and composition summary

Name	Composition	Work zone	Traffic density	Lane deviations	Distraction
Pre	4-lane divided highway at varying speeds. 0% heavy vehicles.	None	0-3 pc/mi/ln (LOS A)	None	None
Task 1	4-lane divided highway at 70 mph. 0% heavy vehicles.	None	25-28 pc/mi/ln (LOS B/C)	Low (1 pc/mi)	None
Task 2	4-lane divided highway at 70 mph. 0% heavy vehicles.	None	35-38 pc/mi/ln (LOS D/E)	Low (1 pc/mi)	None
Task 3	4-lane divided highway at 70 mph. 10% heavy vehicles.	Inactive: left shoulder closed	35-38 pc/mi/ln (LOS D/E)	Medium (2-3 pc/mi)	None
Task 4	10-lane divided freeway at 70 mph. 20% heavy vehicles.	Active: far right two and far left lanes closed	25-28 pc/mi/ln (LOS B/C)	High (3-5 pc/mi)	None
Task 5	10-lane divided freeway at 70 mph. 20% heavy vehicles.	Active on both sides: 3 lanes closed	35-38 pc/mi/ln (LOS D/E)	High (3-5 pc/mi)	None
Task 6	10-lane divided freeway at 70 mph. 20% heavy vehicles.	Active on both sides: 3 lanes closed	35-38 pc/mi/ln (LOS D/E)	High (3-5 pc/mi)	Yes (secondary task)

* passenger cars per mile per lane (pc/mi/ln); level of service (LOS)

Chapter 5 Data Analysis

This section summarizes the data analysis that was undertaken in this project. It was important to synchronize all data as multiple workstations and electronic devices were used to capture and store the data. All start/stop events for the various devices were recorded using the webcam to ensure secondary synchronization in case of system time/network failure.

5.1 Driving Simulator Data

The simulator data were collected at 60Hz and consisted of several variables such as time frame, vehicle speed (m/s), brake pedal force (Newtons), vehicle trajectory x, y, z (m), SDLP (m), collision count, lead vehicle velocity (m/s), lead vehicle trajectory x, y, z (m), time gap (s), headway (m), acceleration (m/s^2), and jerk (m/s^3). Although all tasks were five miles long, only the middle four miles were used during the analysis. Event triggers were set at the beginning and end of these analysis zones during the design phase to permit easy identification. The data collection zones for all the tasks performed by the participants are shown in Figure 5.1.

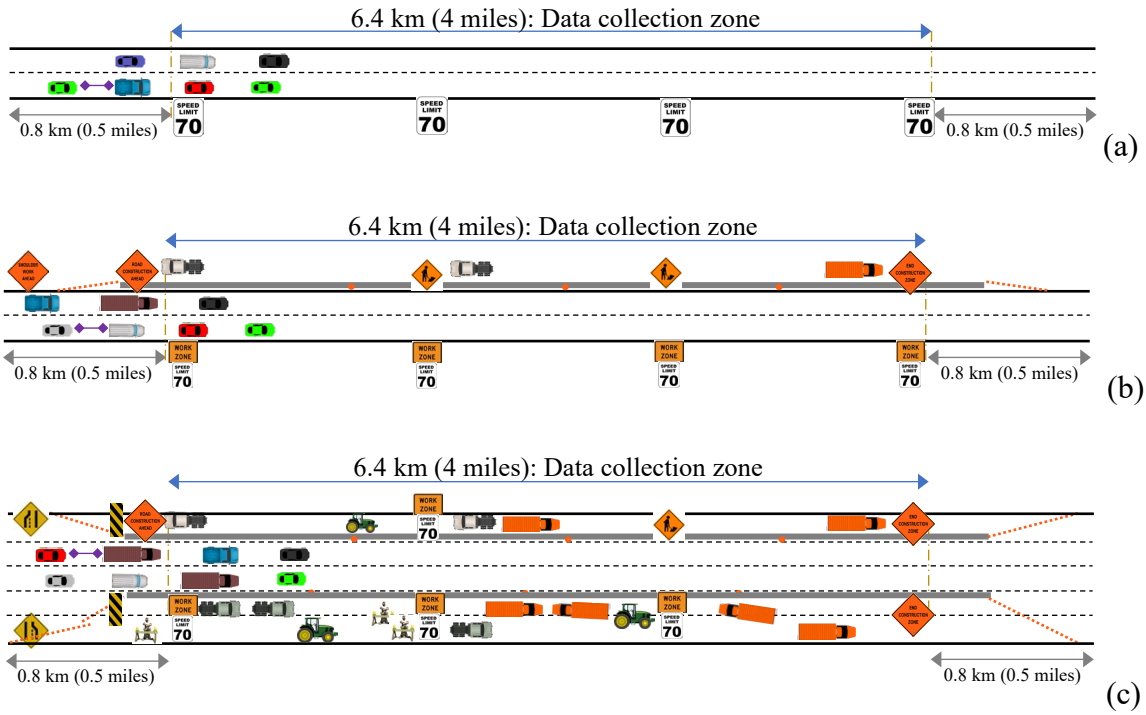

Figure 5.1 (a) Task 1 and 2 analysis zones (b) Task 3 analysis zone and (c) Task 4, 5, and 6 analysis zones

5.2 Subjective Data

We used extensively reviewed techniques for measuring WL (i.e., NASA-TLX) and SA (i.e. SART) to validate our experimental setup. The full NASA-TLX and 10-D SART questionnaires were administered electronically using a windows tablet at the end of each of the six tasks. A visual basic (VBA) version of the SART questionnaire was developed to ensure data was collected and saved securely. A total of 1,208 questionnaires were administered during the data collection. The trends observed from these questionnaires are discussed further in Chapter 6.

5.3 Eye-Tracking Data

The data from the eye-tracker was spilt between continuous, multi-point, and task averages. Task averages were used as a surrogate to NASA-TLX in computing WL. The following sections describe the significance and terminology of the collected variables.

5.3.1 Gaze Position

The concentration of gaze position (i.e., a phenomenon that causes drivers to direct attention towards a specific point of the roadway) has been linked to increased WL (Cooper et al., 2013; He et al., 2014; Li et al., 2018; Kountouriotis et al., 2015; Wang et al., 2014). To facilitate the use of this variable, some assumptions had to be made. From the distribution patterns and heat maps obtained from the data, the gaze concentration area was approximated to represent the area (pixels^2) enclosed by the ellipse formed by one standard deviation in the horizontal and vertical positions of the gaze center (i.e., mean gaze position) shown in figure 5.2.

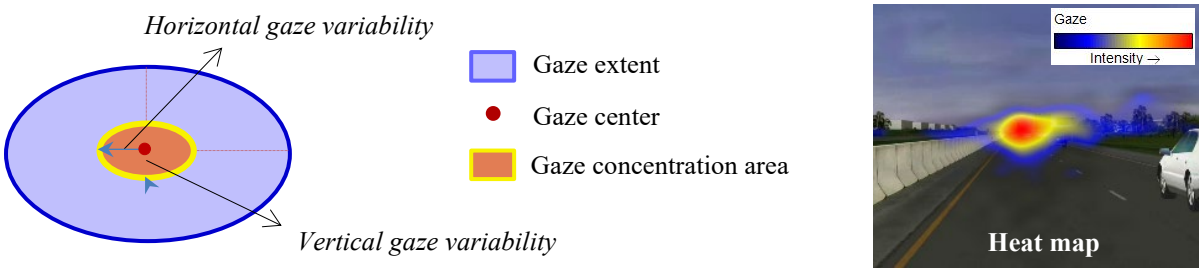

Figure 5.2 Gaze positions and concentration

The horizontal and vertical gaze variabilities were used to identify the role of gaze concentration in determining WL of the driving tasks.

5.3.2 Index of Cognitive Activity (ICA)

The ICA is a patented pupillometric technique that measures frequency of rapid pupil dilations (Vogels et al., 2018). The ICA is a relatively new technique; however, its ability to disentangle pupil response due to changes in lighting conditions makes it an attractive method for use in a driving simulator setting. Bright environments cause the pupil to constrict while dark environments cause them to dilate. As the driving simulator consists of several screens of varying brightness and environments ranging in color schemes, measures taken to systematically

control the lighting conditions may not fully work. EyeTracking Inc. (2019), manufacturer of the Fovio FX3 eye-tracker used in the KU driving simulator, patented the technique and uses custom algorithms along with scaled ICA to predict WL of an individual in increments of one second.

5.3.3 Time to Comprehension

Driver comprehension is one of the more substantial components of SA that involves the ability of an individual to understand the significance of an object, traffic sign, or hazard while driving. The time to comprehension metric was specifically developed to quantify the SA of a driver without being fully subjective in nature (Kummetha et al., 2021). This metric measures the percentage of time taken looking at a cue from the moment it is visible until it has been comprehended. The probe questions listed in table 4.3 were used together with gaze path overlays and regions of interest (shown in figure 5.3) to determine if a cue was comprehended.

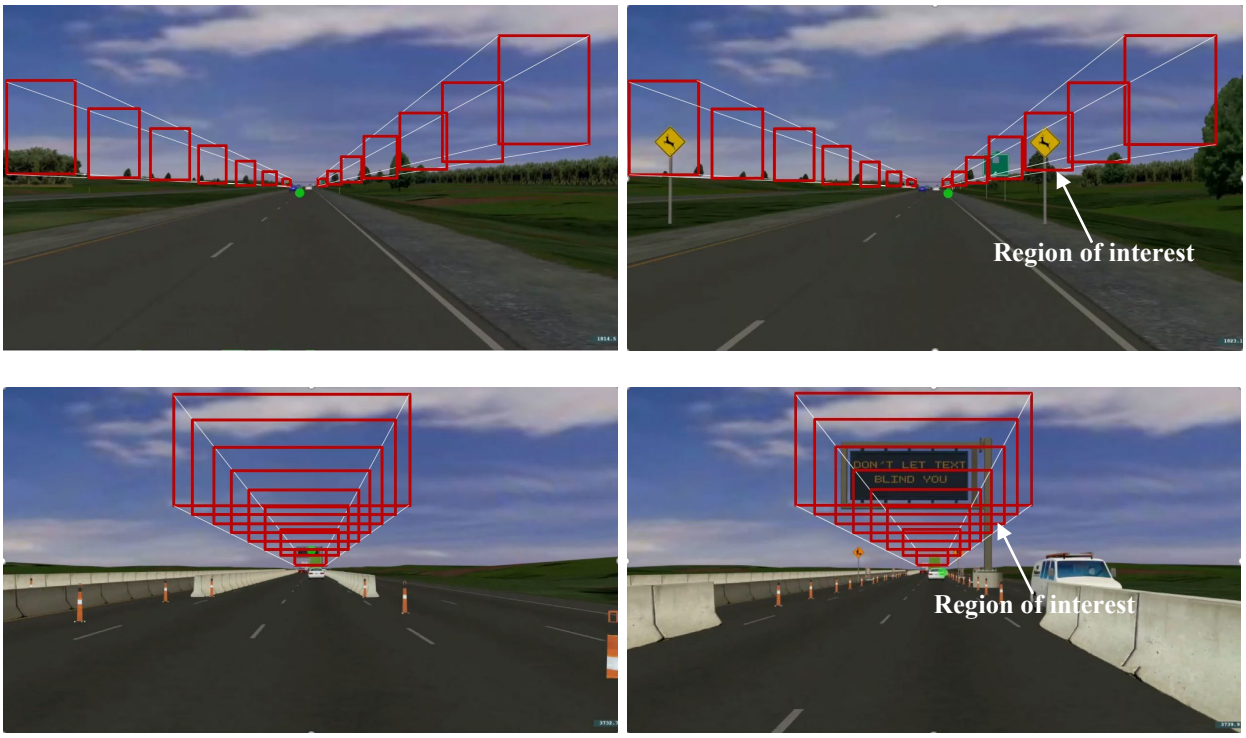

Figure 5.3 Setting up regions of interest

The regions of interest were created in the EyeWorks software. A progressive mesh of rectangular regions of varying size and shape depending on the type of visual cue and the lane position of the driver was created (Kummetha et al., 2021). Multiple events were created before the onset of a cue, which varied in duration between 8 and 12 seconds depending on the size of the cue (i.e., visibility) and vehicle speed.

The total gaze duration in each of the regions of interest was computed and recorded together with participants' verbal confirmation of the cue. Correct responses together with percent time spent gazing from cue onset were combined to form probabilistic distributions for each task as shown in figure 5.4. The key assumption was that a driver would stop gazing at a cue after perceiving and achieving full comprehension. If gazing continued, full comprehension was not achieved. The best-fit distributions from the data were obtained by running the distribution analysis in Minitab 19 (Minitab, LLC., 2019). Weibull distributions were deemed as the best-fit for the cumulative distributive functions (CDFs) of the six tasks, resulting in the highest R-squared values. The parameters for the Weibull distributions are shown in table 5.1.

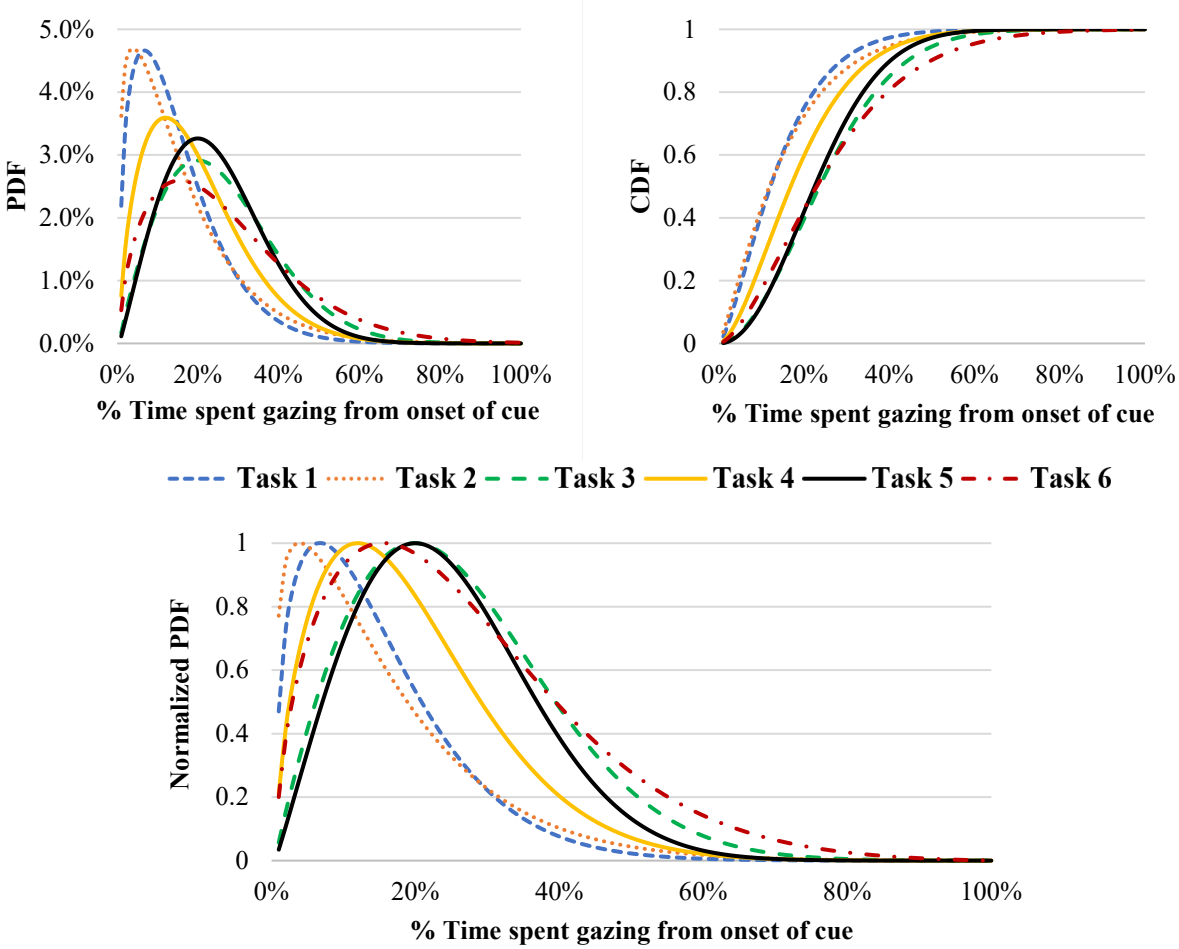

Figure 5.4 Weibull plots for driver comprehension showing (a) PDFs, (b) CDFs, and (c) Normalized PDFs

Table 5.1 Weibull plots parameters

Parameter	**Task 1**	**Task 2**	**Task 3**	**Task 4**	**Task 5**	**Task 6**
Shape	1.3821	1.1866	1.9093	1.5990	2.0631	1.5552
Scale	0.1575	0.1614	0.2859	0.2118	0.2683	0.2906
R-squared	0.9900	0.9821	0.9841	0.9940	0.9821	0.9683

After obtaining the CDFs, the probability density functions (PDFs) were then established. Tasks 1 and 2 showed similar trends of attaining comprehension. Drivers spent between 6 to 7% of the time from the onset of the cue to comprehend it. As the task complexity increased, the optimal time for comprehension increased (figure 5.4). However, in task 6, the optimum time spent to comprehend decreased, indicating the onset of competition for attentional resources with the visual distraction. False positives where participants obtained the correct verbal answer without any gaze match were excluded from the CDF curves. Gaze paths were also manually checked to make sure data were not missed or poorly interpreted from the regions of interest. The regions of interest could not capture gaze matches of 10.4 % of the dataset. However, this could be attributed to the deviations in eye-point calibration during the drive.

The obtained PDF curves were then normalized between 0 and 1 to generate the normalized PDFs (figure 5.4c). These normalized PDF plots were used to interpolate a single value of SA as a probability of achieving comprehension to a given cue in a particular task.

5.4 Heart Rate Data

Heart rate was captured throughout all tasks. The resting heart rate was captured during a short (5 minutes) informative video played before the start of the driving experiments. During the analysis, most participants were observed to have reached a lower heart rate while driving than during the baseline calibration video. This issue was not previously accounted for in the methodology or preliminary testing, thus leading assumptions during the analysis, such as using the absolute minimum HR as a surrogate for the baseline value.

The HR data were normalized between 0 and 1 for each participant with respect to their lowest and highest values. This was also used as an indicator for increased WL, with zero implying low WL and one implying high WL.

5.5 EEG Data

Several steps were followed to obtain LA from the EEG datasets. The obtained data were synchronized with the respective driving simulator data to identify analysis zones (described in Section 5.1). The EEGLAB v14.1.1 toolbox in MATLAB, shown in figure 5.5, was used for postprocessing (Delorme & Makeig, 2004). A description of the steps is provided below.

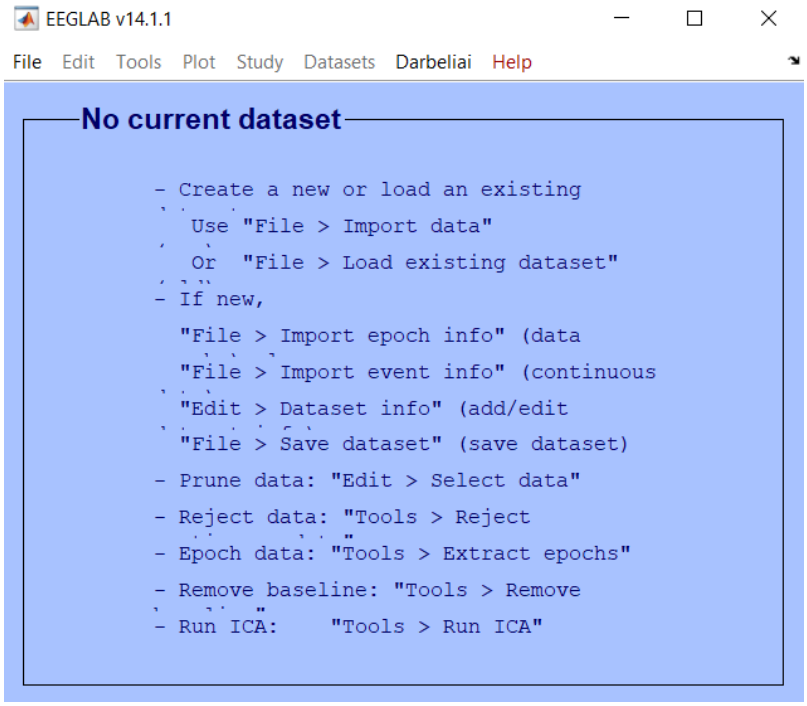

Figure 5.5 EEGLAB interface

Step 1: Set unique identifiers for 10-second events in the EEG dataset. This was done because LA has to be computed in time intervals between 10 and 30 seconds. Each driving task resulted in approximately twenty 10-second events.

Step 2: Load and convert data from Neuroelectrics (.easy) format to EEGLAB (.set) compatible format. This was done by utilizing the Neuroelectrics plugin in EEGLAB. The raw

data collected were down-sampled from 500 Hz to 240 Hz to eliminate some of the artifacts and ease system processing. The following MATLAB code was used to load, convert, assign 3D scalp locations, and resample (from 500 Hz to 240 Hz).

```
     myDir = 'C:\\Users\\path';    % gets directory
     myFiles = dir(fullfile(myDir,'*easy')); % Added
closing parenthese!
     for k = 1:length(myFiles)
          baseFileName = myFiles(k).name;
          fullFileName = fullfile(myDir, baseFileName);  %
Changed myFolder to myDir
          fprintf(1, 'Now reading %s\n', fullFileName);

     [ALLEEG EEG CURRENTSET ALLCOM] = eeglab;
     EEG = pop_easy(fullFileName,0,0,'');
     [ALLEEG EEG CURRENTSET] = pop_newset(ALLEEG, EEG,
0,'gui','off');
     EEG = eeg_checkset( EEG );
     EEG = pop_resample( EEG, 240);
     [ALLEEG EEG CURRENTSET] = pop_newset(ALLEEG, EEG,
1,'gui','off');
     EEG=pop_chanedit(EEG, 'load',{'C:\\Users\\path'
'filetype' 'autodetect'});
     [ALLEEG EEG] = eeg_store(ALLEEG, EEG, CURRENTSET);
     EEG = eeg_checkset( EEG );
     EEG = pop_saveset( EEG,
'filename',baseFileName,'filepath', 'path');
     [ALLEEG EEG] = eeg_store(ALLEEG, EEG, CURRENTSET);
     eeglab redraw;
     end
```

Step 3: The resulting datasets were then filtered. A high-pass filter was applied at 1.6 Hz, followed by a notch filter at 60 Hz to eliminate noise resulting from the 120V powerlines within close proximity to the EEG device. An independent component analysis was then performed to improve signal quality by identifying and pruning any significant artifacts (i.e., blinks, muscle movements). A low-pass filter was then applied to the signal at 40 Hz, essentially rejecting any waveforms above 40 Hz, as they are not required in the analysis.

Step 4: The filtered signal was then split into 2-second epochs with 5% overlap. The overlap ensured signal continuity when the fast Fourier transform (FFT) window was applied. The 2-second epochs essentially provided four to five individual time-series analysis zones (shown by blue dotted lines in figure 5.6) for the 10-second event due to artifact rejection. Each 10-second event resulted in one absolute power value.

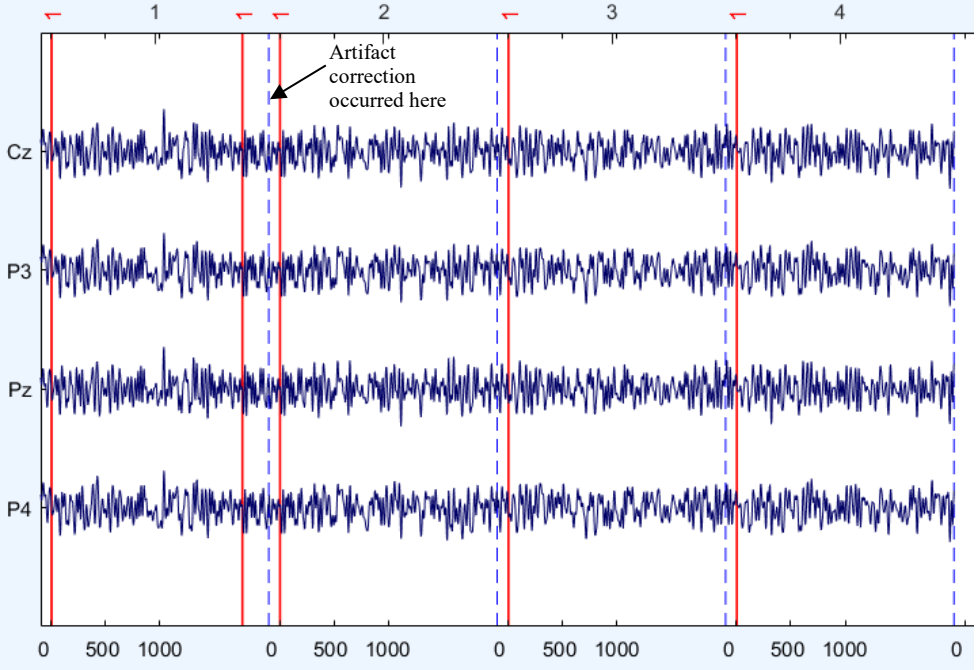

Figure 5.6 2-second epochs

Step 5: The EEG signal was divided into three waveforms for the analysis. Theta waves (4–8 Hz), alpha waves (8–13 Hz), and beta waves (13–22 Hz) as defined by Pope et al. (1995). A 2-second FFT window was applied using the Darbeliai plugin in EEGLAB. The power spectral density (PSD) was calculated by finding the combined PSD for each waveform at the Pz, Cz, P3, and P4 electrode locations (10-20 system) and applying $\beta/(\alpha+\theta)$ (Pope et al., 1995; Prinzel III et al., 2001). The value obtained provided a quantitative measure of LA for the 10-second period.

5.6 Synchronizing and Resampling

All collected variables from the multiple equipment were synchronized using the system time and webcam recordings. This ensured that the lag between the data sets was not offset by more than half of a second across all equipment. Since the data were collected at multiple frequencies, i.e., driving simulator variables at 60 Hz, eye-tracking at 60 Hz, LA at 0.1 Hz, heart rate at 1Hz, SA at 1 Hz, and ICA at 1 Hz, multiple resampling algorithms were used to convert all data to 10 Hz. Lower frequency datasets were up-sampled while larger frequency datasets were down-sampled in MATLAB. Variables that were continuous and showed high deviations were resampled using block averages, while less-volatile variables were resampled by elimination of data points.

Time points with data losses were marked and ignored during model development and validation. The next chapter discusses the task-averaged results to establish a clear biobehavioral distinction between the six driving tasks.

Chapter 6 Results

This section provides the obtained results and discusses their relevance with respect to the six driving tasks. The null hypothesis was that changes in environment complexity do not result in changes to WL and SA and cannot be directly correlated to driving measures (compensation and performance); thus, providing no basis for incorporating these into the IDM. A significance level of 95% was used to substantiate any evidence. The results are presented in four categories: driving variables, physiological measures, subjective measures, and behavioral questionnaires. Multiple repeated measures analysis of variance (ANOVA) were performed to identify any significant differences between the various tasks and variables. Task 1 was used as the baseline.

6.1 Subjective Measures

The average NASA-TLX scores showed no significant differences between the mean scores of the task 2 and task 1 (baseline) with α set to 0.05. However, significant differences in scores were observed for task 3 *($F(1, 83) = 4.087$, $p = 0.046$, $\eta_P^2 = 0.047$, $1\text{-}\beta = 0.515$)*, task 4 *($F(1, 83) = 16.298$, $p < 0.001$, $\eta_P^2 = 0.164$, $1\text{-}\beta = 0.979$),* task 5 *($F(1, 83) = 35.230$, $p < 0.001$, $\eta_P^2 = 0.298$, $1\text{-}\beta = 1.000$),* and task 6 *($F(1, 83) = 201.257$, $p < 0.001$, $\eta_P^2 = 0.708$, $1\text{-}\beta = 1.000$)* with the baseline (shown in Figure 6.1). The increase in NASA-TLX scores suggest that the developed tasks captured a variability in WL due to increased complexity.

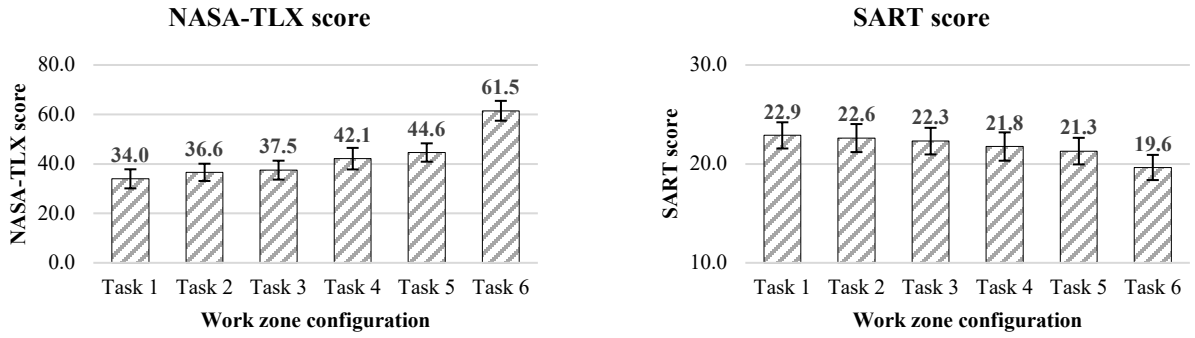

Figure 6.1 Average NASA-TLX and SART scores

Individual NASA-TLX subscales (i.e., mental demand, physical demand, temporal demand, performance, effort, and frustration) were also analyzed for an in-depth understanding of the scores as shown in figure 6.2.

Mean mental demand was found to be significantly different for all tasks when compared to the baseline (task 2 *($F(1, 83) = 5.138$, $p = 0.026$, $\eta_P^2 = 0.058$, $1\text{-}\beta = 0.610$)*; task 3 *($F(1, 83) = 4.939$, $p = 0.029$, $\eta_P^2 = 0.056$, $1\text{-}\beta = 0.594$);* task 4 *($F(1, 83) = 13.448$, $p < 0.001$, $\eta_P^2 = 0.139$, $1\text{-}\beta = 1$)*; task 5 *($F(1, 83) = 30.716$, $p < 0.001$, $\eta_P^2 = 0.270$, $1\text{-}\beta = 1$);* task 6 *($F(1, 83) = 190.880$, $p < 0.001$, $\eta_P^2 = 0.697$, $1\text{-}\beta = 1$)*). Physical demand was also found to be significantly different but only for task 4 *($F(1, 83) = 4.687$, $p = 0.033$, $\eta_P^2 = 0.053$, $1\text{-}\beta = 0.571$)*, task 5 *($F(1, 83) = 9.050$, $p = 0.003$, $\eta_P^2 = 0.098$, $1\text{-}\beta = 0.845$)*, and task 6 *($F(1, 83) = 80.344$, $p < 0.001$, $\eta_P^2 = 0.492$, $1\text{-}\beta = 1$)*. Similar results were also found for the mean of the temporal demand scores, with only task 4 *($F(1, 83) = 14.501$, $p < 0.001$, $\eta_P^2 = 0.149$, $1\text{-}\beta = 0.964$)*, task 5 *($F(1, 83) = 30.301$, $p < 0.001$, $\eta_P^2 = 0.267$, $1\text{-}\beta = 1.000$)*, and task 6 *($F(1, 83) = 156.538$, $p < 0.001$, $\eta_P^2 = 0.653$, $1\text{-}\beta = 1.000$)* configurations showing significant differences to the baseline. Mean performance scores were significantly different for task 5 *($F(1, 83) = 4.624$, $p = 0.034$, $\eta_P^2 = 0.053$, $1\text{-}\beta = 0.566$)* and task 6 *($F(1, 83) = 17.367$, $p < 0.001$, $\eta_P^2 = 0.173$, $1\text{-}\beta = 0.985$)* only.

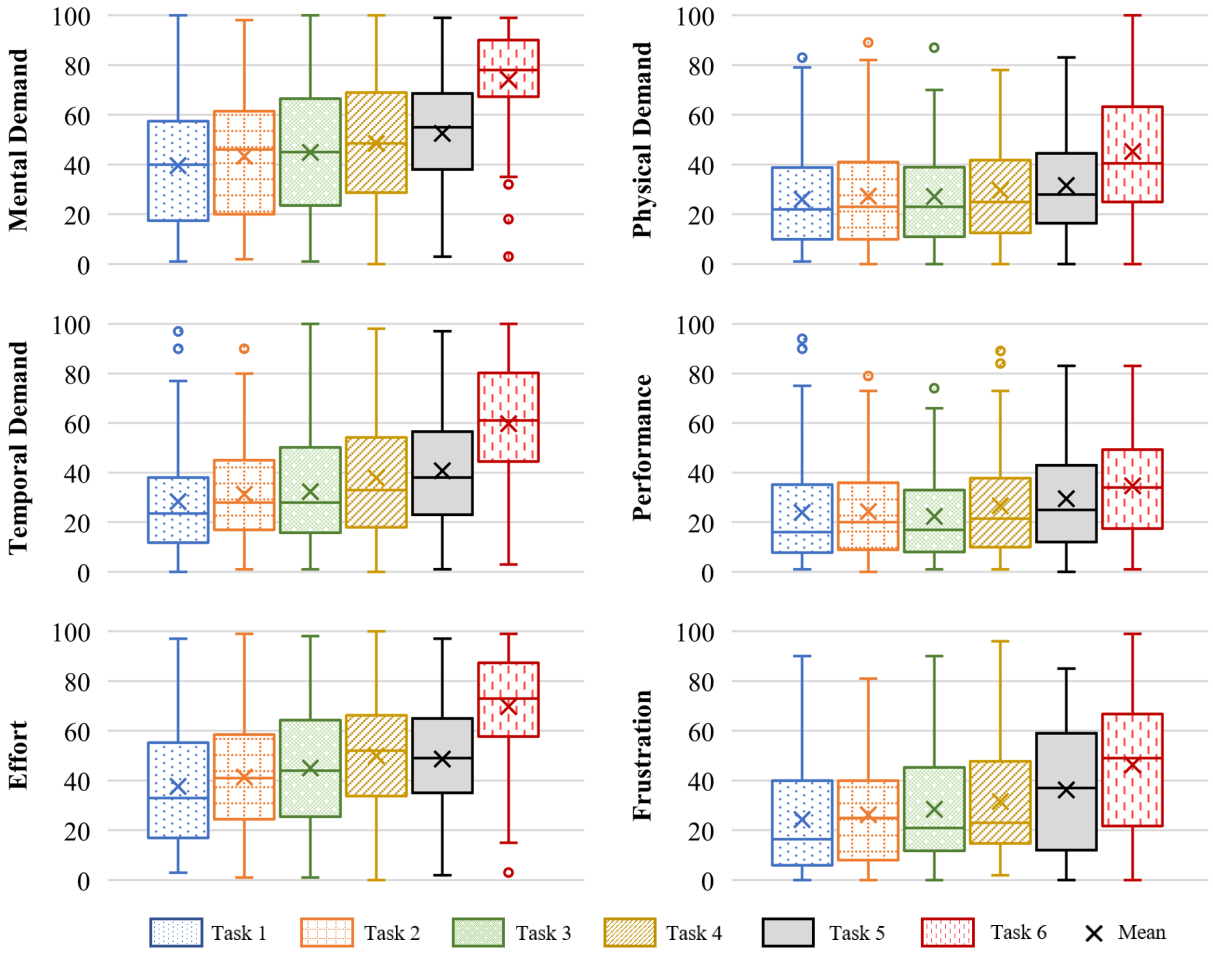

Figure 6.2 NASA-TLX subscale scores by task (a) Mental demand, (b) Physical demand, (c) Temporal demand, (d) Performance, (e) Effort, and (f) Frustration

Mean effort scores were significantly different for task 3 *($F(1, 83) = 10.531$, $p = 0.002$, $\eta_P^2 = 0.113$, $1\text{-}\beta = 0.894$)*, task 4 *($F(1, 83) = 19.722$, $p < 0.001$, $\eta_P^2 = 0.192$, $1\text{-}\beta = 0.992$)*, task 5 *($F(1, 83) = 22.109$, $p < 0.001$, $\eta_P^2 = 0.210$, $1\text{-}\beta = 0.996$)*, and task 6 *($F(1, 83) = 145.655$, $p < 0.001$, $\eta_P^2 = 0.637$, $1\text{-}\beta = 1$)*. Finally, mean frustration scores were significantly different for task 4 *($F(1, 83) = 6.473$, $p = 0.013$, $\eta_P^2 = 0.072$, $1\text{-}\beta = 0.710$)*, task 5 *($F(1, 83) = 24.648$, $p < 0.001$, $\eta_P^2 = 0.229$, $1\text{-}\beta = 0.998$)*, and task 6 *($F(1, 83) = 50.755$, $p < 0.001$, $\eta_P^2 = 0.379$, $1\text{-}\beta = 1$)*. Overall, individual subscale scores showed similar results to the weighted NASA-TLX score.

Increase in mental demand, physical demand, temporal demand, effort, and frustration was observed with complexity. However, an increase in performance scores with an increase in task demand indicated a reduction in driving performance.

Similar trends were observed with the SART scores. No significant differences were observed between the mean scores of the task 2 and task 3 configurations with respect to the baseline, but task 4 *($F(1, 83) = 7.448$, $p = 0.008$, $\eta_P^2 = 0.082$, $1\text{-}\beta = 0.770$)*, task 5 *($F(1, 83) = 7.840$, $p = 0.006$, $\eta_P^2 = 0.086$, $1\text{-}\beta = 0.790$)*, and task 6 *($F(1, 83) = 26.794$, $p < 0.001$, $\eta_P^2 = 0.244$, $1\text{-}\beta = 0.999$)* showed significant differences. With the complexity and demand of the tasks increasing, an increase in subjective workload scores was observed along with a decrease in SART scores. This trend seems consistent with the framework theorized and the TCI. Table 6.1 provides a summary of the descriptive statistics for key variables.

Table 6.1 Descriptive statistics of various measures (mean ± SD)

Variable	N	Task 1	Task 2	Task 3	Task 4	Task 5	Task 6
Avg NASA-TLX Score	84	34.2 ± 18.0	36.5 ± 16.2	37.1 ± 17.8	41.5 ± 20.0	44.5 ± 17.2	61.1 ± 18.6
Avg SART Score	84	22.8 ± 6.1	22.6 ± 6.6	22.1 ± 6.1	21.4 ± 6.4	21.2 ± 6.1	19.5 ± 5.9
Avg Speed (km/h)	84	117.6 ± 3.1	115.1 ± 3.4	114.6 ± 6.4	113.6 ± 3.5	112.8 ± 5.0	109.4 ± 8.7
Avg Headway (m)	83	108.1 ± 81.1	98.4 ± 62.2	86.4 ± 55.0	95.6 ± 75.3	84.5 ± 50.9	111.8 ± 60.8
Avg SDLP (m)	84	0.324 ± 0.084	0.306 ± 0.086	0.309 ± 0.076	0.274 ± 0.066	0.261 ± 0.062	0.286 ± 0.085
Avg Lap Time (s)	85	197.5 ± 5.0	203.8 ± 14.9	203.9 ± 15.0	204.9 ± 9.3	207.9 ± 17.4	213.6 ± 26.4
Avg Heart Rate (beats per minute)	83	75.7 ± 11.7	75.6 ± 11.4	75.0 ± 11.5	75.2 ± 11.9	75.5 ± 11.8	75.4 ± 12.0
Avg Blink Rate (blinks per minute)	85	17.0 ± 5.6	16.5 ± 5.9	16.2 ± 6.0	15.9 ± 6.5	15.5 ± 6.3	14.4 ± 4.7
Avg SD of Horizontal Gaze Position (pixels)	85	128.4 ± 42.9	126.6 ± 44.5	130.6 ± 41.4	99.7 ± 31.2	99.6 ± 33.7	93.0 ± 34.3
Avg SA as a function of comprehension	82	0.704 ± 0.279	0.633 ± 0.292	0.734 ± 0.272	0.733 ± 0.268	0.714 ± 0.279	0.732 ± 0.257
Avg LA	82	1.235 ± 0.355	1.253 ± 0.361	1.240 ± 0.362	1.262 ± 0.382	1.219 ± 0.333	1.236 ± 0.343

6.2 Driving Variables

Driving variables were used to detect imbalance between mental workload and situation awareness. The correlation of these variables to subjective measures discussed in section 6.1 is key to this research. Average headway was one of the key variables in detecting changes to longitudinal control. Significant differences were obtained for tasks 3 *($F(1, 82) = 7.168$, p =*

0.009, η_P^2 *= 0.080, 1-β = 0.754)* and 6 *(F(1, 82) = 8.186, p = 0.005,* η_P^2 *= 0.091, 1-β = 0.807)*, where participants were observed to maintain closer headways than the baseline. It can also be noted that the pairwise tests revealed significant differences between task 5 and task 6 *(Mean difference = -89.510, p = 0.001)* with participants observed maintaining larger headways when engaged in the visual distraction.

Average speed was a more sensitive measure in this study as a decreasing trend was observed across all tasks (from 2 to 6) as shown in figure 6.3. All tasks were significantly different to the baseline: task 2 *(F(1, 83) = 46.897, p < 0.001,* η_P^2 *= 0.361, 1-β = 1.000)*; task 3 *(F(1, 83) = 21.748, p < 0.001,* η_P^2 *= 0.208, 1-β = 0.996)*; task 4 *(F(1, 83) = 133.949, p < 0.001,* η_P^2 *= 0.617, 1-β = 1.000)*; task 5 *(F(1, 83) = 97.801, p < 0.001,* η_P^2 *= 0.541, 1-β = 1.000)*; and task 6 *(F(1, 83) = 98.844, p < 0.001,* η_P^2 *= 0.544, 1-β = 1.000)*. However, tasks 2 and 3 alongside tasks 3, 4, and 5 showed no pairwise differences amongst each other. This could indicate no significant imbalance in the TCI for these tasks. A high inverse correlation can also be observed to the average NASA-TLX scores.

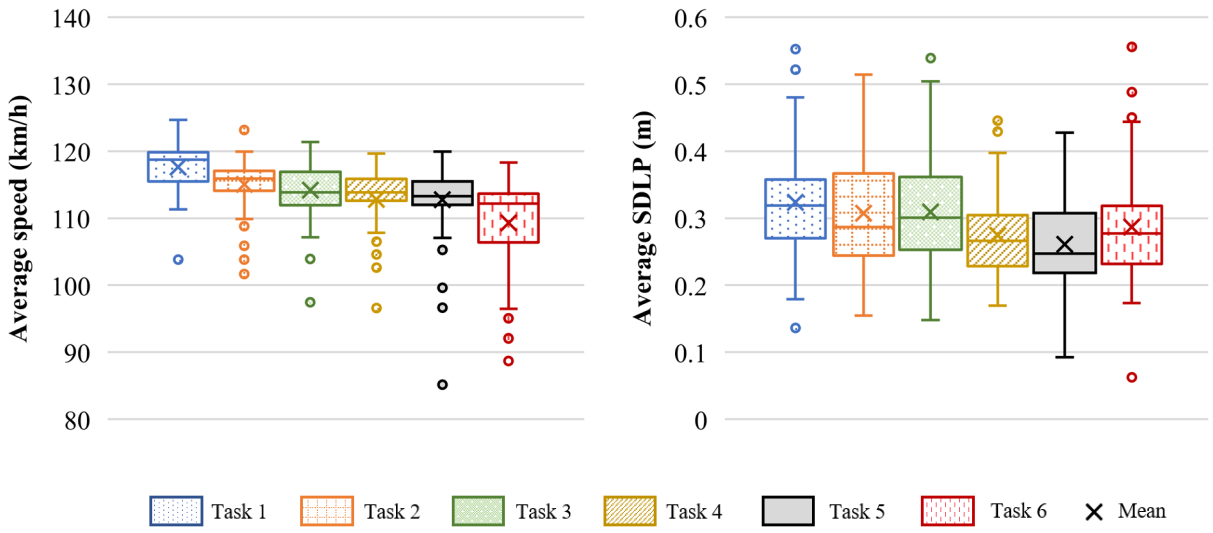

Figure 6.3 (a) Average speed and (b) average SDLP by task

Average standard deviation of lateral position (SDLP) was also found to change along with task complexity. Significant differences were observed between the baseline and tasks 4 *($F(1, 83) = 29.791$, $p < 0.001$, $\eta_P^2 = 0.264$, $1\text{-}\beta = 1.000$)*, 5 *($F(1, 83) = 42.691$, $p < 0.001$, $\eta_P^2 = 0.340$, $1\text{-}\beta = 1.000$)*, and 6 *($F(1, 83) = 10.622$, $p = 0.002$, $\eta_P^2 = 0.113$, $1\text{-}\beta = 0.896$)*. Average SDLP was observed to decrease (improved lane-keeping ability) with substantial increase in task complexity. This was similar to what was observed by past research where a decrease in SDLP was assumed to occur due to lateral position being inherently performed at a level below optimal, unless being subjected to higher cognitive load (Cooper et al. 2013, He et al. 2014, Li et al. 2018, Kountouriotis et al. 2015, Wang et al. 2014).

Average lap time was also used as a driving variable, indicating the time taken to complete a stretch of four miles of roadway across the six tasks. Significant differences were observed across all tasks and the baseline: task 2 *($F(1, 84) = 13.742$, $p < 0.001$, $\eta_P^2 = 0.141$, $1\text{-}\beta = 0.956$)*; task 3 *($F(1, 84) = 17.031$, $p < 0.001$, $\eta_P^2 = 0.169$, $1\text{-}\beta = 0.983$)*; task 4 *($F(1, 84) =$*

61.899, $p < 0.001$, $\eta_P^2 = 0.424$, 1-$\beta = 1.000$); task 5 *($F(1, 84) = 33.030$, $p < 0.001$, $\eta_P^2 = 0.282$, 1-$\beta = 1.000$)*; and task 6 *($F(1, 84) = 38.614$, $p < 0.001$, $\eta_P^2 = 0.315$, 1-$\beta = 1.000$).* This was expected as average speed was observed to decrease with increase in task complexity and demand.

Overall, on a holistic level, some substantial differences were observed across the various tasks, suggesting positive progress towards the theorized framework. Time-series data analysis was performed as described in section 6.5 to study the interaction of these variables and car-following behavior.

6.3 Physiological Measures

As stated in the literature, physiological measures are also observed to change with respect to imbalance in WL and SA. The average heart rate was found to not be significant between most of the tasks except for task 3 *($F(1, 82) = 5.712$, $p = 0.019$, $\eta_P^2 = 0.065$, 1-$\beta = 0.656$)*, which was significantly less than the baseline. However, physiological measures might not be good predictors as an average value, rather using time-series analysis would provide more sensitive results.

SD of horizontal gaze position was also used as a key variable (shown in fig. 6.4). Research has shown a decrease in horizontal gaze variability with increasing cognitive workload. Significant gaze position differences were observed in tasks 4 *($F(1, 84) = 66.023$, $p < 0.001$, $\eta_P^2 = 0.440$, 1-$\beta = 1.000$)*, 5 *($F(1, 84) = 49.379$, $p < 0.001$, $\eta_P^2 = 0.370$, 1-$\beta = 1.000$)*, and 6 *($F(1, 84) = 81.746$, $p < 0.001$, $\eta_P^2 = 0.493$, 1-$\beta = 1.000$)* (Kummetha et al., 2020). A decreasing trend as observed in past research was observed, indicating changes to mental workload across the tasks (Cooper et al. 2013).

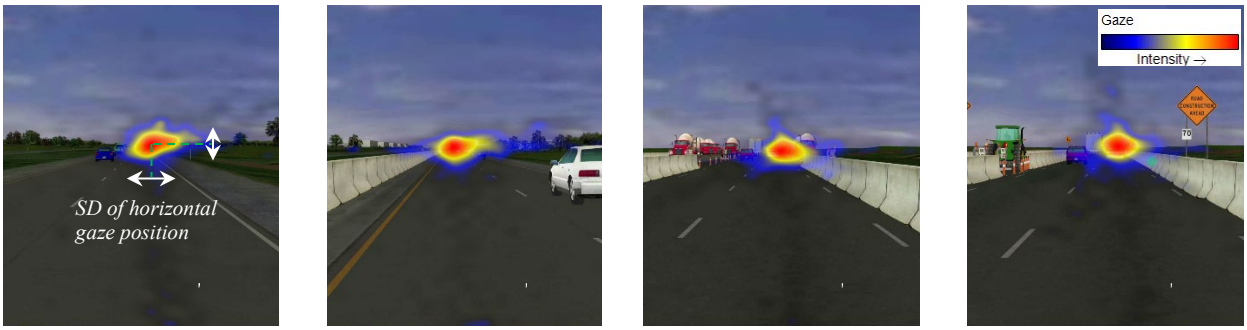

Figure 6.4 Gaze position variability (Driver ID 79)

The average blink rate was also used to determine changes in WL. Significant differences were observed for tasks 3 *($F(1, 84) = 4.262$, $p = 0.042$, $\eta_P^2 = 0.048$, $1\text{-}\beta = 0.532$),* task 4 *($F(1, 84) = 6.680$, $p = 0.011$, $\eta_P^2 = 0.074$, $1\text{-}\beta = 0.724$),* task 5 *($F(1, 84) = 17.765$, $p < 0.001$, $\eta_P^2 = 0.175$, $1\text{-}\beta = 0.986$),* and task 6 *($F(1, 84) = 35.679$, $p < 0.001$, $\eta_P^2 = 0.298$, $1\text{-}\beta = 1.000$)* (Kummetha et al., 2020). A decreasing blink rate with increasing WL was noted from the results.

No significant differences were observed across the six tasks with the average SA score obtained by using driver comprehension. Average LA scores were found to be consistent across all tasks. Also, no correlation was observed between the SART and driver comprehension-based SA scores.

6.4 Behavioral Questionnaires

The relationships between driving performance and the behavioral assessments was measured using a series of Pearson correlations with a statistical significance value set at $p = .05$ (two-tailed). Our dependent measures for the six driving tasks included the following: self-reported estimated miles driven annually; love of driving; self-reported number of traffic violations or tickets/year; self-reported following distance at 70, 50, and 30 mph zones; average driving speed during simulated drive; SD of lateral position in feet; average headway in feet during the simulated drive; average heart-rate in beats per minute; average pupil diameter in mm;

average gaze fixation in seconds; and the index of cognitive activity from the right pupil. We also examined possible relationships between the self-reported behavioral measures and the NASA-TLX as well as the SART.

Participants who scored higher on the PANAS (indicating positive mood) reported significantly higher preference and love of driving *(r = .32, p = .003)* but also deviated significantly from their driving lanes during task 1 *(r = .33, p = .002)* and task 3 *(r = .325, p = .002)*. Participants who scored higher on this scale further showed lower scores on the NASA-TLX index *(r = -.29, p = .007)* indicating lower perceived workload during the simulated drive. Given that the PANAS measured current mood of an individual and was performed during the pre-screening phase (which could have occurred up to two months before the drive), the correlation to the simulated drive and the cognitive load measures for most participants were affected by a time lag. Future studies should implement the administration of the PANAS immediately preceding the simulated drive for the valid examination of the impact of current mood. Nevertheless, these findings point to a relationship between mood and affective disposition and driving performance.

Significant relationships were observed between the CRT and driving behavior and performance measures. Performance on the CRT was negatively correlated with SART scores for tasks 4 *(r = -.28, p = .009)* and 6 *(r = -.27, p = .01),* suggesting that participants with higher cognitive reflection evaluated the driving simulation as less cognitively demanding relative to participants who scored lower on the cognitive reflection task. Given that the CRT is a relatively stable measure of cognitive engagement, this is an aspect of participants' disposition that can add value to understanding driver behavior.

The five-factor model of personality generates scores for each participant on five main aspects of personality that are considered situationally stable: neuroticism, extraversion, openness to experience, agreeableness, and conscientiousness. Participants scoring high in neuroticism tended to drive significantly faster during the simulated drive for the higher difficulty tasks 5 *(r = .25, p = .02)* and 6 *(r = .22, p = .04)*. They also not only showed lower SDLP *(r = -.28, p = .01)* but lower average headway *(r = -.21, p = .047)* for the first task. Participants higher in neuroticism also showed consistently lower gaze fixations across all six tasks *(all ps < .05)*. Neuroticism scores were negatively correlated with extraversion *(r = -.31, p = .003)*, agreeableness *(r = -.28, p = .008)*, and conscientiousness *(r = -.34, p = .001)* scores. Participants higher in extraversion reported significantly higher preference for driving *(r = .36, p = .001)*, but also higher self-reported annual traffic violations *(r = .21, p = .04)*. In line with these findings, participants higher in extraversion deviated significantly from their lanes during task 1 *(r = .30, p = .005)* and task 5 *(r = .28, p = .01)*. They also showed significantly higher pupil dilation for tasks 1 through 4 *(all ps < .05)* indicating higher arousal. Participants scoring higher in openness to experience, also self-reported more annual traffic violations *(r = .28, p = .009)*. Participants higher in agreeableness tended to report that they follow vehicles very closely at 30 mph zones *(r = .24, p = .03)*. Lastly, participants higher in conscientiousness tended to report that they follow vehicles very closely at 30 mph zones *(r = .22, p = .04)*, but also drove slower during task 2 of the simulated drive *(r = .22, p = .04)*. Overall, the findings from the personality measures strongly suggest their importance in driving performance.

To capture different but complimentary aspects of empathy, two measures of empathy were used—the Interpersonal Reactivity Index (IRI) and the Empathy Assessment Index (EAI). The IRI (Davis 1983) is the earliest and most widely used multidimensional measure of empathy,

which includes four factors: perspective taking (i.e., the tendency to spontaneously adopt others' psychological point of view), fantasy (i.e., respondents' tendencies to transpose themselves imaginatively into the feelings and actions of fictitious characters in books, movies, and plays), empathic concern (i.e., the tendency to have sympathy for others' concerns and problems), and personal distress (i.e., feelings of personal anxiety and unease in tense interpersonal settings). We used this measure due to its prevalence in the literature; however, we note that it has been recently re-evaluated as potentially of lower validity and less accuracy of empathy assessments (Chrysikou & Thompson 2016). Our results showed that participants who scored high on the perspective taking subscale of the IRI, reported higher number of traffic violations *($r = .21$, $p = .047$)*, as well as a tendency to follow others closely at 70 mph *($r = -.24$, $p = .02$)* and 50 mph *($r = -.25$, $p = .02$)* zones. Participants who scored higher on the fantasy scale also tended to report significantly more traffic violations *($r = .24$, $p = .025$)* and lower scores on the SART in tasks 4 *($r = -.28$, $p = .008$)* and 5 *($r = -.25$, $p = .02$)*. Higher scores on the personal concern subscale were significantly associated with higher NASA-TLX scores for tasks 1 through 5 *(all $ps < .05$)*. Higher scores on the personal distress subscale were significantly associated with self-reported tendency to allow for a farther following distance at 30 mph zones *($r = .22$, $p = .035$).* On the other hand, during the simulated drive, higher scores on this scale were associated significantly with increased average speeds during tasks 5 *($r = .26$, $p = .016$)* and 6 *($r = .31$, $p = .004$)*, as well as reduced average headway on tasks 1 *($r = -.21$, $p = .049$)*, 2 *($r = -.26$, $p = .016$)*, and 5 *($r = -.36$, $p = .001$)*. These results on the personal distress scale mirror those of the personality trait of neuroticism, suggesting that general self-oriented anxiety may be associated with higher speeds and smaller headway distances—both evidence of a more aggressive driver profile.

The EAI is a more recent measure of empathy that is designed to capture a multidimensional model of empathy that is based on social cognitive neuroscience principles (Gerdes et al. 2011). The scale includes five sub-scales intended to tap on: participants' affective responses, their ability for emotion regulation, their ability for perspective taking, their awareness of self and others, and their empathic attitudes. Higher scores on the emotion regulation subscale were consistently associated with higher average pupil diameter for all tasks *(rs range from .22 to .30 and all ps <.05)* and marginally for task 2 *(r = .21, p = .07)*. Participants scoring higher on perspective taking reported closely following vehicles at 70 mph *(r = -.27, p = .01)*, 50 mph *(r = -.23, p = .03)*, and 30 mph *(r = -.26, p = .01)* zones. Increased scores on self-other awareness were also consistently associated with higher average pupil diameter across all tasks *(all ps < .05)*, whereas increased empathic attitudes were associated with decreased liking of driving overall *(r = -.31, p = .004)* and increased headway in feet but for task 1 only *(r = .23, p = .03)*. Overall, this measure of empathy did not provide as many insights on driving behavior as the IRI.

Consistent with the nature of the scale, increased scores on this scale were associated with decreased likelihood to self-report traffic violations *(r = -.25, p = .016)*. Also, there were no significant relationships between performance on these measures and any self-reported measures or driving performance variables.

In summary, despite the relatively high temporal time between the administration of the behavioral assessments and the driving simulation session, the above results indicate that self-reported assessments of mood, personality, and empathy can be useful indicators of driving behavior. Specifically, a general tendency for positive mood and extraversion may be linked to more traffic violations, higher speeds, and increased lateral position deviations, possibly due to

increased distractibility. On the other hand, neuroticism and empathic distress that can serve as indicators of self-oriented anxiety, were consistently associated with increased speeds and lane deviations during the simulated drive. The examination of these variables in the context of the IDM, might add another dimension to car-following behavior.

6.5 Time-Series Data

Average values of variables do not always provide useful information. Comparing variables at specific points in time shows their probable relationships and correlations. Multiple Pearson correlation tests were carried out with respect to the variables with the greatest potential of being utilized in the car-following model. As speed was one of the most important factors in the model, several other driving and physiological measures were compared to it. Data from all drivers was compiled for all six tasks in one series and analyzed.

A high negative correlation was obtained between speed and SDLP $(r = -.124, p < 0.001)$ indicating lower variability in lane position at high speeds. Heart rate and speed were found to be positively correlated with higher speeds resulting in elevated heart rates $(r = 0.019, p < 0.001)$. This can be clearly observed in figure 6.5. No significant correlation was obtained between true LA (not normalized) scores and speed $(r = -0.001, p = 0.372)$. A significant correlation was observed between Speed and WL established from ICA of the left eye $(r = 0.022, p < 0.001)$. The data shows some valid relationships that might be useful to predict speeds during car-following. Figure 6.5 shows a sample time-series plot during the sixth task and the blue arrows indicate the duration of the distraction events. SDLP, heart rate, and WL_ICA can be observed to increase during the distractions.

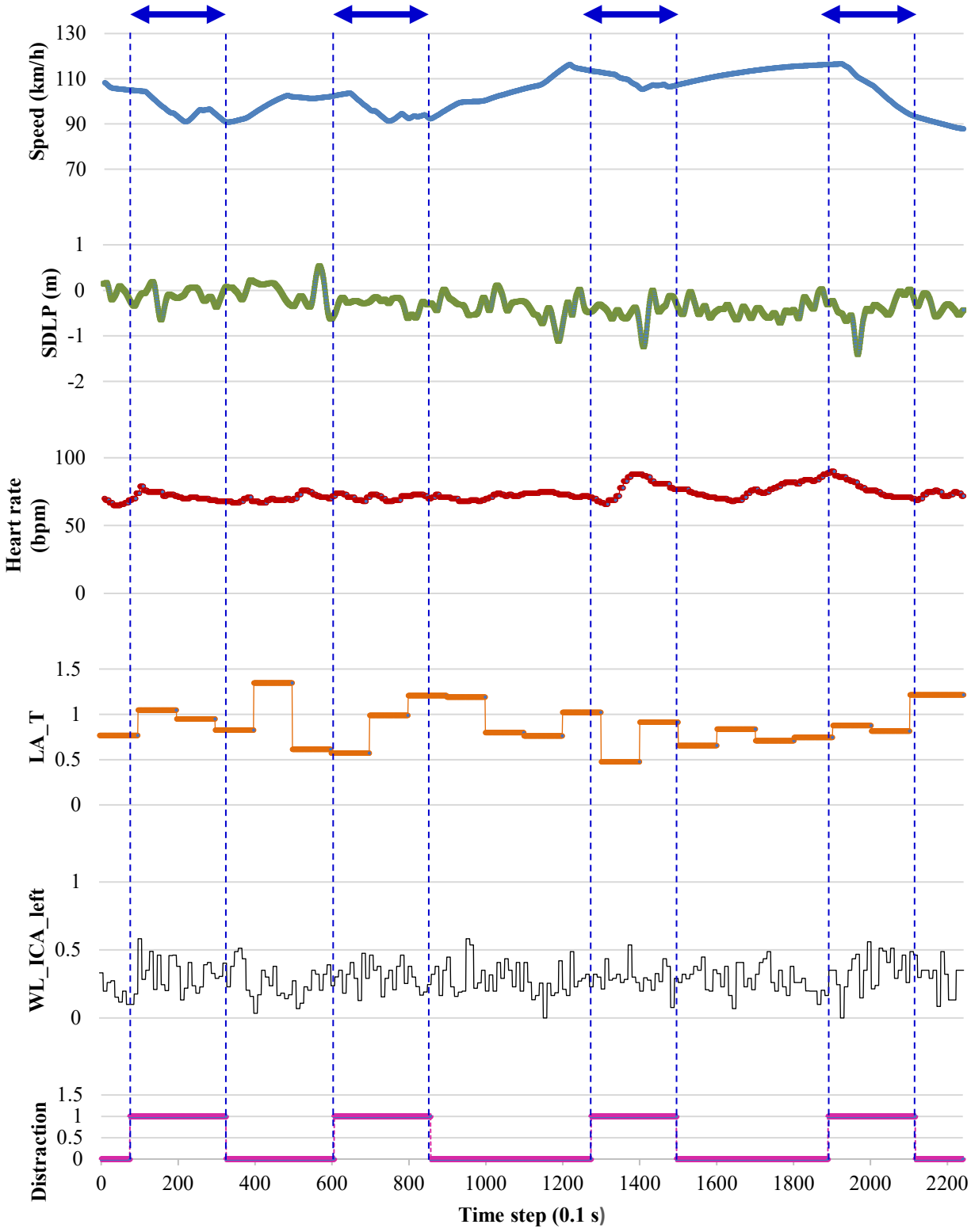

Figure 6.5 Time-series profile for driver ID 3 (a) Speed, (b) SDLP, (c) Heart rate, (d) true LA score, (e) WL as a function of the left eye, and (f) Distraction – Task 6

6.6 Summary

In summary, average scores of driving variables (i.e., speed, headway, and SDLP) and subjective measures (i.e., NASA-TLX and SART) were effective in establishing the demand of the tasks. However, physiological measures were not sensitive due to the high variance between individuals. Variability in physiological measures was more apparent in time-series analysis.

Behavioral questionnaire data showed some promising results such as the tendency for positive mood and extraversion to be linked to more traffic violations, higher speeds, and increased lateral position deviations. This information was used in grouping individuals during the model development.

Chapter 7 Model Development and Validation

The proposed behavioral IDM (b-IDM) was assumed to optimize calibrating multiple car-following trajectories by grouping drivers with similar performance traits (i.e., supervised learning). In this research, participants were categorized based on their driving performance across all six tasks by evaluating their maximum speed (m/s), absolute maximum jerk (m/s^3), and minimum time gap (s). Only 80 participants were used in the clustering as four datasets showed bad/noisy data especially from the EEG device and eye tracker while data from six participants were excluded due to simulator sickness. A 75/25 split was used for model development and validation, respectively.

Multiple clustering algorithms (Two-Step, K-Means, and Hierarchical) were used to obtain distinct groups of drivers. The K-Means clustering algorithm resulted in the most distinct clusters (i.e., $p < 0.001$). Figure 7.1 shows the obtained driver groups.

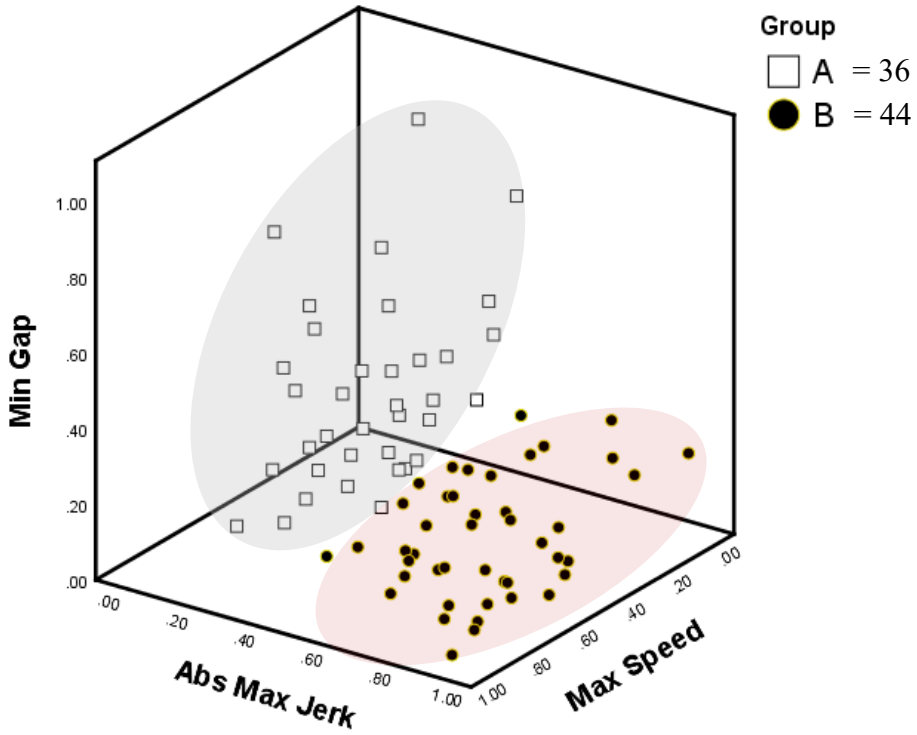

Figure 7.1 Established driver clusters

An optimal solution was reached with two distinctive clusters of similar size. Group A consisted of 36 drivers and group B consisted of 44 drivers (*Minimum gap*: $F(1, 78) = 27.187$, $p < 0.001$; *Absolute maximum jerk*: $F(1, 78) = 164.415$, $p < 0.001$; *Maximum speed*: $F(1, 78) = 17.456$, $p < 0.001$).

Table 7.1 shows the properties of the obtained driver groups. Both groups consisted of a similar number of male and female drivers. Group A consisted of drivers that followed larger gaps, lower maximum jerk, and lower maximum speeds, while they also had a lower average age and driving experience. Group B consisted of more aggressive drivers who exhibited greater overall speeds, shorter following gaps, and larger maximum jerk. Cluster properties also indicated that group B drivers had more driving experience, annually drove more miles, and

experienced a lower maximum NASA-TLX score (i.e., experienced less WL in the most complex driving task).

Table 7.1 Cluster properties

Variables	Normalized cluster centers			Mean ± SD	
	A	B	Sig.	A	B
Minimum Gap (s)	0.36	0.16	< 0.001	1.12 ± 0.51	0.67 ± 0.23
Absolute Maximum Jerk (m/s^3)	0.31	0.78	< 0.001	4.29 ± 1.40	8.16 ± 1.30
Maximum Speed (m/s)	0.42	0.60	< 0.001	35.69 ± 1.27	37.05 ± 1.55
Age (years)				27.06 ± 11.65	34.25 ± 14.17
Driving Experience (years)				10.42 ± 12.20	17.82 ± 14.85
Annual Mileage				10740 ± 7450	13890 ± 9390
Maximum SDLP (m)				0.37 ± 0.21	0.39 ± 0.08
Maximum Acceleration (m/s^2)				0.828 ± 0.269	1.647 ± 0.816
Maximum Deceleration (m/s^2)				-2.644 ± 1.404	-4.541 ± 1.481
Maximum NASA-TLX score				64.05 ± 14.90	60.29 ± 19.17
Minimum SART score				17.31 ± 5.73	17.41 ± 5.85

To correlate the self-reported questionnaire data (i.e. driving experience, traffic violations, following gap, accident history, take pleasure in driving, braking behavior, cell phone usage, CRT score, PANAS, IRI, PES, EAI, moral dilemmas, and neuroticism) and the subjective

behavioral traits (i.e. NASA-TLX and SART) with performance variables, additional clustering was conducted. This could not be accomplished perfectly; however, it was noted that participants were able to accurately gauge their desired speeds. A significant correlation was obtained between the self-reported speeds and the maximum speeds (figure 7.2) recorded from the driving study. A Pearson correlation coefficient of 0.362 was attained *($N = 80$, $p < 0.001$)*. The observed offset could be a result of using the maximum achieved speed in a simulator setting versus a generalized self-reported question.

No significant correlation *($r = 0.211$)* was observed between the self-reported and simulator-recorded gaps *($N = 80$, $p = 0.06$)*. Since gaps are not usually displayed in the instrument cluster of a vehicle, they are largely estimated by drivers and thus the result seemed intuitive.

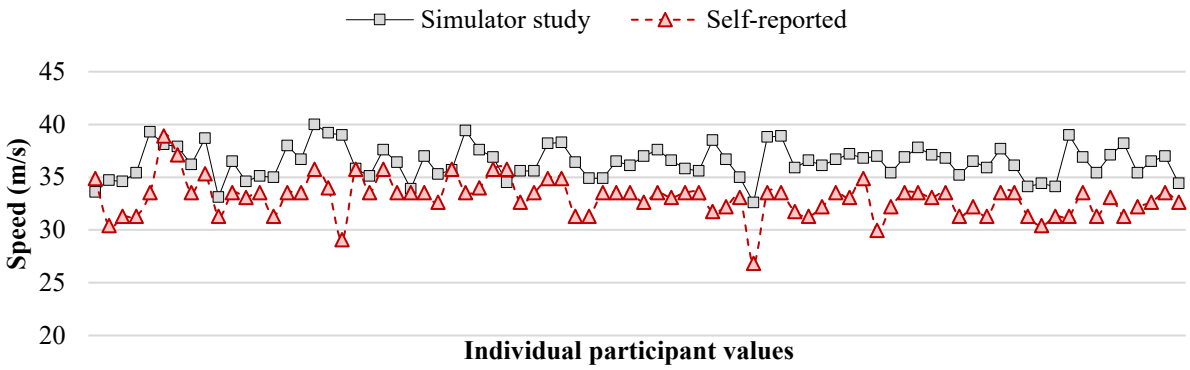

Figure 7.2 Comparison of self-reported and simulator-recorded speeds

It was concluded that overall driving performance cannot be predicted solely based on demographic and subjective data. Driving metrics are a crucial part of the puzzle and cannot be entirely substituted for subjective data.

Three variations of the IDM were compared: calibrated IDM, group IDM, and b-IDM. The calibrated IDM utilized individual-specific parameters rather than the identified group traits. Basic calibration was carried out using the naturalistic driving parameters provided in table 2.1.

The group IDM and b-IDM are modeled using the group maximum speeds, group minimum gaps, group maximum accelerations, and group minimum decelerations. The unchanged group parameters for the group IDM and b-IDM are shown in table 7.2.

Table 7.2 IDM group parameters

IDM Variables	**Group A**	**Group B**
$v_0(t)$ – maximum speed	37.0 m/s	38.6 m/s
a_{max} – maximum acceleration	1.097 m/s^2	2.464 m/s^2
b_{max} – maximum deceleration	4.048 m/s^2	6.022 m/s^2
T_n – minimum gap	0.610 s	0.440 s
δ – unchanged parameter	4	4
s_0 – standstill distance	2 m	2 m

The top four variables (i.e., $v_0(t)$, a_{max}, b_{max}, and T_n) for the groups are obtained by taking one upper standard deviation of the relevant cluster properties obtained in table 7.1. This made sure that at least two-thirds of the group population were accounted for by the chosen interval.

The goal seek function in excel was used to attain values of α shown in equation 7.1. Any value of alpha that exceeded the constraint $0 < \alpha \leq 1$ was set to 1. Equation 7.1. revisits the theorized additions to the IDM.

$$a_n(t) = a_{max}\left[1 - \left(\frac{v_n(t)}{(\alpha)v_0(t)}\right)^{\delta} - \left(\frac{s^*{}_n(t)}{s_n(t)}\right)^2\right]; \quad 0 < \alpha \leq 1 \tag{7.1}$$

$$s^*{}_n(t) = s_0 + \left(\frac{1}{\alpha}\right)T_n v_n(t) + \frac{v_n(t)\Delta v_n(t)}{2\sqrt{a_{max}b_{max}}}$$

Several variables were used as inputs to the model and they include: WL from ICA, WL from normalizing heart rate (WL_HR), raw pupil diameter, raw heart rate, raw LA, normalized LA, normalized SA, leader brake-light activation, presence of distraction (1 = distracted, 0 = not distracted), leader acceleration, and leader velocity. Each driver could exhibit multiple trajectories. This was a result of considering car-following with a constraint gap of five seconds, as past research indicates that any car-following gap that exceeds five seconds cannot be considered as a following trajectory.

Three levels of interaction terms were used when building the model and the terms were dropped if found to be insignificant ($\alpha > 0.05$). Several linear transformations (natural log, exponential, square root, and inverse) and univariate ANCOVAs (analysis of covariance) were performed on the datasets and the natural log transformation resulted in the most appropriate fit, as confirmed by the box-cox results in RStudio (RStudio, 2020).

7.1 Group A Model

Datasets from 27 out of the 36 drivers were randomly selected to build the model while the datasets from the remaining 9 drivers were preserved for the validation set.

The residual plots for the group A participants are shown in figure 7.3. The residual plots satisfied the normality and equal variance assumptions. Although some of the interaction terms were significant, their contribution towards the R-squared value of the model were negligible and were dropped in order to prevent overfitting that could potentially hinder the validation process.

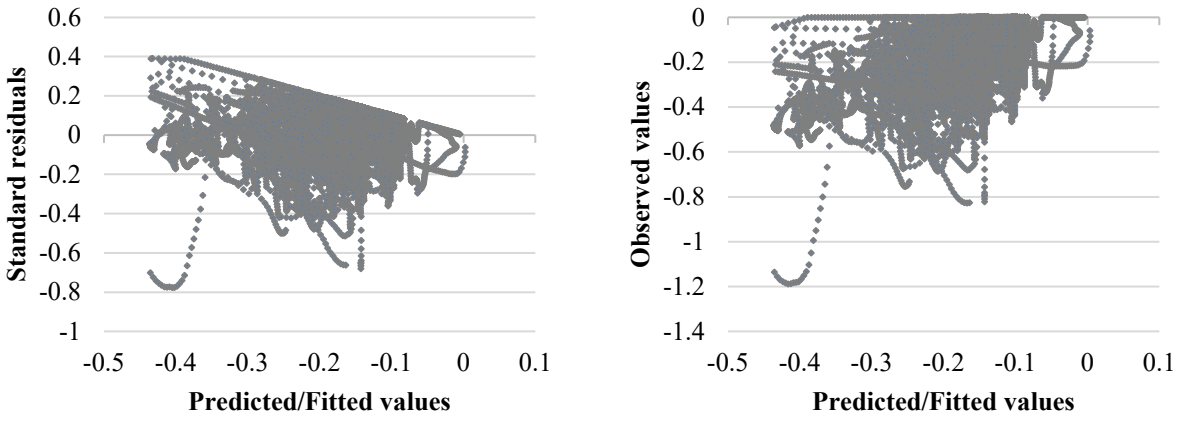

Figure 7.3 Residual plots for group A showing (a) Residuals vs predicted values and (b) Observed vs predicted values

The finalized non-linear model resulted in an R-squared value of 0.17. Although this is low, most behavioral models tend to have similar values of R-squared (between 15-40%) as having the exact same variability in physical and cognitive properties is uncommon among individuals. Also, the relatively conservative sample size used for the study restricts the predictability. Table 7.3 shows the properties of the model selected for group A drivers.

Table 7.3 Group A regression model statistics

Regression Statistics	
Multiple R	0.412
R Square	0.170
Adjusted R Square	0.170
Standard Error	0.0757
Observations	206674

ANCOVA

	df	*SS*	*MS*	*F*	*Sig*
Regression	5	241.68	48.3368	8439.464	< 0.001
Residual	206668	1183.68	0.0057		
Total	206673	1425.37			

	Coefficients	*Standard Error*	*t Stat*	*P-value*	η_p^2	*1-β*
Intercept	-2.9615	0.01441	-205.540	< 0.001	0.170	1.000
ln (LA)	-0.0005	0.00026	-1.9756	0.0482	0	0.506
ln (SA)	-0.0011	0.00026	-4.1811	< 0.001	0	0.987
ln (WL_HR)	-0.0014	0.00029	-4.7149	< 0.001	0	0.997
Distraction	-0.0324	0.00072	-44.903	< 0.001	0.010	1.000
ln (Lead v(t))	0.81614	0.00417	195.677	< 0.001	0.156	1.000

*ln denotes natural log

Achieved Model:

ln (α) = –2.9615 – 0.0005*ln (LA) – 0.0011*ln (SA) – 0.0014*ln (WL_HR) – 0.0324*Distraction – 0.81614*ln (Lead v(t))

Final model:

$$\alpha = e^{-2.9615-0.0324*Distraction} LA^{-0.0005} SA^{-0.0011} WL\_HR^{-0.0014} Lead\ v(t)^{0.81614} \quad (7.2)$$

7.2 Group B Model

Group B consisted of 44 drivers, out of which 33 were used to build the model and 11 were used for validation. The same methods described in the previous section were used. The residual plots for the observed and predicted set are shown in figure 7.4. The residual plots were observed to satisfy the normality and equal variance assumptions.

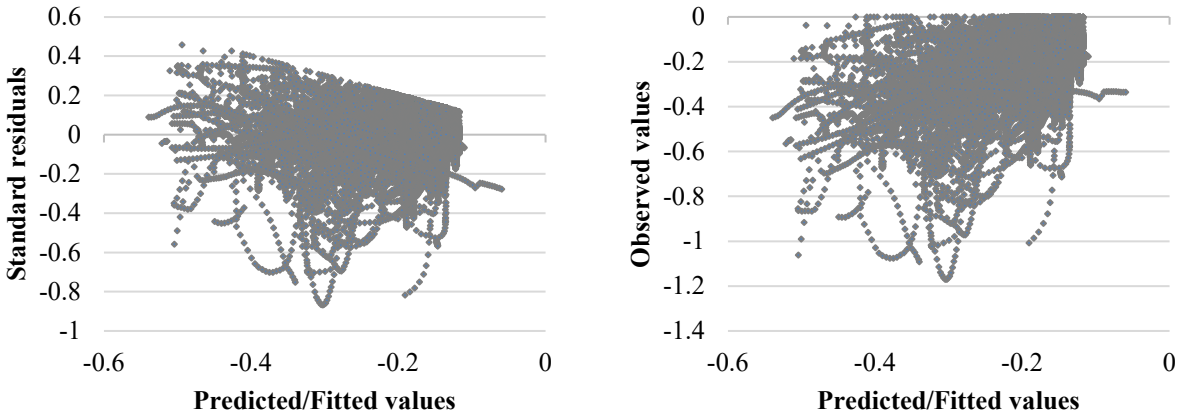

Figure 7.4 Residual plots for group B showing (a) Residuals vs predicted values and (b) Observed vs predicted values

The finalized model was also non-linear and resulted in an R-squared value of 0.205. Table 7.4 shows the properties of the model selected for group B drivers. Group B drivers also resulted in the same significant model parameters as group A, i.e., WL from normalizing heart rate (*WL_HR*), normalized LA (*LA*), normalized SA (*SA*), presence of distraction (*Distraction*), and leader velocity (*Lead v(t)*).

Table 7.4 Group B regression model statistics

Regression Statistics	
Multiple R	0.452
R Square	0.205
Adjusted R Square	0.205
Standard Error	0.073
Observations	293532

ANCOVA

	df	*SS*	*MS*	*F*	*Sig*
Regression	5	403.65	80.7310	15094.810	< 0.001
Residual	293526	1569.85	0.0053		
Total	293531	1973.51			

	Coefficients	*Standard Error*	*t Stat*	*P-value*	η_p^2	*1-β*
Intercept	-3.2796	0.01182	-277.493	< 0.001	0.208	1.000
ln (LA)	0.00104	0.00022	4.6554	< 0.001	0	0.996
ln (SA)	0.00082	0.00024	3.3808	< 0.001	0	0.922
ln (WL_HR)	-0.00051	0.00025	-2.0469	0.0407	0	0.535
Distraction	-0.0344	0.00058	-59.548	< 0.001	0.012	1.000
ln (Lead v(t))	0.89750	0.00341	263.216	< 0.001	0.191	1.000

*ln denotes natural log

Achieved Model:

ln (α) = –3.2769 + 0.00104*ln (LA) + 0.00082*ln (SA) – 0.00051*ln (WL_HR) – 0.0344*Distraction – 0.89750*ln (Lead v(t))

Final model:

$$\alpha = e^{-3.2769-0.0344*Distraction} LA^{0.00104} SA^{0.00082} WL\_HR^{-0.00051} Lead\ v(t)^{0.89750} \quad (7.3)$$

7.3 Group A Validation

Validation charts for two drivers from group A for all tasks are shown in figures 7.5 to 7.7. Graphs for the remaining participants are shown in Kummetha (2020).

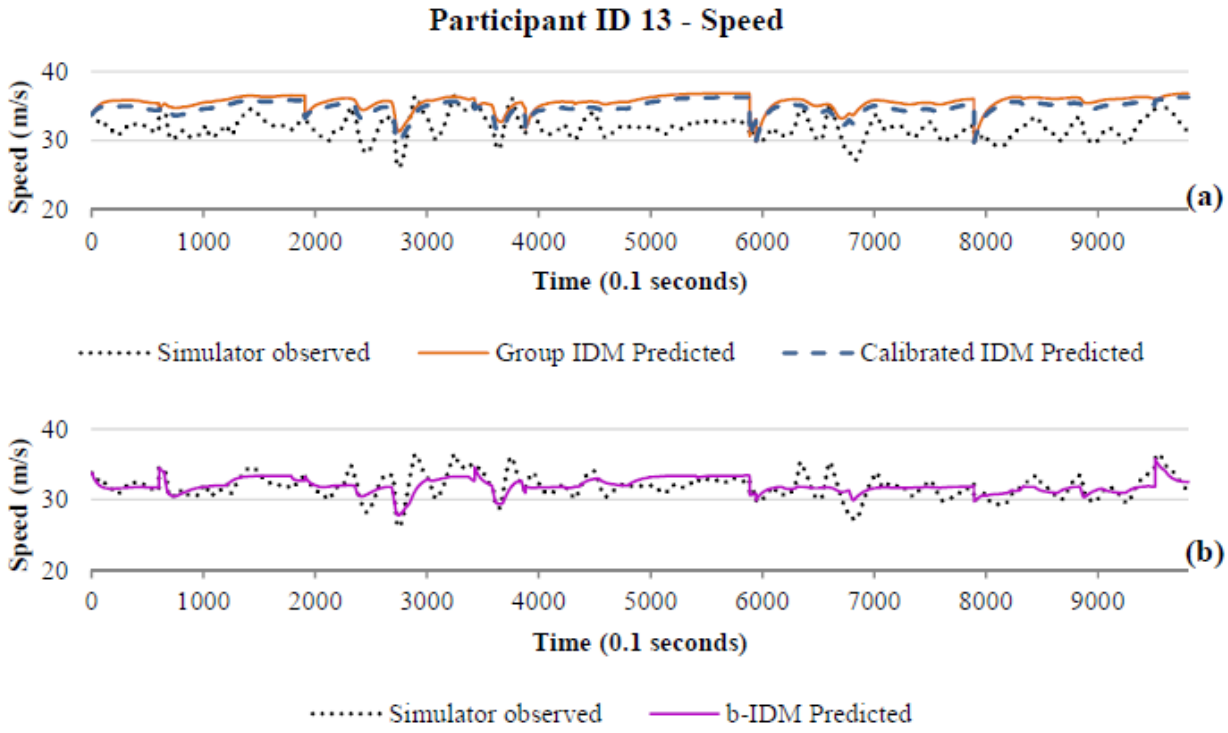

Figure 7.5 Speed validation plots for participant ID 13– (a) calibrated and group IDM predicted and (b) b-IDM predicted

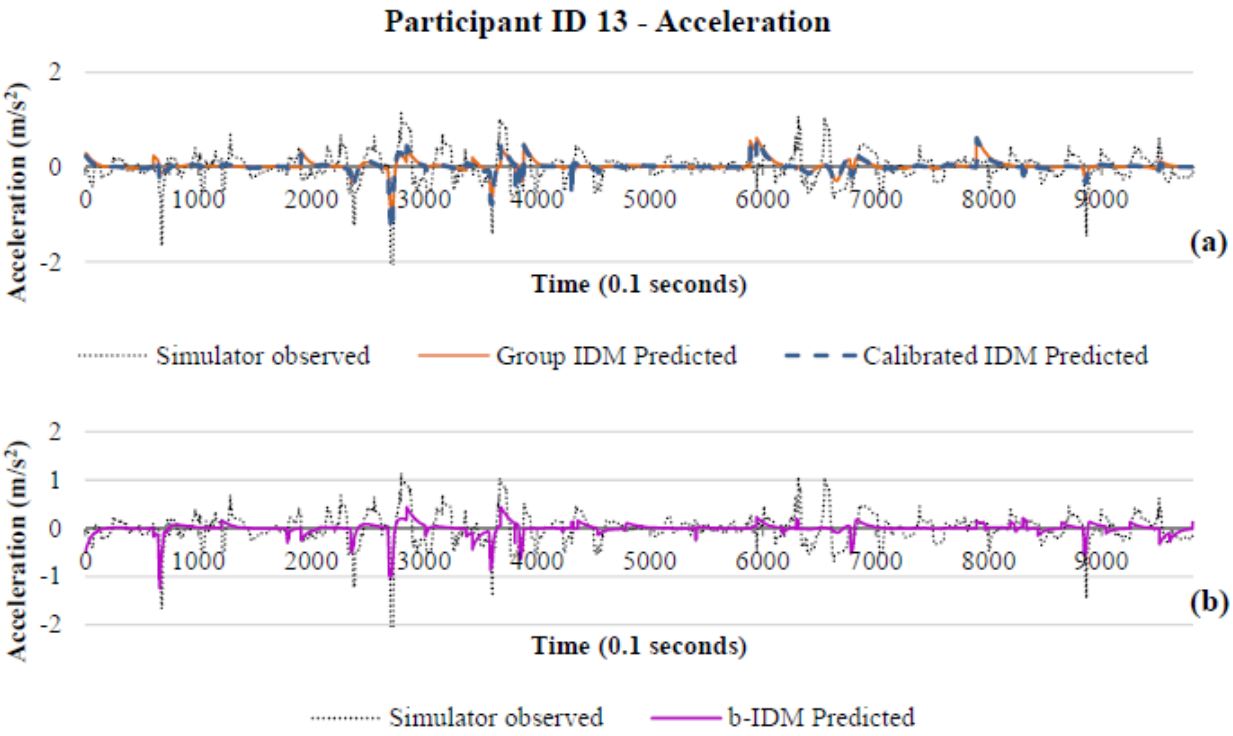

Figure 7.6 Acceleration validation plots for participant ID 13 – (a), calibrated and group IDM predicted and (b) b-IDM predicted

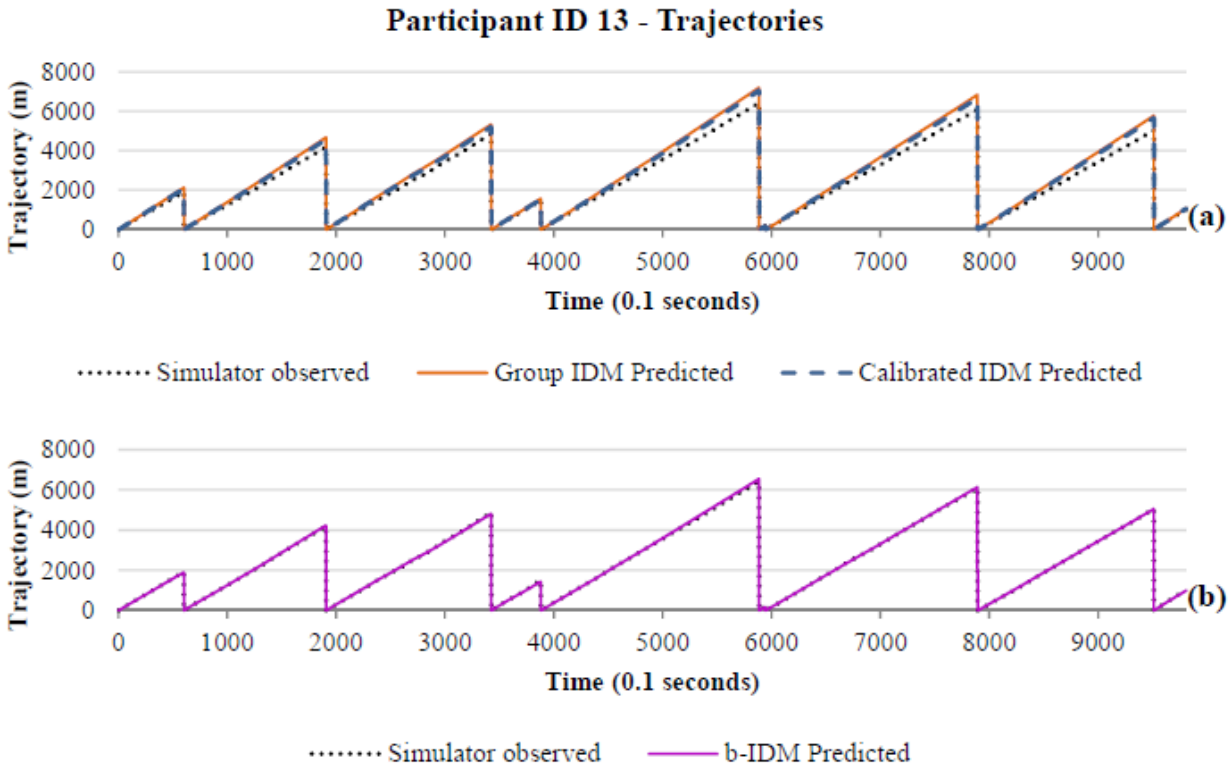

Figure 7.7 Trajectory validation plots for participant ID 13 – (a) calibrated and group IDM predicted and (b) b-IDM predicted

From the figures the b-IDM better predicts all three validation variables. Goodness-of-fit calculations are shown in section 7.5. Figures 7.8 to 7.10 show the combined speed, acceleration, and trajectory charts for all participants in the group A validation set. Similar trends are observed with the b-IDM resulting in a better fit.

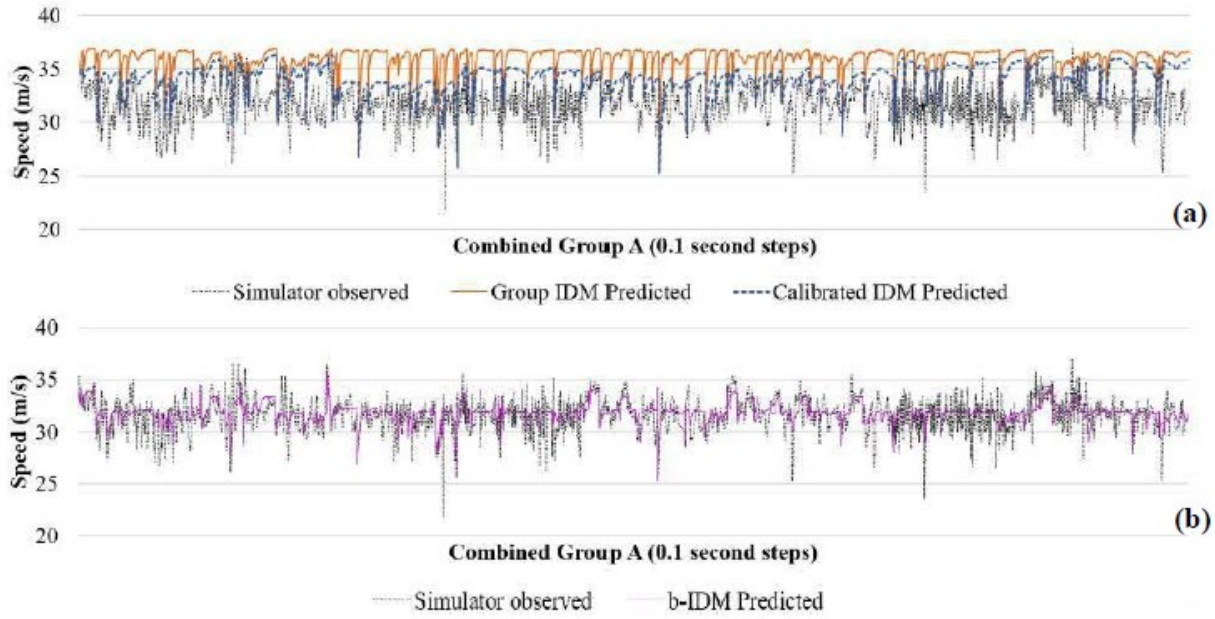

Figure 7.8 Speed plots for the entire group A validation set (a) Calibrated and group IDM predicted and (b) b-IDM predicted

The b-IDM also resulted in better predictions for decelerations, as seen in figure 7.9. For in-depth results, individual participant validation charts are presented in Kummetha (2020).

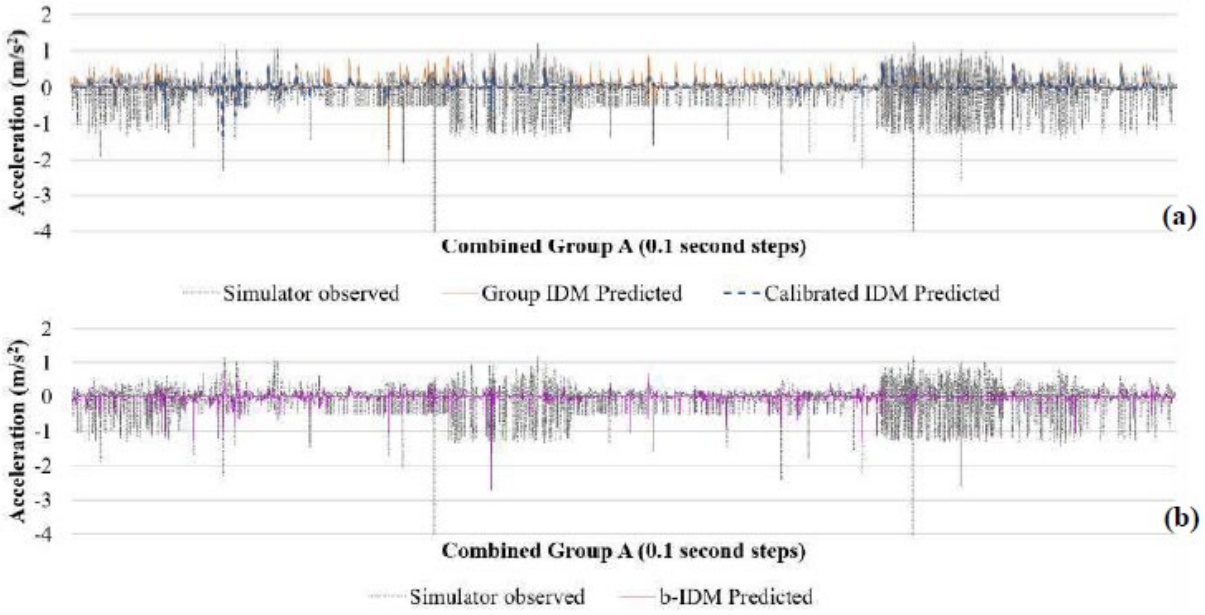

Figure 7.9 Acceleration plots for the entire group A validation set (a) Calibrated and group IDM predicted and (b) b-IDM predicted

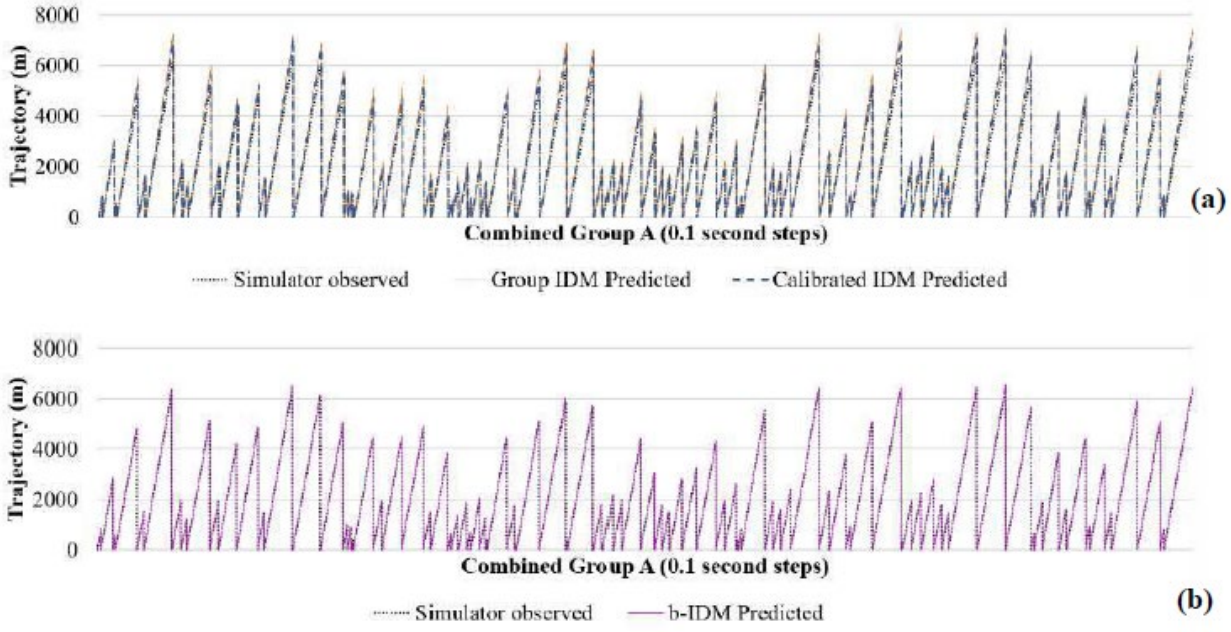

Figure 7.10 Trajectory plots for the entire group A validation set (a) Calibrated and group IDM predicted and (b) b-IDM predicted

7.4 Group B Validation

Similar trends seen in group A were observed in the group B validation dataset. Example comparisons of speed, acceleration, and trajectory time-series data from participant ID 18 are presented in figures 7.11 to 7.16 below. Graphs for the remaining participants are shown in Kummetha (2020). The individual participant and group validation charts show a much better fit from the b-IDM.

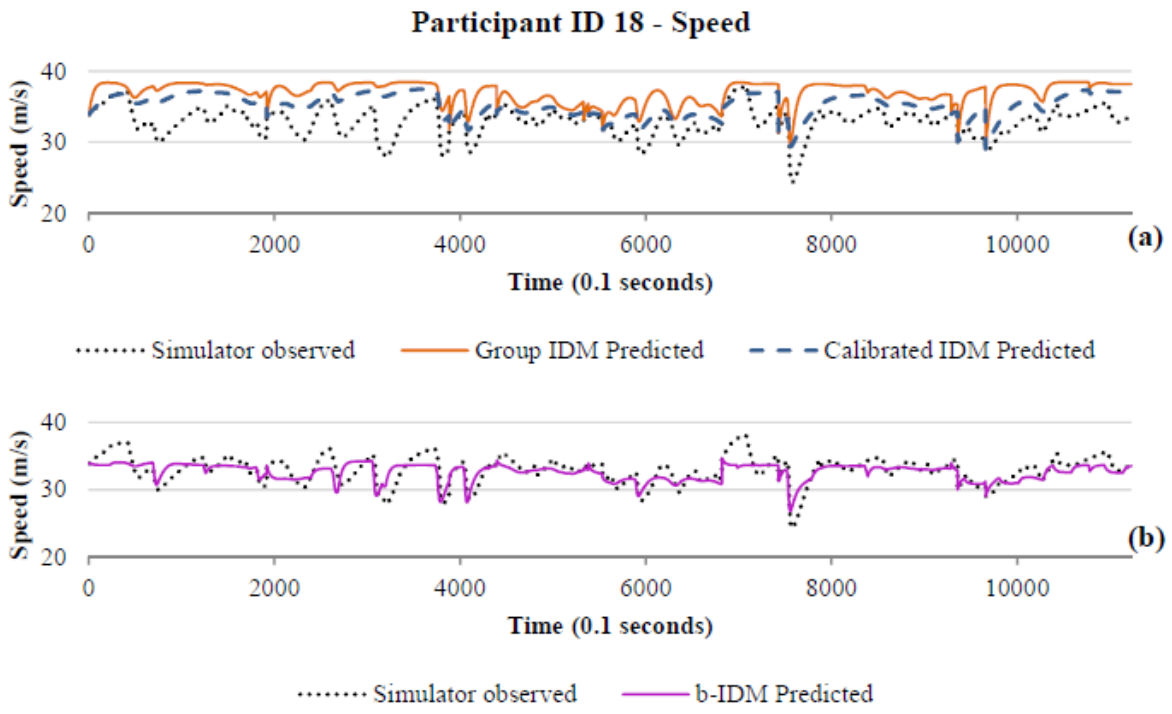

Figure 7.11 Speed validation plots for participant ID 18 - (a) Calibrated and group IDM predicted (b) b-IDM predicted

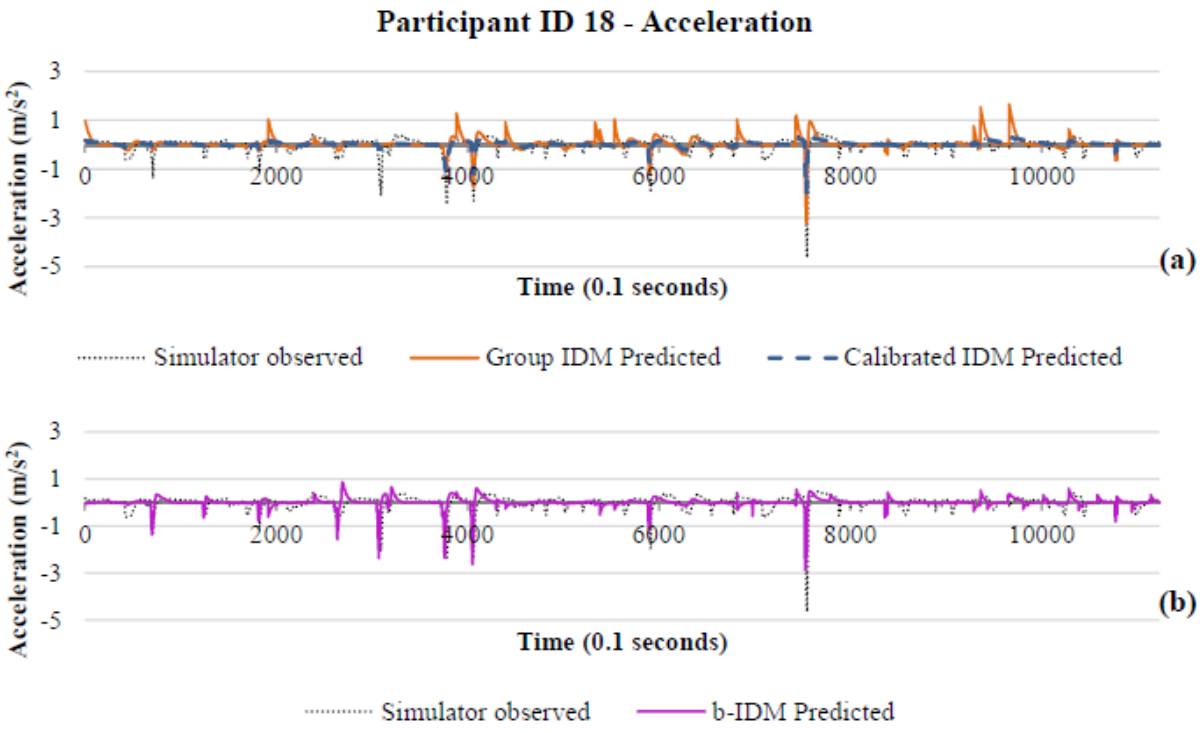

Figure 7.12 Acceleration validation plots **for participant ID 18 -** (a) Calibrated and group IDM predicted and (b) b-IDM predicted

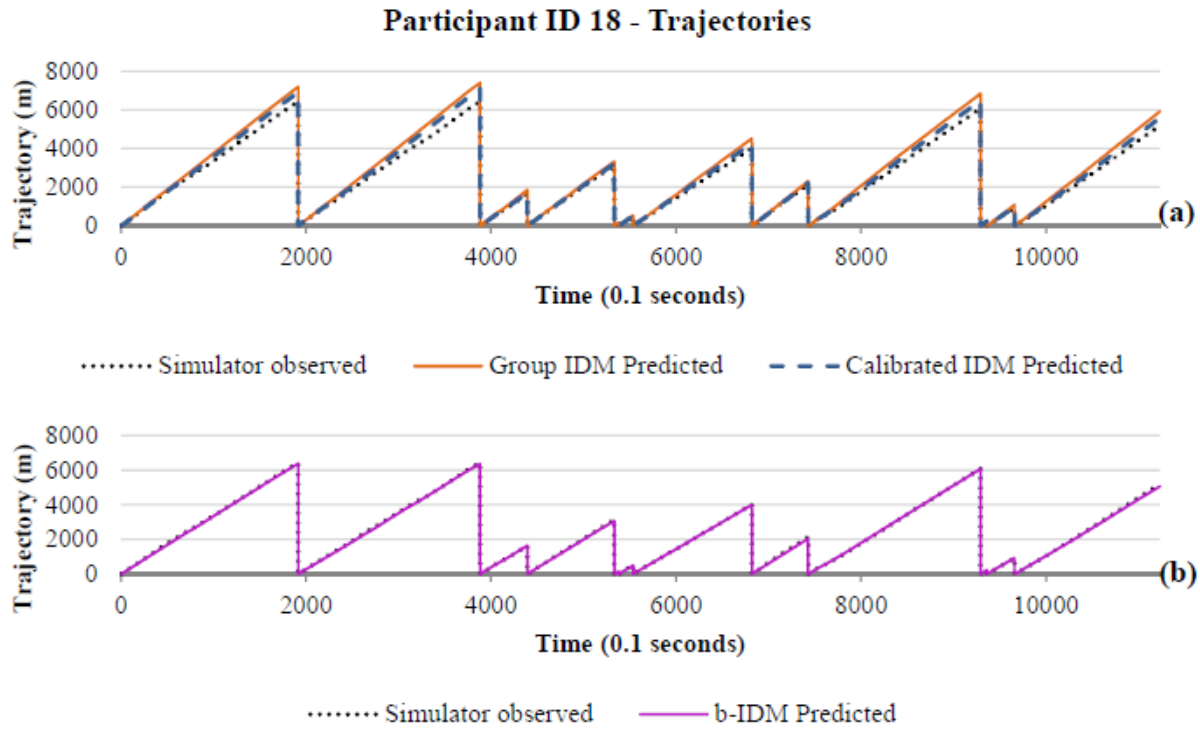

Figure 7.13 Trajectory validation plots for participant ID 18 – (a) Calibrated and group IDM predicted and (b) b-IDM predicted

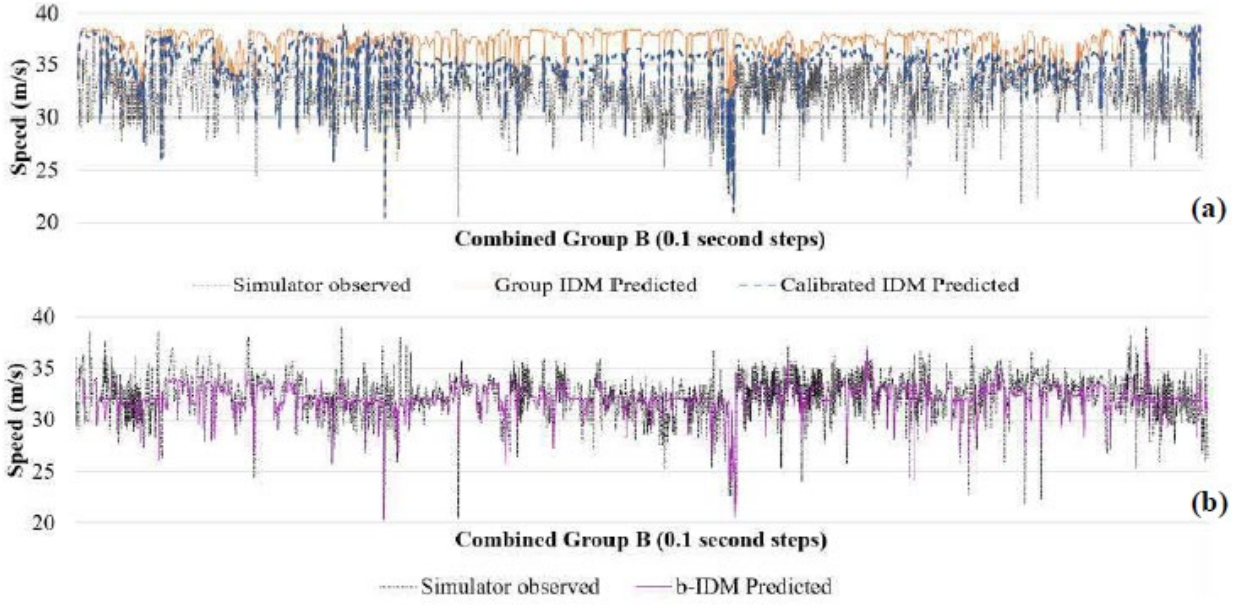

Figure 7.14 Speed plots for the entire group B validation set (a) Calibrated and group IDM predicted and (b) b-IDM predicted

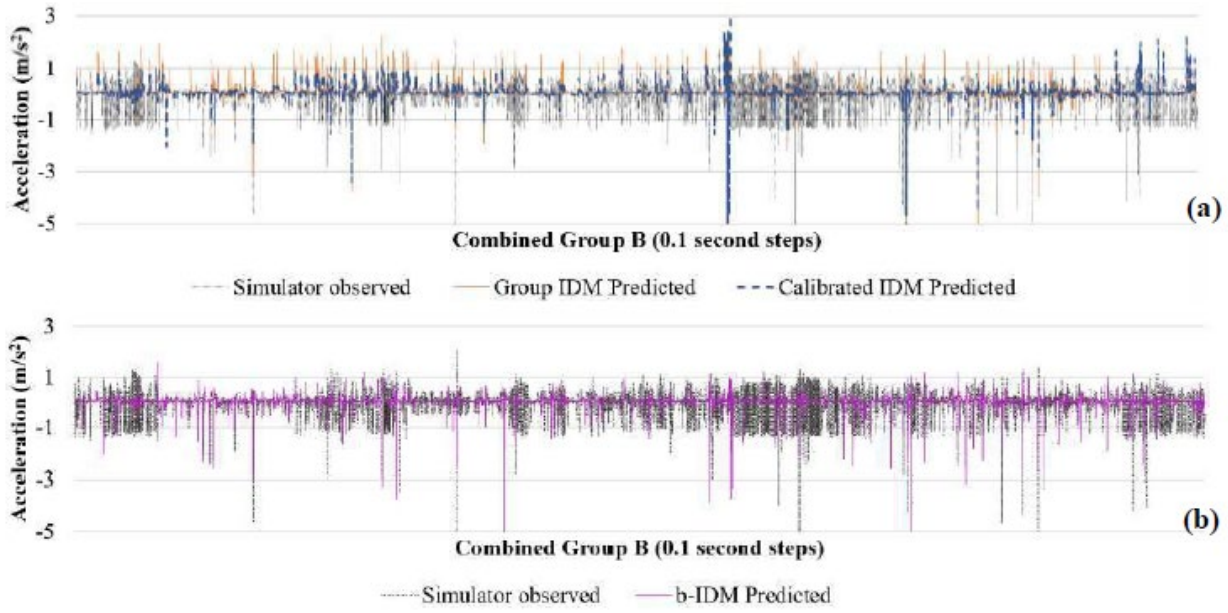

Figure 7.15 Acceleration plots for the entire group B validation set (a) Calibrated and group IDM predicted and (b) b-IDM predicted

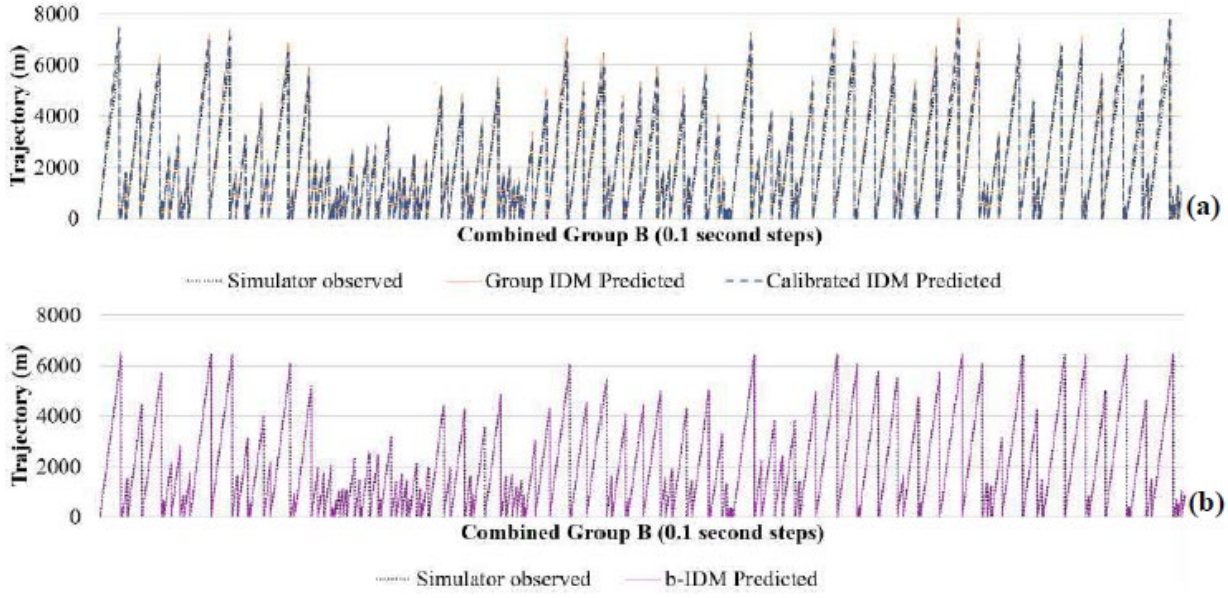

Figure 7.16 Trajectory plots for the entire group B validation set (a) Calibrated and group IDM predicted and (b) b-IDM predicted

7.5 b-IDM Validation Metrics Summary

To determine the goodness of fit, the normalized root mean square error (NRMSE) and mean absolute percentage error (MAPE), shown in equations 7.4 and 7.5 were used. NRMSE normalizes the data with respect to the range of the time series, thus allowing for an easier comparison of the errors. The NRMSE is expressed as a percentage in the results.

$$\%\, NRMSE = \frac{\sqrt{\sum_{t=1}^{n}(\hat{y}_t - y_t)^2/n}}{y_{max} - y_{min}} \times 100\ \% \tag{7.4}$$

$$MAPE = \frac{100\ \%}{n}\sum_{t=1}^{n}\left|\frac{y_t - \hat{y}_t}{y_t}\right| \tag{7.5}$$

Where,

y represents the parameters obtained from the IDM and b-IDM (i.e. speed, acceleration, and trajectory),

$\hat{y}_t$ represents the estimated parameter values output from the IDM and b-IDM at time *t*,

y_t represents the actual value of the parameter at time *t*,

n represents the number of individual time points (0.1 second time steps),

y_{max} is the maximum value of y_t from *t* = 1 to *t* = *n*, and

y_{min} is the minimum value of y_t from t = 1 to *t* = *n*.

The goodness of fit comparisons suggest that the b-IDM resulted in a much better fit with respect to speed and trajectories. However, acceleration did not result in a substantial improvement. This is expected as most car-following models are calibrated using speeds and trajectories due to the highly variable nature of acceleration. The obtained results are shown in table 7.5 and figure 7.17.

Table 7.5 Goodness of fit comparisons using % NRMSE and MAPE

Variable	NRMSE (%)				MAPE (%)			
	Group A		Group B		Group A		Group B	
	IDM	b-IDM	IDM	b-IDM	IDM	b-IDM	IDM	b-IDM
Speed	30.13	8.32	28.69	8.14	13.77	3.09	15.55	3.63
Acceleration	6.36	6.05	6.24	5.76	160.74	127.58	191.84	143.33
Trajectories	5.82	0.59	6.47	0.63	11.28	1.50	13.83	1.75

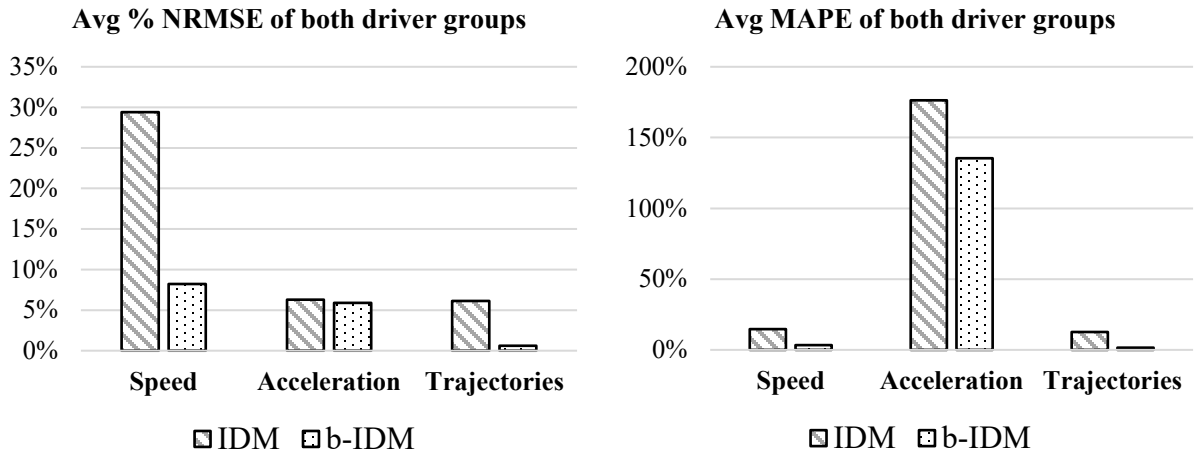

Figure 7.17 Goodness of fit averages (a) % NRMSE and (b) MAPE for both driver groups

Although the MAPE results in much poorer goodness of fit for acceleration, this was expected due to the mean values of acceleration being closer to zero. The MAPE is usually not recommended for values close to zero as it significantly overestimates the error, however, similar results to the % NRMSE were observed with the speeds and trajectories suggesting a better b-IDM fit. The calibrated IDM resulted in a better fit than the uncalibrated group IDM. This was

expected due to the individual-specific parameters used. Overall, the b-IDM resulted in much closer predictions even though group traits were used.

In conclusion, the general form of the biobehavioral parameter α was modeled to be expressed as follows:

$$\boldsymbol{\alpha} = \boldsymbol{e}^{\mu_0+\mu_1 \boldsymbol{Distraction}} \times \boldsymbol{LA}^{\mu_2} \times \boldsymbol{SA}^{\mu_3} \times \boldsymbol{WL\_HR}^{\mu_4} \times \boldsymbol{Lead\ v(t)}^{\mu_5} \quad (7.6)$$

Where,

$\mu_0, \mu_1, \mu_2, \mu_3, \mu_4, \mu_5$ are all coefficients that can be established from a group of participants.

Chapter 8 Conclusions and Recommendations

This project designed a framework to utilize the TCI to incorporate biobehavioral parameters and predict changes to driving performance, specifically to car-following. Ninety drivers were recruited to validate the framework by participating in virtual scenarios within a driving simulator environment. The scenarios were created to capture all the necessary parameters by varying the situation complexity of individual tasks. Participants had to complete an extensive behavioral questionnaire that was used to correlate subjective and experimental data.

A biobehavioral extension to the IDM (b-IDM), using the collected data, was developed to easily calibrate predicted and observed values by grouping individual driver performance and behavioral traits. The model was validated and found to be an effective way of utilizing behavioral and performance variables to efficiently predict car-following behavior.

8.1 Conclusions

The overall objective of incorporating biobehavioral architecture into the IDM was achieved. Several physiological and driving performance variables were examined in this research. The following conclusions were derived from the methodology, experimentation, and data analysis:

- The developed theoretical framework (figure 3.2) proved to be an effective method by utilizing the TCI to monitor changes in WL, SA, and LA of drivers.
- The developed simulator scenario effectively captured varying WL and SA as noted from the NASA-TLX and SART scores. Averaged driving performance measures such as speed, SDLP, and headway were also observed to significantly differ between the six tasks.

- It was discovered that a four-way interaction between WL, SA, LA, and performance was being experienced by the driver at any given time point. For example, an increase in WL due to a complex task leads to a reduction in driving speed, but the newly decreased driving speed could improve SA and make the task less complex, thus reducing WL.
- A new method of quantifying SA was developed by using probe questions, regions of interest, and gaze paths to track driver comprehension.
- Participants were successfully clustered into two groups with significantly different driving performance traits. However, these differed performance traits did not correspond to any substantial cognitive or behavioral characteristics obtained from the questionnaires.
- It was observed that the overall driving performance cannot be predicted solely based on demographic and subjective data. Driving metrics were found to be a crucial part of the puzzle and cannot be entirely substituted for subjective data. However, speed was noted to be a consistent metric in both formats.
- The following variables were crucial to the developed b-IDM: WL from normalizing heart rate (*WL_HR*), normalized LA (*LA*), normalized SA (*SA*), presence of distraction (*Distraction*), and leader velocity (*Lead v(t)*).
- Although the developed models resulted in low R-squared values, all selected variables were highly significant. Low R-squared are generally expected in behavioral models due to the high variance between individuals in terms of cognitive, physical, and mental properties.

- The developed model was validated using a 75/25 data split. Large improvements were seen to the overall fit of the IDM, especially with respect to the speed and trajectory predictions.
- Grouping driver traits proved to be a useful tool in decreasing individual-specific calibration efforts.
- Although the findings of this research were validated, the use of a driving simulator does not guarantee similar results in naturalistic settings. Using instrumented vehicles to collect similar physiological and performance measures would further refine the model. Also, using a much larger sample size to both build and validate the model might improve the overall fit and predictability.

A few challenges experienced during this project are as follows:

- The main limitation of the framework was the assumption that changes to driving performance was sequential. The change in equilibrium between driver capability and task demand simultaneously led to changes in WL, SA, LA, and driving performance.
- The process of synchronizing all the physiological measures to the driving simulator data and appropriately resampling the data for further analysis was intensive. Several VBA and MATLAB scripts were developed to prepare the dataset.
- Incomplete data due to equipment malfunction, corrupt files, and simulator sickness posed a huge challenge to the aggregation and analysis. Also, the relatively large data files required substantial computational power and experienced lots of system crashes.

8.2 Recommendations and Future Research

This research provided some valuable insights into using biobehavioral variables to enhance the calibration and prediction of car-following models. The main focus of this project

was the IDM; however, applying the same theories to other models might add to the scalability of the methodology.

The inclusion of distractions in the developed model provides a new take on predicting speeds and trajectories of distracted drivers and how these values affect the overall traffic flow. More detailed analysis using various naturalistic driving trajectories might aid in better understanding the car-following and lane changing dynamics of distracted driving.

As more car manufacturers are standardizing partial automation features such as adaptive cruise control (ACC) and automatic lane following (ALF) in their vehicles, predicting car-following behavior when engaged in these modes can further benefit traffic flow and demand predictions. A key focus area would be to understand car-following behavior right before engaging or right after disengaging automation systems. The TCI could be used to determine the levels of WL and SA at the instance automation is engaged. Once engaged in automation, the task-automation interface (TAI) determines when a driver engaged in automation, decides to take over due to an imbalance resulting from the demand of the task and trust in automation capability. A theoretical framework, shown in figure 8.1, was established to facilitate the development of experimental strategies to collect the required variables (Kummetha, 2020).

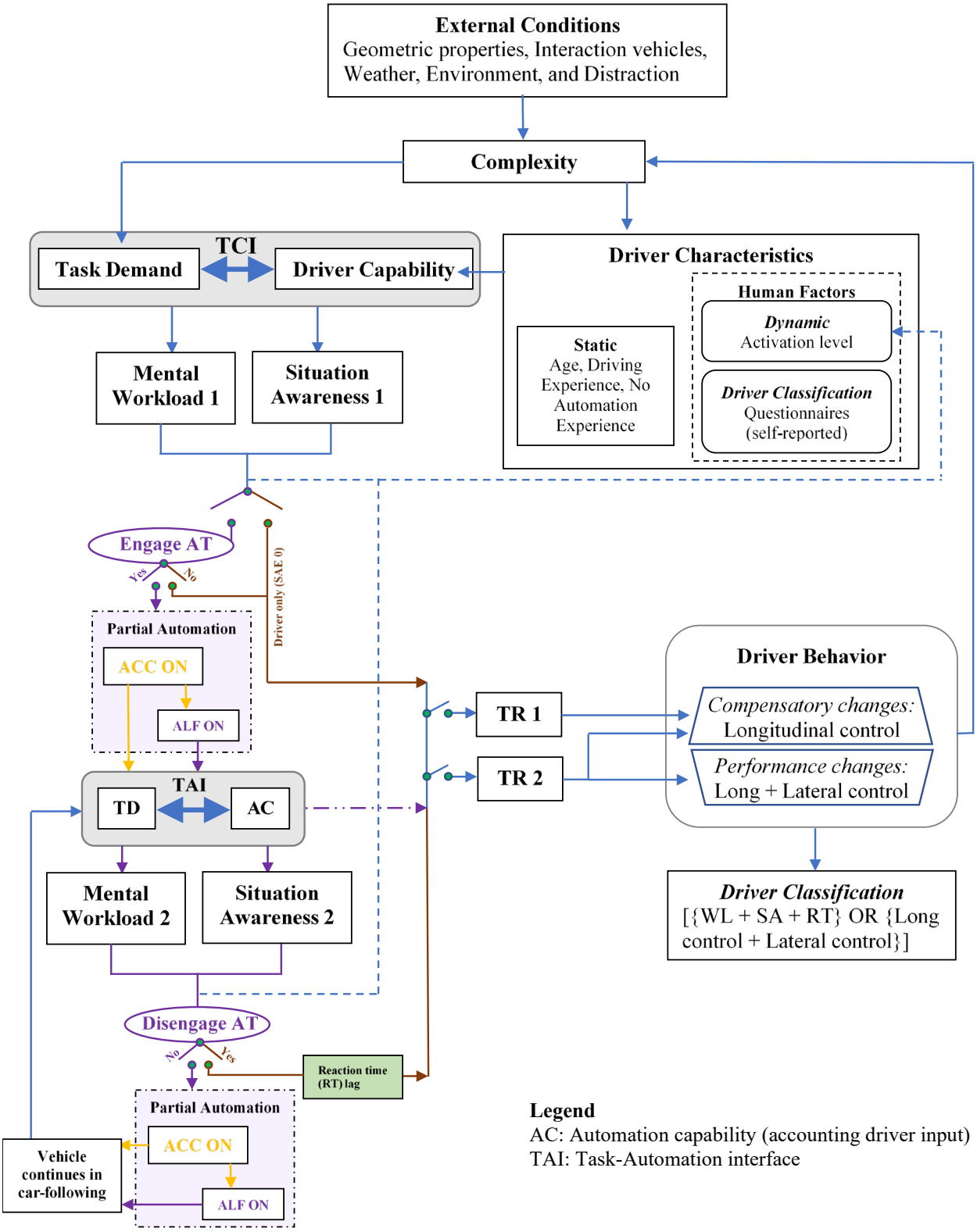

Figure 8.1 Extended framework to include automation

References

Agarwal, Anirudh. 2017. “Human Anatomy.” Link: https://www.knowyourbody.net /parietal-lobe.html. Accessed: Jan 2018.

Alm, Hakan, and Lena Nilsson. 1995. “The Effects of a Mobile Telephone Task on Driver Behavior in a Car Following Situation.” *Accident, Analysis, and Prevention,* 27(5): 707-715.

Baron-Cohen, Simon, and Sally Wheelwright. 2004.“The Empathy Quotient: An Investigation of Adults with Asperger Syndrome or High Functioning Autism, and Normal Sex Differences.” *Journal of Autism and Developmental Disorders*, 34(2): 163-175.

Brookhuis, Karel A., and Dick De Waard. 2010. “Monitoring Drivers’ Mental Workload in Driving Simulators Using Physiological Measures.” *Accident Analysis and Prevention*, 42(3): 898-903.

Brookhuis, Karel A., and Dick De Waard. 1994. “Measuring Driving Performance by Car-Following in Traffic.” *Ergonomics*, 37(3): 427-434.

Brookhuis, Karel A., Gerbrand De Vries, and Dick De Waard. 1991. “The Effects of Mobile Telephoning on Driving Performance.” *Accident Analysis and Prevention*, 23(4): 309-316.

Brookhuis, Karel A., Jan Willem Louwerens, and J. O’Hanlon. 1985. “The Effect of Several Antidepressants on EEG and Performance in a Prolonged Car Driving Task.” *Sleep’84,* 129-131.

Cacioppo, John T., Richard E. Petty, and Chuan F. Kao. 1984. “The Efficient Assessment of Need for Cognition.” *Journal of Personality Assessment*, 48: 306-307.

Campbell, Keith W., Angelica M. Bonacci, Jeremy Shelton, Julie J. Exline, and Brad J. Bushman. 2004. "Psychological Entitlement: Interpersonal Consequences and Validation of a Self-Report Measure." *Journal of Personality Assessment*, 83(1): 29-45.

Causse, Mickael, Eve Fabre, Louise Giraudet, Marine Gonzalez, and Vsevolod Peysakhovich. 2015. "EEG/ERP as a Measure of Mental Workload in a Simple Piloting Task." *Procedia Manufacturing,* 3: 5230-5236.

Chrysikou, Evangelia G., Jake W. Thompson. 2016. "Assessing Cognitive and Affective Empathy Through the Interpersonal Reactivity Index: An Argument Against a Two-Factor Model." *Assessment*, 23(6): 769-777.

Cooper, Joel M., Nathan Medeiros-Ward, and David L. Strayer. 2013. "The Impact of Eye Movements and Cognitive Workload on Lateral Position Variability in Driving." *Human Factors,* 55 (5): 1001-1014.

Costa, Paul T., and Robert R. McCrae. 1989. "The NEO-PI/NEO-FFI Manual Supplement." Psychological Assessment Resources, Odessa, FL.

Coyne, Joseph T., and Ciara M. Sibley. 2015. "Impact of Task Load and Gaze on Situation Awareness in Unmanned Aerial Control." *Naval Research Laboratory*, Defense Technical Information Center, VA.

Dahl, Hartvig, and Donald P. Spence. 1971. "Mean Heart Rate Predicted by Task Demand Characteristics." *Psychophysiology,* 7(3):369-376.

Davis, H. Mark. 1983. "Measuring Individual Differences in Empathy: Evidence for a Multidimensional Approach." *Journal of Personality and Social Psychology*, 44(1): 113-126.

De Waard, Dick, and Karel. A. Brookhuis. 1991. “Assessing Driver Status: A Demonstration Experiment on the Road.” *Accident Analysis and Prevention*, 23(4): 297-307.

De Waard, Dick. 1996. “The Measurement of Drivers' Mental Workload.” Netherlands: Groningen University, Traffic Research Center.

Dijksterhuis, Chris, Dick De Waard, Karel A. Brookhuis, Ben L. Mulder, and Ritske de Jong. 2013. “Classifying Visuomotor Workload in a Driving Simulator Using Subject Spatial Brain Patterns.” *Frontiers in Neuroscience*, 7(149).

Endsley, Mica R., and Daniel J. Garland. 2000. “Direct Measurement of Situation Awareness Validity and use of SAGAT.” *Situation Awareness analysis and Measurement*, Mahwah, NJ.

Endsley, Mica R., and David B. Kaber. 1999. “Level of Automation Effects on Performance, Situation Awareness and Workload in a Dynamic Control Task.” *Ergonomics,* 42(3): 462-492.

Endsley, R. Mica. 1995. “Toward a Theory of Situation Awareness in Dynamic Systems.” *Human Factors,* 37(1): 32-64.

Eriksen, Charles W., and Derek W. Schultz. 1979. “Information Processing in Visual Search: A Continuous Flow Conception and Experimental Results.” *Perception & Psychophysics,* 25: 249-263.

EyeWorks 3 User Manual. 2019. EyeTracking, Inc., Solana Beach, California.

Feng, Fred, Shan Bao, James R. Sayer, Carol Flannagan, Michael Manser. 2017. “Can Vehicle Longitudinal Jerk be used to Identify Aggressive Drivers? An Examination using Naturalistic Driving Data.” *Accident Analysis and Prevention,* 104: 125-136.

Frederick, Shane. 2005. “Cognitive Reflection and Decision Making.” *Journal of Economic Perspectives,* 19(4): 25-42.

Fuller, Ray. 2005. “Towards a General Theory of Driver Behavior.” *Accident Analysis and Prevention,* 37(3): 461-472.

Gangeddula, Viswa, Maud Ranchet, Abiodun E. Akinwuntan, Kathryn Bollinger and Hannes Devos. 2017. “Effect of Cognitive Demand on Functional Visual Field Performance in Senior Drivers with Glaucoma.” *Frontiers in Aging Neuroscience*, 9(286).

Gerdes. Karen E., Elizabeth A. Segal, and Cynthia A. Lietz. 2011. “Measuring Empathy in the 21st Century: Development of an Empathy Index Rooted in Social Cognitive Neuroscience and Social Justice.” *Social Work Research*, 35(2): 83-93.

Grabner, Roland H., and Bert De Smedt. 2012. “Oscillatory EEG Correlates of Arithmetic Strategies: A Training Study.” *Frontiers in Psychology*, 195(4): 635-642.

Hamdar, Samer H., Hani S. Mahmassani, Martin Treiber. 2015. “From Behavioral Psychology to Acceleration Modeling: Calibration, Validation, and Exploration of Drivers’ Cognitive and Safety Parameters in a Risk-Taking Environment.” *Transportation Research Part B,* 78: 32-53.

Hart, Sandra G., and Lowell E. Staveland. 2013. “Development of NASA-TLX (Task Load Index): Results of Empirical and Theoretical Research.” *Advances in psycholog*y, 53: 139-183.

He, Jibo, Jason S. McCarley, and Arthur F. Kramer. 2014. “Lane keeping under cognitive load: Performance changes and mechanisms.” *Human Factors*, 56 (2): 414-426.

Hess, Eckhard, and James M. Polt. 1964. “Pupil Size in Relation to Mental Activity during Simple Problem-Solving.” *American Association for the Advancement of Science*, 143(3611): 1190-1192.

Hoogendoorn, G. Raymond. 2012. “Empirical Research and Modeling of Longitudinal Driving Behavior Under Adverse Conditions.” Delft University of Technology, Netherlands.

Hoogendoorn, Raymond G., Serge P. Hoogendoorn, Karel A. Brookhuis, and Winnie Daamen. 2010. “Psychological Elements in Car-Following Models: Mental Workload in case of Incidents in the Other Driving Lane.” *Procedia Engineering,* 3: 87-99.

Hoogendoorn, Raymond. G., Bart van Arem, Serge P. Hoogendoorn, and Karel A. Brookhuis. 2012. “Applying the Task-Capability-Interface Model to the Intelligent Driver Model in Relation to Complexity.” *TRB 2013 Annual Meeting.*

Hossain, Gahangir, and Mohammed Yeasin. 2014. “Understanding Effects of Cognitive Load from Pupillary Responses Using Hilbert Analytic Phase.” *2014 IEEE Conference on Computer Vision and Pattern Recognition Workshops,* 375-380.

Hurwitz, David, Michael A. Knodler, Daniel M. Dulaski. 2005. “Speed Perception Fidelity in a Driving Simulator Environment.” DSC 2005 North America, Orlando, Florida.

Ikenishi, Toshihito, Takayoshi Kamada, and Masao Nagai. 2013. “Analysis of Longitudinal Driving Behaviors During Car Following Situation by the Driver’s EEG Using PARAFAC.” *12th IFAC Symposium on Analysis, Design, and Evaluation of Human-Machine Systems,* Las Vegas, NV, USA.

ISO 17488: International Organization for Standardization. 2016. “Road Vehicles – Transport Information and Control Systems – Detection Response Task (DRT) for Assessing Attentional Effects of Cognitive Load in Driving.” Switzerland.

Just, Marcel A., and Patricia A. Carpenter. 1980. “A Theory of Reading: From Eye Fixations to Comprehension.” *Psychological Review,* 87(4): 329-354.

Kahneman, Daniel. 1973. “Attention and Effort.” Prentice-Hall, Inc., Englewood Cliffs, NJ.

Kahneman, Daniel, Bernard Tursky, David Shapiro, and Andrew Crider. 1969. “Pupillary, Heart Rate, and Skin Resistance Changes During A Mental Task.” *Journal of Experimental Psychology,* 79(1): 164-167.

Karwowska, Ewa, Przemyslaw Siminski. 2015. “Analysis of the Influence of Perception Time on Stopping Distance from the Angle of Psychophysical Factors.” *The Archives of Automotive Engineering-Archiwum Motoryzacji,* 70(4): 59-74.

Kesting, Arne, and Martin Treiber. 2013. “Traffic Flow Dynamics: Data, Models and Simulation.” *Springer-Verlag Berlin Heidelberg*.

Kim, Hyun Suk, Yoonsook Hwang, Daesub Yoon, Wongeun Choi, and Cheong Hee Park. 2014. “Driver Workload Characteristics Analysis using EEG Data from an Urban Road.” *IEEE Transactions on Intelligent Transportation Systems,* 15(4): 1844-1849.

Kincses, Wilhelm E., Stefan Hahn, Michael Schrauf, and Eike A. Schmidt. 2008. “Measuring Driver’s Mental Workload using EEG.” *ATZ worldwide,* 110(3): 12-17.

Klingner, Jeff. 2010. “Measuring Cognitive Load During Visual Tasks by Combining Pupillometry and Eye Tracking.” Stanford University, Stanford, CA.

Klingner, Jeff, Rakshit Kumar, and Pat Hanrahan. 2008. “Measuring the Task-Evoked Pupillary Response with a Remote Eye Tracker.” *Proceedings of the 2008 symposium on Eye Tracking research & applications,* 69-72.

Kondyli, Alexandra. 2009. “Breakdown Probability Model at Freeway-Ramp Merges Based on Driver Behavior.” University of Florida, Gainesville, FL.

Kondyli, Alexandra, and Lily Elefteriadou. 2011. “Modeling Driver Behavior at Freeway-Ramp Merges.” *Transportation Research Record: Journal of the Transportation Research Board,* 2249: 29-37.

Kondyli, Alexandra, Evangelia. G. Chrysikou, Christopher. H. Ramey, Vishal C. Kummetha. 2018. “Modeling Driver Behavior and Aggressiveness Using Biobehavioral Methods – Part I”. (Report No. 25-1121-0005-153-1). Lincoln, Nebraska: Mid-America Transportation Center, University of Nebraska-Lincoln.

Kondyli, A., E. G. Chrysikou, V. C. Kummetha. 2020. “Modeling Driver Behavior and Aggressiveness Using Biobehavioral Methods – Part II”. (Report No. 25-1121-0005-153-2). Lincoln, Nebraska: Mid-America Transportation Center, University of Nebraska-Lincoln.

Kountouriotis, Georgios K., Richard M. Wilkie, Peter H. Gardner, and Natasha Merat. 2015. “Looking and thinking when driving: The impact of gaze and cognitive load on steering.” *Transportation Research Part F*, 34: 108-12.

Kramer, Arthur F. 1991. “Physiological Metrics of Mental Workload: A Review of Recent Progress.” *Multiple Task Performance*, 279-328.

Kummetha, Vishal C. 2020. “Incorporating Biobehavioral Architecture into Car-Following Models: A Driving Simulator Study”. PhD Dissertation, University of Kansas.

Kummetha, Vishal C., Alexandra Kondyli, Hannes Devos. 2021. “Evaluating Driver Comprehension of the Roadway Environment to Retain Accountability of Safety During Driving Automation”. Transportation Research Part F, 81, pp. 457-471.

Kummetha, Vishal C., Alexandra Kondyli, Evangelia G. Chrysikou and Steven D. Schrock. 2020. “Safety Analysis of Work Zone Complexity with respect to Driver Characteristics- A Simulator Study Employing Performance and Gaze Measures.” *Accident Analysis & Prevention,* 142.

Kummetha, Vishal C., Alexandra Kondyli, and Steven D. Schrock. 2018. “Analysis of the Effects of Adaptive Cruise Control on Driver Behavior and Awareness using a Driving Simulator.” *Journal of Transportation Safety & Security*.

Lehr, P. Robert. 2015. “Brain Function and Deficits.” Department of Anatomy, Southern Illinois University. Center for Neuro Skills, [URL: https://www.neuroskills.com/brain-injury/brain-function.php], Accessed Nov 2018.

Li, Penghui, Gustav Markkula, Li Yibing, and Natasha Merat. 2018. “Is improved lane keeping during cognitive load caused by increased physical arousal or gaze concentration toward the road center?” *Analysis & Prevention*. 117: 65-74.

Li, Yiyang, Norihide Kitaoka, Chiyomi Miyajima, and Kazuya Takeda. 2014. “Evaluation Method for Aggressiveness of Driving Behavior Using Drive Recorders." *Journal of Industry Applications,* 4(1): 59-66.

Light, Gregory A., Lisa E. Williams, Falk Minow, Joyce Sprock, Anthony Rissling, Richard Sharp, Neal R. Swerdlow, and David L. Braff. 2010. “Electroencephalography (EEG) and Event-

Related Potentials (ERPs) with Human Participants." *Current Protocols in Neuroscience,* 52(1): 6.25.2-6.25.24.

Lin, Chin-Teng, Sheng-Fu Liang, Wen-Hung Chao, Li-Wei Ko, Chih-Feng Chao, Yu-Chieh Chen, and Teng-Yi Huang. 2006. "Driving Style Classification by Analyzing EEG Responses to Unexpected Obstacle Dodging Tasks." *IEEE International Conference on Systems, Man, and Cybernetics,* Taipei, Taiwan, 4916-4919.

Loft, Shayne, Lisa Jooste, and Yanqi R. Li. 2018. "Using Situation Awareness and Workload to Predict Performance in Submarine Track Management: A Multilevel Approach." *Human Factors,* 60(7): 978-991.

Lu, Zhenji, Xander Coster, and Joost De Winter. "How Much Time do Drivers Need to Obtain Situation Awareness? A Laboratory-based Study of Automated Driving." *Applied Ergonomics,* 60: 293-304.

Ma, Ruiqi, and David B. Kaber. 2005. "Situation Awareness and Workload in Driving While Using Adaptive Cruise Control and a Cell Phone." *International Journal of Industrial Ergonomics*, 35(10): 939-953.

Ma, Ruiqi, and David B. Kaber. 2007. "Situation awareness and driving performance in a simulated navigation task." *Ergonomics,* 50(8): 1351-1364.

Manjunatha, Pruthvi, Alexandra Kondyli, and Lily Elefteriadou. 2017. "How Has Driver Behavior Been Considered in Traffic Microsimulation and How Can We Use Cognitive Sciences and Psychology Studies to Enhance Them?" *96th Annual Meeting of the Transportation Research Board,* Washington, DC.

Manjunatha, Pruthvi, and Lily Elefteriadou. 2019. "A Framework for Incorporating Human Factors in Microsimulation Using Driving Simulator Observations." *98th Annual Meeting of the Transportation Research Board,* Washington, DC.

Manjunatha, Pruthvi, Vishal C. Kummetha, Alexandra Kondyli, and Lily Elefteriadou. 2019. "Validating the Task-Capability Extension to the Intelligent Driver Model (IDM) Using Driving Simulator Data." *98th Annual Meeting of the Transportation Research Board,* Washington, DC.

Marquart, Gerhard, and Joost De Winter. 2015. "Workload Assessment for Mental Arithmetic Tasks Using the Task-evoked Pupillary Response." *PeerJ Computer Science*, 1(16).

MiniSim User's Guide. 2015. The National Advanced Driving Simulator, Document Version 19, The University of Iowa, Iowa City, Iowa.

Mosaly, Prithima R., Lukasz Mazur, Fei Yu, Hua Guo, Merck Derek, David Laidlaw, Carlton Moore, Lawrence Marks, and Javed Mostafa. 2017. "Relating Task Demand, Mental Effort and Task Difficulty with Physicians' Performance during Interactions with Electronic Health Records." *International Journal of Human-Computer Interaction,* 34(5): 467-475.

Murphey, Yi Lu, Robert Milton, and Leonidas Kiliaris. 2009. "Driver's Style Classification Using Jerk Analysis." *IEEE Workshop on Computational Intelligence in Vehicles and Vehicular Systems*, Nashville, TN.

Neuroelectrics User Manual: Enobio 8. 2019. Neuroelectrics, Barcelona, Spain.

Nguyen, Thanh, Chee P. Lim, Ngoc D. Nguyen, Lee Gordon-Brown, and Saeid Nahavandi. 2018. "A Review of Situation Awareness Assessment Approaches in Aviation Environments." Cornell University Library-arXiv:1803.08067.

Olstam, Janson J., and Andreas Tapani. 2004. “Comparison of Car-Following Models.” Swedish National Road and Transport Research Institute, VTI meddelande 960A.

Patten, Christopher J., Albert Kircher, Joakim Östlund, Lena Nilsson, and Ola Svenson. 2006. “Driver Experience and Cognitive Workload in Different Traffic Environments.” *Accident Analysis & Prevention,* 38(5): 887-894.

Pauzie, Annie. 2008. “A Method to Assess the Driver Mental Workload: The Driving Activity Load Index (DALI).” *IET Intelligent Transport Systems*,2: 315-322.

Pauzie, Annie. 2008. “Evaluating Driver Mental Workload Using the Driving Activity Load Index (DALI).” *In Proceedings European Conference on Human Centered Design for Intelligent Transport Systems*, 67-77.

Pekkanen, Jami, Otto Lappi, Teemu H. Itkonen, and Heikki Summala. 2017. “Task-Difficulty Homeostasis in Car Following Models: Experimental Validation Using Self-Paced Visual Occlusion.” *PLoS ONE*, 12(1).

Pope, Alan T., Edward H. Bogart, and Debbie S. Bartolome. 1995.“Biocybernetic System Evaluates Indices of Operator Engagement in Automated Task.” *Biological Psychology,* 40: 187-195.

Prinzel III, Lawrence J., Alan T. Pope, Frederick G. Freeman, Mark W. Scerbo, and Peter J. Mikulka. 2001. “Empirical Analysis of EEG and ERPs for Psychophysiological Adaptive Task Allocation.” *National Aeronautics and Space Administration*, Report No. NASA/TM-2001-211016.

Quintero, Christian G., Jose Onate Lopez, and Andres C. Cuervo Pinilla. 2012. "Driver Behavior Classification Model based on an Intelligent Driving Diagnosis System." *15th International IEEE Conference on Intelligent Transportation Systems*, Anchorage, Alaska, 894-899.

Ranchet, Maud, John C. Morgan, Abiodun E. Akinwuntan, and Hannes Devos. 2017. "Cognitive Workload Across the Spectrum of Cognitive Impairments: A systematic Review of Physiological Measures." *Neuroscience and Biobehavioral Reviews*, 80: 516-537.

Saifuzzaman, Mohammad, and Zuduo Zheng. 2014. "Incorporating Human-Factors in Car-Following Models: A Review of Recent Developments and Research Needs." *Transportation Research Part C,* 48: 379-403.

Saifuzzaman, Mohammad, Zuduo Zheng, Mazharul Haque, and Simon Washington. 2015. "Revisiting the Task-Capability Interface Model for Incorporating Human Factors into Car-Following Models." *Transportation Research Part B,* 82: 1-19.

Saifuzzaman, Mohammad, Zuduo Zheng, Mazharul Haque, and Simon Washington. 2017. "Understanding the Mechanism of Traffic Hysteresis and Traffic Oscillations through the Change in Task Difficulty Level." *Transportation Research Part B,* 105: 523-538.

Salmon, Paul, Neville Stanton, Guy Walker, and Damian Green. 2006. "Situation Awareness Measurement: A Review of Applicability for C4i Environments." *Applied Ergonomics,* 37(2): 225-238.

Salmon, Paul, Neville Stanton, Guy Walker, Daniel Jenkins, Darshna Ladva, Laura Rafferty, and Mark Young. 2009. "Measuring Situation Awareness in Complex Systems: Comparison of Measures Study." *International Journal of Industrial Ergonomics,* 39: 490-500.

Salvucci, D. Dario. 2006. “Modeling Driver Behavior in a Cognitive Architecture.” *Human Factors: The Journal of the Human Factors and Ergonomics Society,* 23(2): 362-380.

Sanches, Charles L., Olivier Augereau, and Koichi Kise. 2018. “Estimation of Reading Subjective Understanding Based on Eye Gaze Analysis.” *PLoS One,* 13(10).

Sartang, Ghanbary A., M. Ashnagar, E. Habibi, and S. Sadeghi. 2017. “Evaluation of Rating Scale Mental Effort (RSME) Effectiveness for Mental Workload Assessment in Nurses.” *JOHE,* 5(4): 211-217.

Schomig, Nadja, and Barbara Metz. 2013. “Three Levels of Situation Awareness in Driving with Secondary Tasks.” *Safety Science,* 56: 44-51.

Schulze, Thomas, and Thomas Fliess. 1997. “Urban Traffic Simulation with Psycho-Physical Vehicle-Following Models.” *Proceedings of the 1997 Winter Simulation Conference,* 1222-1229.

Selcon, Stephen J., and R. Taylor. 1989. “Evaluation of the Situational Awareness Rating Technique (SART) as a Tool for Aircrew System Design.” *Proceedings of the AGARD AMP Symposium on Situational Awareness in Aerospace Operations*, CP478, France.

Sirevaag, Erik J., Arthur F. Kramer, Christopher D. Wickens, Mark Reisweber, David L. Strayer, and James F. Grenell. 1993. “Assessment of Pilot Performance and Mental Workload in Rotary Wing Aircraft.” *Ergonomics,* 36(9): 1121-1140.

So, Winnie K., Sovio W. H. Wong, Joseph N. Mark, and Rosa H. M. Chan. 2017. “An Evaluation of Mental Workload with Frontal EEG.” *PLoS ONE,* 12(4).

Stojmenova, Kristina, and Jaka Sodnik. 2015. "Methods for Assessment of Cognitive Workload in Driving Tasks." *ICIST 2015 5th International Conference on Information Society and Technology,* 229-234.

Strayer, David L., Joel M. Cooper, Jonna Turrill, James R. Coleman, Nate Medeiros-Ward, and Francesco Biondi. 2013. "Measuring Cognitive Distraction in the Automobile." *AAA Foundation for Traffic Safety*, Washington, DC.

Strayer, David L., Jonna Turrill, James R. Coleman, Emily V. Ortiz, and Joel M. Cooper. 2014. "Measuring Cognitive Distraction in the Automobile II: Assessing In-Vehicle Voice-Based Interactive Technologies." *AAA Foundation for Traffic Safety*, Washington, DC.

Stroop, J. Ridley. 1935. "Studies of Interference in Serial Verbal Reactions." *Journal of Experimental Psychology,* 18: 643-662.

Szulewski, Adam, Shannon M. Fernando, Jared Baylis, and Daniel Howes. 2014. "Increasing Pupil Size is Associated with Increasing Cognitive Processing Demands: A Pilot Study Using a Mobile Eye-Tracking Device." *Journal of Emergency Medicine*, 2: 8-11.

Tampere, Chris M. J., Serge P. Hoogendoorn, and Bart van Arem. 2009. "Continuous Traffic Flow Modeling of Driver Support Systems in Multiclass Traffic with Intervehicle Communication and Drivers in the Loop." *IEEE Transactions on Intelligent Transportation Systems,* 10(4): 649-657.

Tejero, Pilar, and Mariano Choliz. 2002. "Driving on the Motorway: The Effect of Alternating Speed on Driver's Activation Level and Mental Effort." *Ergonomics,* 45(9): 605-618.

Transportation Research Board National Research Council. 2016. "Highway Capacity Manual." *TRB Business Office*.

Treiber, Martin, Ansgar Hennecke, and Dirk Helbing. 2000. "Congested Traffic States in Empirical Observations and Microscopic Simulations." *Physical Review E,* 62(2): 1805-1824.

Treiber, Martin, Arne Kesting, and Dirk Helbing. 2006. "Delays, Inaccuracies, and Anticipation in Microscopic Traffic Models." *Physica A,* 360: 71-88.

Wageningen-Kessels, Femke, Hans van Lint, Kees Vuik, and Serge Hoogendoorn. 2015. "Genealogy of Traffic Flow Models." *Euro Journal on Transportation and Logistics,* 4(4): 445-473.

Walter, Carina B. 2015. "EEG Workload Prediction in a Closed-loop Learning Environment." Universität Tübingen, Germany.

Wang, Ying, Bryan Reimer, Jonathan Dobres, and Bruce Mehler. 2014. "The sensitivity of different methodologies for characterizing drivers' gaze concentration under increased cognitive demand." *Transportation Research Part F*, 26(A): 227-237.

Wiedemann, Rainer. 1974. "Simulation des StraBenverkehrsflusses. Institut fur Verkehrswesen," University of Karlsruhe, Germany.

Young, Mark S., Karel A. Brookhuis, Christopher D. Wickens, and Peter A. Hancock. 2015. "State of science: mental workload in ergonomics." *Ergonomics*, 58(1): 1-17.

Zheng, Yang, Jianqiang Wang, Xiaofei Li, Chenfei Yu, Kenji Kodaka, and Keqiang Li. 2014. "Driving Risk Assessment Using Cluster Analysis Based on Naturalistic Driving Data." *IEEE 17th International Conference on Intelligent Transportation Systems (ITSC),* 2584-2589.

Zhang, Yuyu, and Takatsune Kumada. 2017. “Relationship Between Workload and Mind Wandering in Simulated Driving.” *PLoS ONE* 12(5).

Appendix A Participant Demographics

ID	Age	Gender	Age of license	Annual mileage	Education level	Enjoy driving	Cellphone usage	Crash history	Ticket history	Current Insurance
M001	23	1	9	6500	2	7	8	1	1	1
M002	28	2	15	15000	5	6	4	1	1	3
M003	22	1	2	4000	2	8	3	1	1	1
M004	21	1	3	7500	2	9	8	1	1	2
M005	21	1	0	10000	2	8	3	1	1	2
M006	20	1	4	10000	2	10	8	1	1	2
M007	18	1	3	6000	2	10	3	1	1	3
M008	19	1	4	7000	2	10	3	1	1	3
M009	22	1	0	10000	2	7	4	2	1	3
M010	19	1	1	2000	2	7	2	1	1	1
M011	19	1	5	7000	2	10	10	1	1	1
M012	20	1	4	8000	2	5	1	1	1	2
M013	21	1	6	6000	2	8	4	1	1	3
M014	19	1	3	7000	2	9	3	1	1	NA
M015	21	1	6	10000	2	10	3	1	1	3
M016	20	1	3	20000	2	6	4	1	1	3
M017	37	2	23	10000	3	4	1	1	1	1
M018	23	1	8	5000	2	7	7	1	1	1
M019	19	1	3	15000	2	10	2	1	2	1
M020	18	1	3	20000	2	10	10	1	3	1
M021	19	1	4	7500	2	9	1	2	1	1
M022	22	1	7	12000	3	10	8	1	2	3
M023	21	1	0	1000	2	NA	4	1	1	1
M024	21	1	5	10000	2	7	4	1	1	2
M025	18	1	4	6000	2	10	3	1	1	3
M026	21	2	6	12000	2	7	3	1	1	NA
M027	20	2	5	6000	2	6	3	1	1	3
M028	21	2	0	10000	2	8	4	1	1	1
M029	59	2	26	6000	2	9	1	2	1	1
M030	51	2	33	25000	3	8	3	1	1	3
M031	23	2	8	20000	2	8	4	1	1	3
M032	21	2	7	8000	2	9	1	1	1	1
M033	50	2	35	10000	2	7	6	1	1	1
M034	22	2	0	10000	4	8	2	1	1	3
M035	19	2	4	12500	2	10	2	1	3	1
M036	18	2	0	6500	2	7	4	1	1	3
M037	19	2	0	10000	2	8	1	1	1	2
M038	19	2	4	1000	2	9	4	1	1	3
M039	21	2	6	1000	2	6	5	1	1	2
M040	19	2	4	15000	2	8	7	1	1	1
M041	20	2	4	12000	2	10	10	1	1	3

ID	Age	Gender	Age of license	Annual mileage	Education level	Enjoy driving	Cellphone usage	Crash history	Ticket history	Current Insurance
M042	21	2	4	25000	2	6	2	1	1	1
M043	20	2	5	10000	2	8	1	1	2	3
M044	22	2	0	5000	2	9	4	2	1	2
M045	20	2	5	10000	2	7	5	1	3	1
M046	54	2	38	25000	4	10	7	1	1	3
M047	21	2	4	9000	2	8	8	1	1	2
M048	19	2	3	10000	2	8	4	1	1	1
M049	20	1	5	5000	2	8	1	1	1	1
M050	23	1	7	10000	4	8	2	1	1	3
M051	27	1	8	30000	3	10	2	1	1	1
M052	46	1	28	20000	3	9	4	1	1	1
M053	48	1	31	12000	3	8	1	1	1	1
M054	27	1	0	8000	5	10	NA	2	1	3
M055	31	1	17	10000	5	7	3	1	1	3
M056	46	1	29	1700	5	4	2	1	1	1
M057	29	1	14	15000	5	6	3	1	2	3
M058	26	1	0	13000	3	5	2	2	1	3
M059	36	1	20	15000	2	10	2	1	1	1
M060	49	1	33	45000	3	8	4	1	1	1
M061	25	1	0	11000	1	10	3	1	1	3
M062	46	1	30	20000	3	10	3	1	1	3
M063	38	1	22	45000	3	7	6	2	1	1
M064	35	2	20	2000	2	6	1	1	1	1
M065	26	2	2	12000	4	10	7	1	1	1
M066	42	2	26	16000	3	9	3	1	1	3
M067	40	2	22	27000	3	9	NA	1	1	1
M068	26	2	3	10000	5	NA	5	1	1	3
M069	42	2	27	2000	3	7	4	1	1	2
M070	36	2	22	19000	5	8	6	1	1	3
M071	34	2	19	40000	3	10	2	2	1	3
M072	48	2	32	8000	5	8	1	1	1	3
M073	31	2	17	10000	1	10	9	1	1	3
M074	30	2	15	13000	5	9	4	1	1	3
M075	32	2	16	24000	5	NA	7	1	1	2
M076	28	2	12	12000	3	6	4	1	1	3
M077	56	1	37	1200	5	5	1	1	1	1
M078	58	1	45	7500	1	9	2	1	1	1
M079	61	1	46	15000	2	10	5	1	1	3
M080	53	1	37	18000	2	10	1	1	1	1
M081	56	1	41	20000	2	10	2	1	1	1
M082	56	1	41	5000	1	8	1	1	1	1
M083	25	1	9	11000	2	8	4	1	1	3
M084	53	2	36	10000	2	10	1	1	1	3

ID	Age	Gender	Age of license	Annual mileage	Education level	Enjoy driving	Cellphone usage	Crash history	Ticket history	Current Insurance
M085	60	2	46	1000	1	6	NA	1	1	3
M086	64	2	49	8000	3	8	NA	1	1	3
M087	57	2	41	10000	5	9	2	1	1	3
M088	57	2	41	13000	3	8	5	1	1	3
M089	20	2	5	12000	2	6	3	1	1	1
M090	55	2	40	15000	3	10	3	1	1	3
Mean	**31.4**	**1.5**	**14.6**	**12043.3**	**2.6**	**8.2**	**3.8**	**1.1**	**1.1**	**NA**
SD	**14.2**	**0.5**	**14.6**	**8561.1**	**1.1**	**1.6**	**2.4**	**0.3**	**0.4**	**NA**

*NA indicates missing or not completed information.

Education level {1: High school; 2: Current college student; 3: Finished college; 4: Current graduate student; 5: Finished graduate school with at least a master's degree}

Current insurance {1: Liability; 2: Comprehensive; 3: Collision}